Energy Policy and Development Centre (KEPA)
National and Kapodistrian University of Athens

Центр Энергетическая Политики и Развития
Национального и Каподистриайского Университета Афин

Volume 4, Number 1, January - June 2011
Собрание 4, Номер 1, Январь - июнь 2011

Euro - Asian Journal of sustainable energy development policy

Евро-Азиатский журнал по политике развития устойчивой энергетики

Athens 2013

Euro - Asian Journal of sustainable energy development policy

Евро-Азиатский журнал по политике развития устойчивой энергетики

Energy Policy and Development Centre (KEPA)

National and Kapodistrian University of Athens (NKUA)

Центр Энергетическая Политики и Развития

Национального и Каподистриайского Университета Афин

COPYRIGHT TRANSFER AGREEMENT

Date:…………………………………………………………………………………….

To: ………………………………………………………………………………...

Re: Manuscript entitled. ………………………...…………………………………..

(the “Contribution”) for publication in ……………………………………………...

……………………………………………………………………………………….

(the “Journal”) published on behalf of the Energy Policy and Development Centre (KEPA) of the National and Kapodistrian University of Athens.

Thank you for submitting your contribution for publication. In order to expedite the publishing process and enable your work to be disseminated to the fullest extent, we need to have this Copyright Transfer Agreement signed and returned to us as soon as possible. If the Contribution is not accepted for publication this Agreement shall be null and void.

A. Copyright

1. The Contributor assigns to the Energy Policy and Development Centre (KEPA) of the National and Kapodistrian University of Athens (NKUA), hereafter mentioned as KEPA – NKUA, during the full term of copyright and any extensions or renewals of that term, all copyright in and to the Contribution, including but not limited to the right to publish, republish, transmit, distribute and otherwise use the Contribution and the material contained therein in electronic and print editions of the Journal and in derivative works throughout the world, in all languages and in all media of expression now known or later developed, and to license or permit others to do so.
2. Reproduction, posting, trasmission or other distribution use of the Contribution or any material contained therein, in any medium as permitted hereunder, requires a citation to the Journal as the copyright owners, suitable in form and contents as follows: (Title of Article, Author, Journal Title, Volume/Issue, Copyright © [year] National and Kapodistrian University of Athens).
3. Permission grants - if the manuscript contains extracts, including illustrations, from other copyright works (including material from on-line or intranet sources) it is the author's responsibility to obtain written permission from the owners of the publishing rights to reproduce such extracts.

B. Other rights of Contributor

KEPA - NKUA grant back to the Contributor the following:

1. The right to share with colleagues print or electronic “preprints” of the unpublished Contribution, in form and content as accepted by KEPA - NKUA for publication in the Journal. Such preprints may be posted as electronic files on the Contributor’s own website for personal or professional use, or on the Contributor’s internal university or corporate networks/intranet, or secure external website at the Contributor’s institution, but not for commercial sale or for any systematic external distribution by a third party (eg: a listserver or database connected to the public access server). Prior to the publication, the Contributor must include the following notice on the preprint: “This is a preprint of the article accepted for publication in [Journal title] Copyright © [year] Energy Policy and Development Centre of the National and Kapodistrian University of

Athens". After publication of the Contribution by KEPA-NKUA, the preprint notice should be amended to read as follows: "This is a preprint of the article published in [include the complete citation information for the final version of the Contribution as published in the print edition of the [Journal title] Copyright © [year] Energy Policy and Development Centre of the National and Kapodistrian University of Athens" and should provide an electronic link to the Journal's web site, located at the following URL: http://www.promitheasnet.kepa.uoa.gr. The Contributor agrees not to update the preprint or replace it with the published version of the Contribution.

2. The right without charge to photocopy or to transmit on-line or to download, print out and distribute to a colleague a copy of the published Contribution in whole or in part, for the Contributor's personal or professional use, for the advancement of scholarly or scientific research or study, or for corporate informational purposes.

3. The right to republish, without charge, in print format, all or part of the material from the published Contribution in a book written or edited by the Contributor.

4. The right to use selected figures or tables, and selected text from the Contribution, for the Contributor's own teaching purposes, or for incorporation within another work by the Contributor that is made part of an edited work published (in print or electronic format) by a third or for presentation in electronic format on the internal computer network or external website of the Contributor or the Contributor's employer.

5. The right to include the Contribution in a compilation for classroom use (course packs) to be distributed to students at the Contributor's institution free of charge or to be stored in electronic format in data rooms for access by students at the Contributor's institution as part of their course work (sometime called as "electronic reserve rooms") and for in-house training programmes at the Contributor's employer.

C. Contributors Representations

The Contributor represents that the Contribution is the Contributor's original work. If the Contribution was prepared jointly, the Contributor agrees to inform the co-Contributors of the terms of this Agreement and to obtain their signature(s) to this Agreement or their written permission to sign on their behalf. The Contribution is submitted only to this Journal and has not been published before, except for "preprints" as permitted above.

Contributor's signature______________________________________Date____________

Type or print name and title____

Co-Contributor's signature___________________________________Date____________

Type or print name and title____

To enable the journal editor to disseminate the author's work to the fullest extent, the author must sign the Copyright Transfer Agreement, transferring copyright in the article from the author to the journal editor and submit the original signed agreement with the article presented for publication. A copy of the agreement to be used (which may be photocopied) can be found in each issue of the journal or on the website at http://www.promitheasnet.kepa.uoa.gr. Copies may also be obtained from the journal editor.

Dear Reader,

The *"Euro-Asian Journal of Sustainable Energy Development Policy"* is the outcome of the established cooperation among scientists from Europe, Black Sea, Caspian Sea and Central Asia.

It is part of a growing cooperation in the frame of PROMITHEASnet activities. A network that includes members from sixteen countries and remains open to new participants, while its range of activities includes an Annual Scientific Conference, scientific awards, workshops, seminars and joint participation in EU financing research activities.

In addition the PROMITHEAS network disseminates relevant information through its newsletter, to more than 23,000 registered recipients from 170 countries all over the world.

In this context we do encourage scientific synergies and we invite colleagues to join us as authors, article-reviewers or even as partners in research projects.

Our continuous effort is the quality upgrade of the journal's content and to this aim we welcome your contribution.

The editor

Prof. Dimitrios Mavrakis

Дорогой читатель,

“Евро-Азиатский журнал по политике развития устойчивой энергетики” является результатом сотрудничества, налаженного между учеными из Европы, регионов Черного моря, Каспийского моря и Центральной Азии.

Он является частью растущего сотрудничества в рамках деятельности сети PROMITHEAS. Это сеть, включает в себя членов из шестнадцати стран и остается открытой для новых участников, а также спектр ее мероприятий включает Ежегодную Научную Конференцию, научные награды, совещания, семинары и совместное участие в исследованиях, финансируемых Европейским Союзом.

Кроме того, через сеть PROMITHEAS распространяется соответствующая информация посредством ее информационного бюллетеня, более чем 23,000 зарегистрированным получателем из 170 стран по всему миру.

В связи с этим, мы также поддерживаем научное сотрудничество и приглашаем коллег присоединиться к нам в качестве авторов, обозревателей или даже в качестве партнеров в научно-исследовательских проектах.

Наши непрерывные усилия направлены на обеспечение качества содержания журнала, и мы приветствуем Ваш вклад для обеспечения этой цели.

В заключение, я хотел бы поприветствовать Профессора Эльмиру Рамазанову, директора Научно-исследовательского Института Геотехнологических Проблем Нефти, Газа и Химии (GPOGC) Азербайджанской Государственной Нефтяной Академии, как старшего редактора этого журнала, и выразить свою искреннюю благодарность за ее постоянную поддержку издании этого журнала.

Редактор

Проф. Димитриос Мавракис

Aim and scope

The PROMITHEAS scientific journal titled "***Euro-Asian Journal of Sustainable Energy Development Policy***" is a semi-annual bilingual (English, Russian) publication addressing policy issues on energy and climate change, mainly from the Black Sea, Caspian, Central Asia and S.E. Europe regions. The aim of the publication is to motivate and encourage the scientific and research human potential of these regions to present their research work in the aforementioned areas. Thus, it is expected that the regional scientific potential will be more easily identified and able to be contacted by regional and EU energy policy and environmental stakeholders. Efforts will be made so as the journal contains articles produced through joint efforts among researchers from the regions and the PROMITHEAS network participants.

The scientific journal will also host articles and executive summaries of scientific reports and studies presented during workshops, organized by the PROMITHEAS Network, regarding energy and climate policy issues. The contents of each issue will be determined by the editorial board.

Major articles will cover a comprehensive range of topics such as:

Energy supply and geopolitics;

Strategic energy planning;

Socio-economics of hydrocarbon reserves exploitation;

Energy interconnections;

Regional Energy Market development;

Emerging hydrogen technologies;

Socio-economics of transcontinental energy corridors;

Implementation of Kyoto Protocol mechanisms;

Analysis and implementation of climate policy instruments;

RTD policies and socio-economics for new forms of energy.

Цели и задания

Научный журнал сети PROMITHEAS под названием **«Евро-Азиатский журнал по политике развития устойчивой энергетики»** является полугодичной и двуязычной (Английский, Русский) публикацией, которая уделяет основное внимание вопросам политики в области энергетики и изменения климата, в основном для регионов Черного и Каспийского морей, Центральной Азии и Юго-Восточной Европы. Целью публикации является стимулирование и поддержка научно-исследовательского человеческого потенциала этих регионов что бы представить свою исследовательскую работу в вышеперечисленных областях. Ожидается, что региональный научный потенциал будет легче идентифицироваться и заинтересованным сторонам, региональным, связаным с энергетической политике ЕС и экологии, будет легче с ним связаться. Это будет осуществляться путем включения в журнал научных статей, написанных в результате совместного сотрудничества ученых из вышеперечисленных регионов и участников сети PROMITHEAS.

Научный журнал также будет размещать материалы и краткие обзоры научных отчетов и исследований, представленных во время разных семинаров, организованных Сетью PROMITHEAS, которые касаются тем энергетической и климатической политики. Содержание каждого выпуска будет отбираться ученым советом.

Основные статьи, в меру возможностей, будут покрывать следующие темы:

- энергоснабжение и геополитика;

- стратегическое энергетическое планирование;

- социально-экономические аспекты использования углеводородных запасов;

- энергетические взаимосвязи;

- развитие Регионального Энергетического Рынка;

- новосоздающиеся водородные технологии;

- социально-экономические аспекты трансконтинентальных энергетических коридоров;

- механизмы осуществления Киотского Протокола;

- анализ и внедрение инструментов климатической политики;

- политики научных технических исследований и социальноэкономические аспекты новых форм энергии.

Contents

Volume 4, Number 1

About some features of the power transfer mode on the long transmission line

Berzan V.P., Rimschi V.X., Tirsu M.S., Patsyuk V.I., Uzun M.N.

Institute of Power Engineering of Academy of Sciences of Moldova

E-mail: berzan@ie.asm.md

Abstract. The features of electric power transmission over long lines, processes in which can be described by the telegraph equations in the dimensionless units, have been considered. The boundary conditions are given in this case in the form of differential-integral equations. The using of the relative load parameter z allows obtaining aggregate data about working regime of a long line when you change the load under the limits $-\infty < R_S < +\infty$. Numerical method of finite differences, called as "Albatros" method, has been used during study of working modes of a long line. The method has a homogeneous structure and allows to carry out through calculation of discontinuous solutions. Wave fronts and other discontinuities values of the unknown parameters are allocated automatically and are represented in the form of large gradients of the wave field. Basic modes of transmission of power have been investigated in dependence of the values of the linear parameters of the line, of its length and of the load features. It has been shown that from electrical point of view a long line is non-uniform object, which is characterized by the singular points in order to transfer maximum power to the load. The location of these points depends on the length of the electromagnetic wave, and also depends on parameters of the line loss. At singular points of the AC lines active power at its input (generator power) is the same as in the idle mode (XX), and also is the same as in a short-circuit current (SCC) for this singular point of the line. The line length influences mostly strongly at the mode of transmission of power. At the same time it is necessary to distinguish modes of operation of the line under conditions of the maximum line transmission capacity, of the maximum value of the coefficient of performance (COP), of the maximum value of power factor (PF), and of the maximum energy injection level in the line by a sinusoidal voltage generator. It have been presented characteristics of changing of power at the beginning and at the end of the line, of power factor, of the coefficient of performance (COP) of power transmission lines, and of the currents, in dependence on the length of line, on the line parameters and load parameters.

Keywords: long line, mode of operation, transmitted power.

1. Introduction

Currently, there are new qualitative changes in the technologies of energy supply, particularly due to increased share of renewable energy in the consumption balance. The problem of greater involvement of renewable energy will require a new approach in the organization of production and transport of electrical energy, because it is necessary to ensure a constant balance between production and consumption, as an example, due to the parallel operation of solar power plants located in different time zones and climate zones.

Possibility of production of large amount of electricity by solar power plants has been proved by long-term experience in this field. For example, the world's most powerful solar power plant has been opened in Portugal in 2007, with the installed capacity equal to 11 MW [1]. In this case solar PV modules occupy an area of about 60 hectares. There are also other projects of solar power plants. In particular, in accordance with the elaborated in the USA project for Arizona state it is planned to construct and put into operation in 2011 solar power plant with capacity equal to 280 MW [2]. Also, technical proposal regarding construction of a solar power station in the Sahara desert in Africa has been presented, with electric power generation at the level of 100 GWh [3].

Taking into consideration continuous increasing the share of generation from renewable energy sources, reliable and sustainable energy supply can be possible by realization of concept of planetary electrical power system [4].

Trends of continuous increasing of power generation sources and of increasing of distance of transmission electric lines are typical for the whole period of development of power engineering. In particular, rated voltage of electric lines has been increased from 1.5-2 kW (1882) to 1150 kW at the present time, and distance of electric power transmission lines has been increased from 57 km to 1500 km and more [1-3, 5-7]. These quantitative changes in the structure, in the structures of circuits of transmission and distribution of electrical energy are accompanied by the emergence of new scientific and technological problems that are not typical for small power systems.

In the consolidated regional electric power transmission systems, line distance will be comparable with the wavelength of the electromagnetic wave. Under these dimensions problems of efficiency and reliability of the system are relevant as to a whole system and also to its components. So, investigation of characteristics of transmission of electric power on a long distance is not only theoretical problem but has also big practical relevance for modern electrical power engineering.

2. Problem of statement

Creation of the big power supply systems with lingering electric lines, for example, within the frame of the West-east project, a power ring round Black sea (regional association of power supply systems) or in case of electric energy transit from Sahara solar power station to Europe [3] demands more intensive research of energy transmission features on the big distances. Besides, at creation of power corridors use of new technical solutions, for example such as superconducting electrical transmission line (ETL) or separate sites of electricity transmission on the basis of superconductivity effect, that will affect works modes of such non-uniform lines is not excluded.

Quantitative changes in structure of electropower systems (EPS) generate some question on which now is not present clear and definite answers, for example such as:

Modern methods of the processes analysis in long lines are how much exact and whether there are borders of their applicability, for example in case of line lost-free.

Under what conditions it is possible to provide the greatest transferred power, the greatest value of line EFFICIENCY, including at compensation of reactive components of loading and line.

As line heterogeneity, its length and values of longitudinal parameters influences characteristics of electric power transfer at normal and emergency operation.

The problem of the given work consists in the analysis of scale (linear) and parametrical factors influence on efficiency of electric power transfer on the big distances. At the analysis of features of long electric lines functioning, for example, as a part of regional EPS, the cable equations are used.

3. Research method

Heterogeneity of long lines and dependence of energy transmission mode of, both on loading parameters, and on line parameters are complicating factors at research of features of their work in EPS structure.

At the analysis we will start with position, that any established mode is preceded always by non-stationary wave process. The most convenient tools for the problem solution in such statement are in our opinion the method of characteristics and method of final differences "Albatross" [8]. Differential numerical scheme "Albatross" is offered and strictly proved by Institute of power engineering of Academy of Sciences of Moldova (ASM). Using this approach it is possible to solve easily and simply the cable equations for non-uniform lines and chains with any losses, the branching points, several generating both loading knots and other complicating factors [8].

In a method of characteristics it is necessary to allocate and trace a priori configuration of wave fronts (strong ruptures) which considerably become complicated eventually. Therefore the method of characteristics is expedient for using, basically, for test calculations of ideal and not deforming lines for the purpose of the control of accuracy of numerical solutions. The method of final differences "Albatross" possesses homogeneous structure and carries out the through account of explosive solutions where fronts of waves and other jumps are allocated automatically and are represented in the form of places of the big gradients of wave field. This conclusive advantage, in combination to practically absolute accuracy, allows to carry out calculation of the transitive and established processes under uniform formulas of predictor - corrector type taking into account a various type of heterogeneities without excessive physical and geometrical idealisation of investigated electric systems and devices [8-10].

Thanks to conservatism, zero differential dissipation and minimum dispersion of the numerical scheme the calculations error on it does not collect, that allows to count non-stationary processes on the big intervals of time corresponding 300 … 500 run of an electromagnetic wave on length of line up to reception of the established mode. Thus parameters of loadings can suddenly vary, modelling, for example, emergencies of type short circuit (SC) or rupture of line.

The method of final differences "Albatross" is based on the known cable equations of long line which well describe processes in two-wire, multiwire and coaxial lines. These structures are most widely used in practice as longitudinal-regular directing structures in which energy extends in the form of cross-section electromagnetic waves (T-waves). As is known, the field T - waves in transversal section coincides with stationary field in the same structure, and currents in conductors proceed only in longitudinal direction (conductivity currents). Therefore at the features analysis of electric processes course in long line voltage u and current intensity in conductor i can be considered as independent variables and to carry out the analysis of voltage and currents "waves" in line on the basis of the cable equations [8-10]:

$$L\frac{\partial i}{\partial t}+\frac{\partial u}{\partial x}+Ri=0;\quad C\frac{\partial u}{\partial t}+\frac{\partial i}{\partial x}+Gu=0 \qquad (1)$$

where L, C, R, G - longitudinal inductance, capacity, active resistance and conductivity of insulation.

At the analysis of these processes it is expedient to use system of dimensionless sizes that allows to obtain the generalised data about processes course in long lines in not dependences on frequency of current (50 or 60 Hz). The considered problem belongs to the class of mathematical physics problems with initial-boundary conditions. At the solution of such problems transition to dimensionless (normalized) sizes is carried out under formulas:

$$u = \frac{u^o}{U^o}; \quad i = \frac{i^o Z_B^o}{U^o}; \quad t = \frac{t^o}{\Delta^o}; \quad x = \frac{x^o}{\lambda^o};$$

$$R = \frac{R^o \lambda^o}{Z_B^o}; \quad R_S = \frac{R_S^o}{Z_B^o}; \quad G = G^o \lambda^o Z_B^o; \qquad (2)$$

$$Z_B^o = \sqrt{L^o / C^o}; \quad a^o = 1/\sqrt{L^o C^o}, \quad z = \frac{R_S^0 - Z_B^0}{R_S^0 + Z_B^0}$$

where U - some rated voltage; Z_B - wave resistance of ideal line; R_S -resistance of loading; λ = a/f - wave length on frequency of chain power supplies source;

Δ - wave transit time on length of line equal λ: $\Delta = \lambda / a$; a - speed of electromagnetic indignations distribution along a line; the degree mark is present at dimensional sizes.

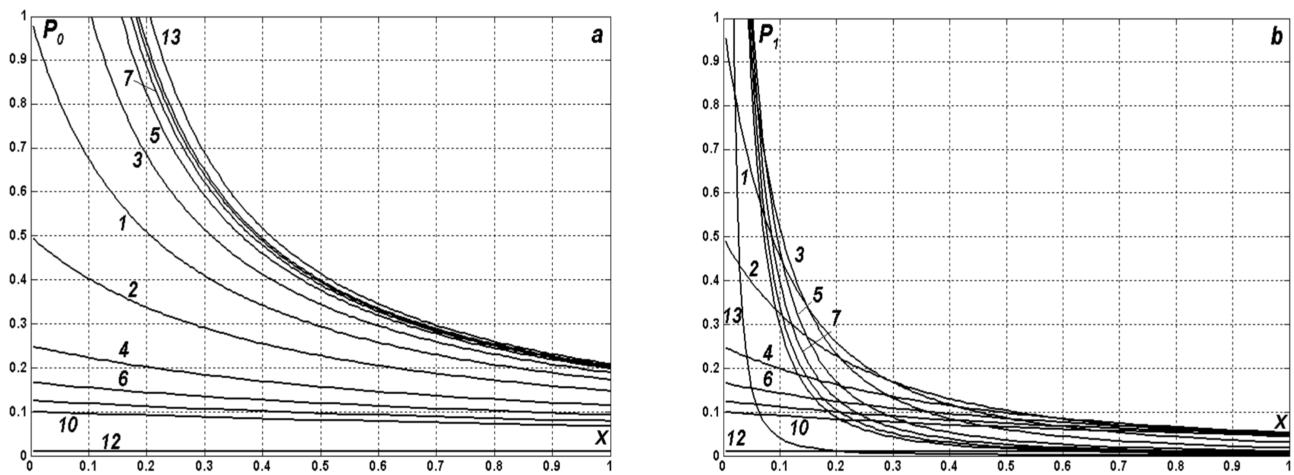

Fig. 1. Dependence of generated (a) and transferred (b) powers from length of line at various resistance of loading: R_S = 1 (1); 2 (2); 1/2 (3); 4 (4); 1/4 (5); 6 (6); 1/6 (7); 8 (8); 1/8 (9); 10 (10); 1/10 (11); 100 (12); 1/100 (13) and R = 4.8, G = 0

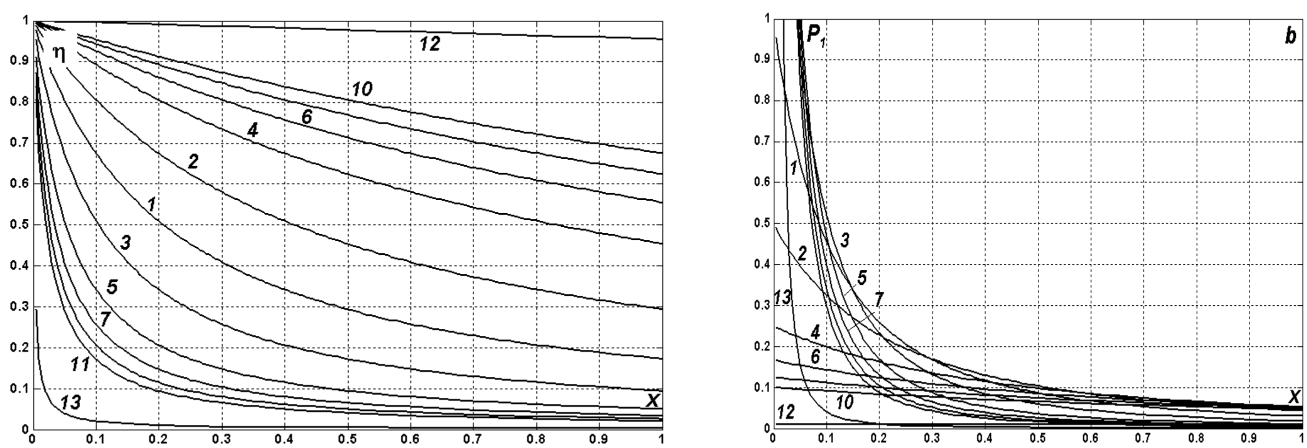

Fig. 2. Dependence of EFFICIENCY on length of a line at various resistance of loading: RS = 1 (1); 2 (2); 1/2 (3); 4 (4); 1/4 (5); 6 (6); 1/6 (7); 8 (8); 1/8 (9); 10 (10); 1/10 (11); 100 (12); 1/100 (13) at R = 4.8, G=0 (a) and G = R/5 (b).

4. Features of a long lines mode

4.1. A direct current line

Let a homogeneous line of length *l*, having longitudinal parameters: $R > 0$; $G = 0$, it is connected to a source of direct voltage: $u = U_0$, and its reception end will close on purely active loading with resistance $Z_S = R_S$. In this case as voltage generator internal resistance we used full line resistance: $R_g = lR$. In the given chain the condition of maximum power transfer P_1 in loading R_S is known, i.e. $R_S = lR$ [11].

Results of the parametrical analysis show (fig. 1), that function of generator power $P_0(x)$ reaches limiting values in mode close to SC at $R_S \to 0$, whereas maxima of loading power function $P_1(x)$ obviously depend on length of line *x*.

The efficiency of direct current line monotonously decreases with increase in length of line and losses in it (fig. 2), and in case of losses in insulation decrease in value of line EFFICIENCY with growth of its length is expressed more strongly.

4.2. An alternating current line

Let's consider instant inclusion on alternating voltage of not charged line (u = i = 0 at t = 0), loaded on concentrated resistance RS:

$$u = U_0(t) \quad \text{at } x = 0,\ t > 0;$$
$$u = R_S \quad \text{at } x = l,\ t > 0. \qquad (3)$$

It is obvious, that at $R_S = 0$ we receive a short circuit mode: $u = 0$, and condition $R_S = \infty$ corresponds to line in idling mode (IM): $i = 0$ (loading is disconnected). Similar degenerated loadings (IM or SC) in practice meet rather seldom, however their studying represents doubtless interest as an initial step at transition to real (non-degenerated) loading modes.

Let the electric chain (fig. 3) joins during the initial moment of time t = 0 an external source of voltage:

$u = u_0(t)$ at $x = 0$,

and its end will close on RLC - loading:

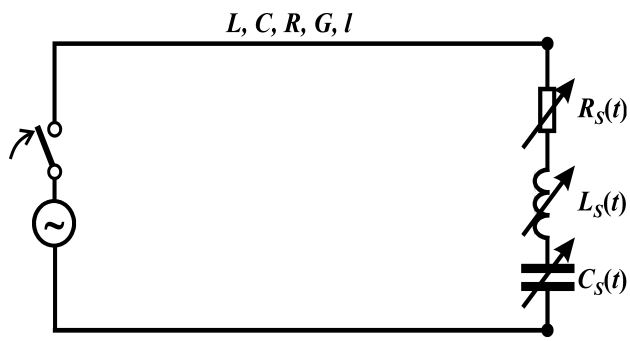

Fig. 3. Alternating voltage line with RLC-loading on the end.

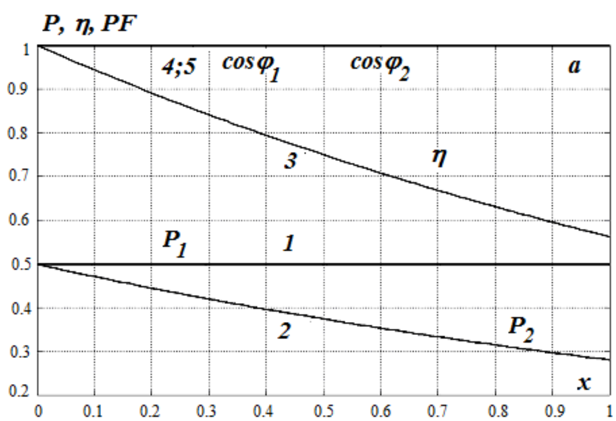

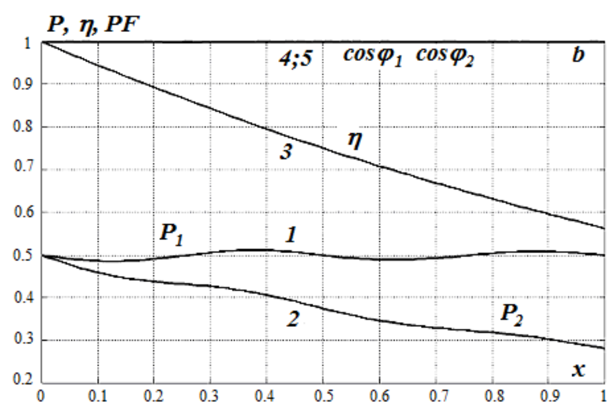

Fig. 4. Dependence of generated and transferred power, EFFICIENCY and PF of source and receiver from line length x at $Z_S = Z_0$ (a); Z_B (b); R = 0.48; G = R/5.

$$u = R_S i + L_S \frac{di}{dt} + \frac{1}{C_S}\int_0^t i(\tau)d\tau \quad \text{at } x = l.$$

It is obvious, that at $R_S = L_S = 0$, $C_S = \infty$ we receive a short circuit mode: $u = 0$, and condition

$R_S = \infty$ corresponds to line idling: i =0 (loading is disconnected).

At sinusoidal voltage $u = U_0 \sin(2\pi ft)$ power rating value we defined from relation $P = \frac{U_0^2}{2Z_B}$ in dimensional or $P = \frac{1}{2}$ in dimensionless kind. At constant value of variable voltage amplitude on line input: $U_m = const = U_0$ we received $P = \frac{U_0^2}{Z_B}$ or $P = 1$

On fig. 4 change of average (dimensionless) values of generated and transferred power (curves 1; 2), EFFICIENCY (3), power factor (PF) ($\cos\varphi$) of source and receiver (4; 5) is shown depending on line length x at $Z_S = Z_0$ (a); Z_B (b); $R = 0.48$, G=R/5, where Z_0-complex wave resistance at which the line works in mode of running waves; Z_B - wave resistance at which the line works in mode of the mixed waves and which is purely active resistance.

Apparently from schedules with increase of line length transferred power and EFFICIENCY monotonously decrease, and generated power remains practically invariable, testing only insignificant (within 1 … 3 %) fluctuation at Z_S = Z_B.

On fig. 5 dependence of investigated values on line length x is presented at Z_S = $Z_B + j\omega L_S$ (a); $Z_B - j/(\omega C_S)$ (b); L_S =1/8 (0.66 H); C_S =1/5 (15.23 mkF); R = 0.48; G = R/5**.** Presence of reactive elements in loading resistance leads to sharp change of chain entrance resistance and as consequence all values characterising process of power transfer by alternating current test fluctuations for tens percent. For a half-wave line transferred power and EFFICIENCY are maximum, when loading on its reception end purely active. In case of line with losses (fig. 5b) wavy character of power given by the generator in network is similar as for line lost-free.

With increase of line length, power function of the generator aspires to the established value at increase of longitudinal transversal active resistance of this line faster. Thereof there is an easing of scale factor influence on process of transfer to line of active power by generator.

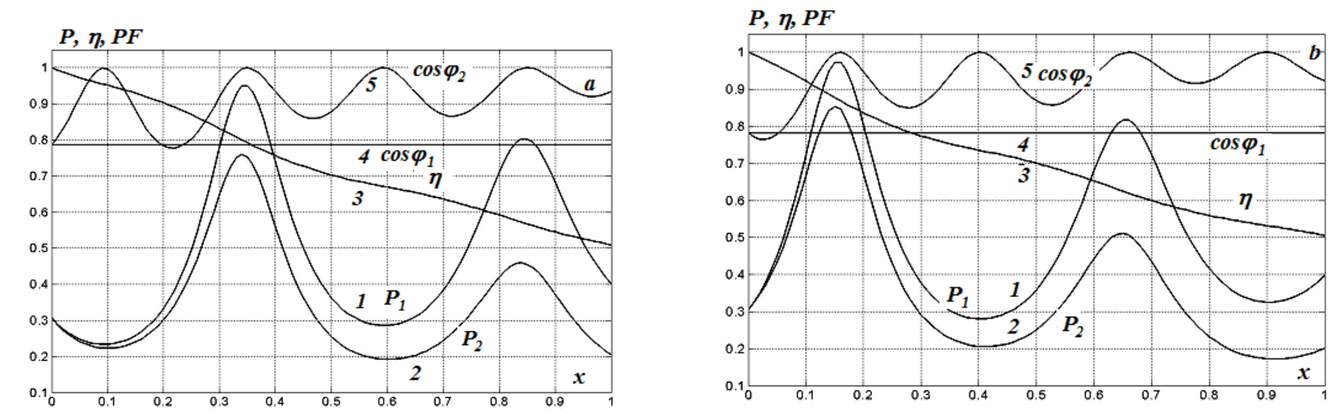

Fig. 5. Dependence of generated and transferred power, EFFICIENCY and PF of source and receiver from line length x at $Z_S = Z_B + j\omega L_S$ (a); $Z_B - j/(\omega C_S)$ (b); L_S =1/8; C_S =1/5; R = 0.48; G = R/5.

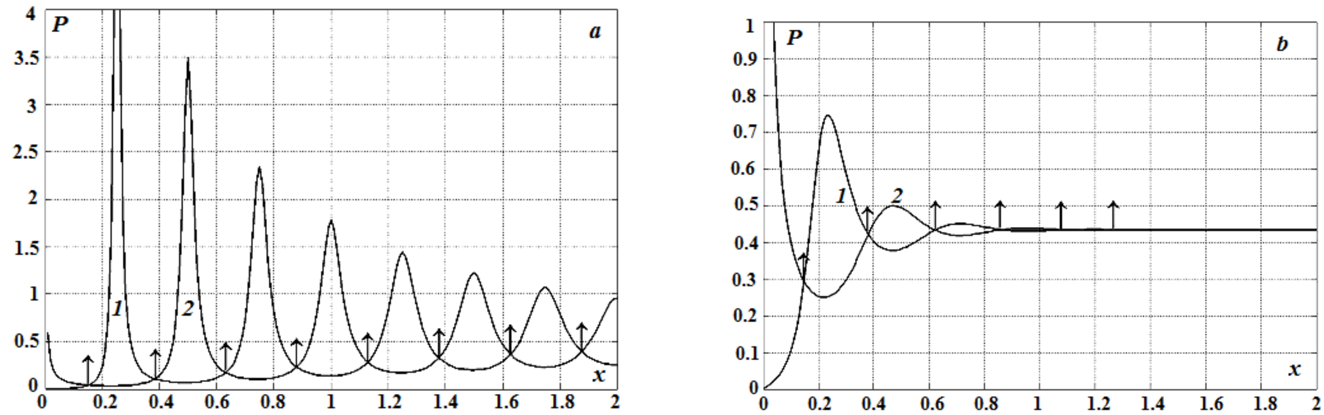

$l_1 = 0.1517, l_2 = 0.3859, l_3 = 0.6317, l_4 = 0.8798, l_5 = 1.1287, l_6 = 1.3780, l_7 = 1.6275, l_8 = 1.8772$ $l_1 = 0.1481, l_2 = 0.3809, l_3 = 0.6211, l_4 = 0.8619, l_5 = 1.1027, l_6 = 1.3434, l_7 = 1.5842, l_8 = 1.8250$

Fig. 6. Dependence of generator power P_0 on line length x in IM (1) and SC mode (2) at R = 0.48 (a); R = 4.8 (b); G = R/5.

Research of generator power change given to lines in IM and SC mode shows, that there are special points (length of line) for which this power is identical on value both to IM and SC mode in the given section (fig. 6 - special points are designated by arrows).

Growth of longitudinal active resistance R reduces number of such points. Generator active power function $P_0(x)$ connected to line, for this condition reaches faster the established value at line length increase. Hence, for generator instant power amplitude condition $P_{02}(x) < P_{01}(x)$ for $R_2 > R_1$, where R_1, R_2 - running resistance of long line (fig. 6) is satisfied.

It is established also, that in a vicinity of line special points active longitudinal resistance does not influence value of power given to lines by generator. For example, at increase in longitudinal active resistance from 0.48 to 4.8 relative units for the line lengths defined by co-ordinates of special points placement, identical values of generator active power connected to such line are received.

Unlike of direct voltage line where idling generator power always is less, than at short circuit, here we have on 4 points of crossing of these curves on each piece of length of the line, equal to λ. Co-ordinates of these points on line length are next: $l_1 = 0.1481$; $l_2 = 0.3809$; $l_3 = 0.6211$; $l_4 = 0.8619$; $l_5 = 1.1027$; $l_6 = 1.3434$; $l_7 = 1.5842$; $l_8 = 1.825$.

The parametrical analysis of electric energy transfer processes on line length has shown in the electric plan, that the transmission line is non-uniform object. Generator working conditions in the line beginning depends on many factors: line wave length, loading connection point, loading character and devices for reactive power compensation, the connection scheme of compensating device, transformers for voltage increase and-or drop in line, schemes of loading connection to line and both in any points and special points of long line.

As an example on fig. 7 the equivalent circuit of long line with indication of special points of loadings connection, compensating devices and transformers providing transfer of the greatest power in loading is shown.

For any not deforming line: $RC = GL$ generators powers at IM and SC mode coincide in points x = λ/8, 3 λ/8, 5 λ/8 etc. If $RC > GL$ owing to diffraction of waves these curves are displaced little to the right: x = 0.15 λ, 0.386 λ, 0.63 λ. From here follows, that the maximum selection power from alternating voltage line on site:

$0.15\lambda \le x \le 0.386\lambda$ it is possible in a mode close to IM, and on sites:

$0 < x \le 0.15\lambda$ and $0.386\lambda \le x \le 0.63\lambda$ in a mode close to SC. Such situation repeats through each pieces of length the lines equal approximately λ/4.

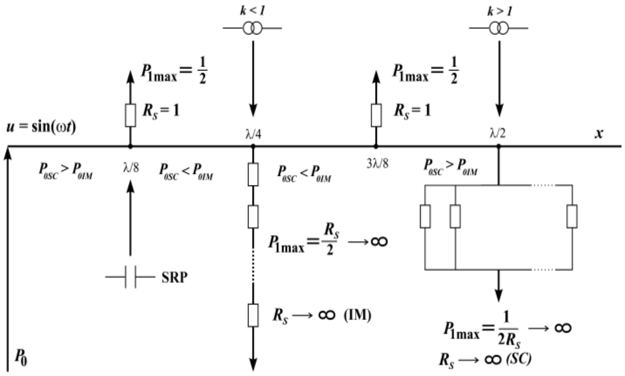

Fig.7. The special points of a long line and suggested technical solutions to incorporate compensating devices, transformers and loads to the line.

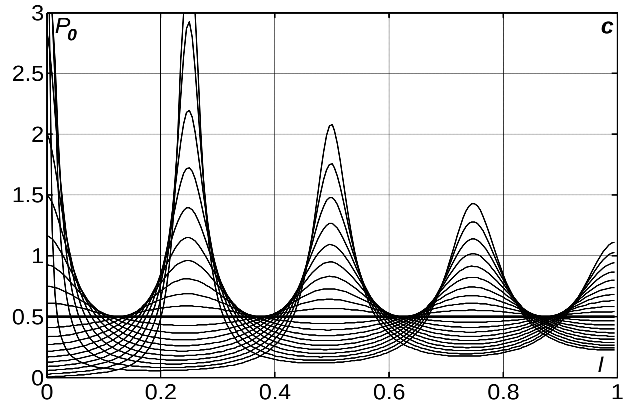

Fig. 8. Character of active power change on input of line with losses in function from its length at co-ordinated loadings.

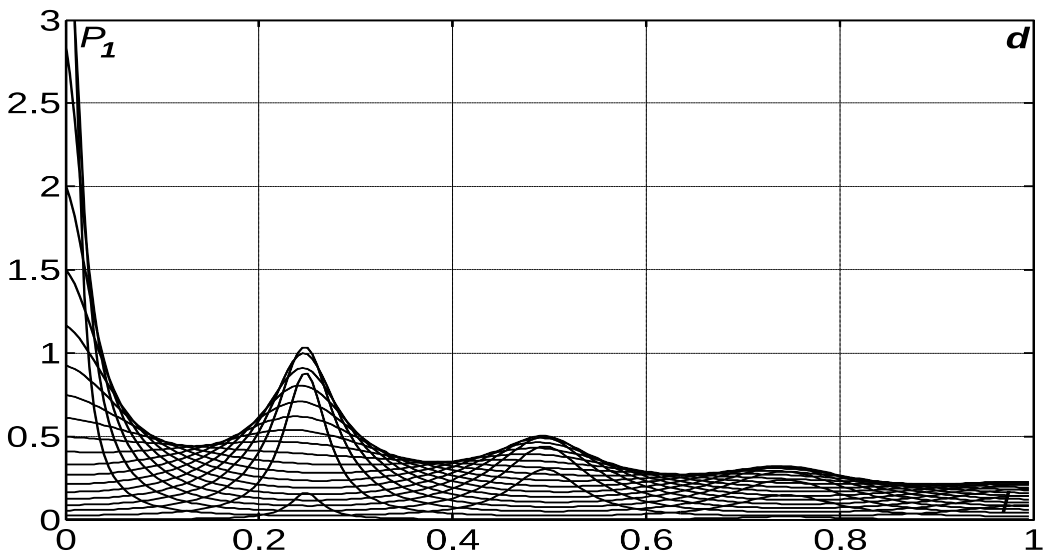

Fig. 9. Character of active power change (transit) on the line end with losses in function from its length at co-ordinated loading

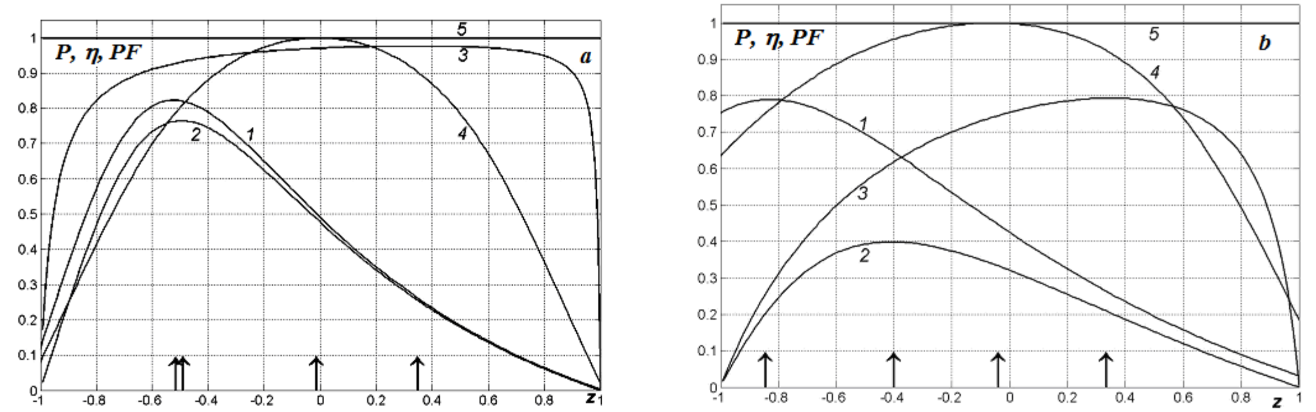

Fig. 10. Dependence of generated and transferred power, EFFICIENCY and PF of source and receiver on resistance of loading R_S at l = 0.0516; R = 0.48 (a); 4.8 (b); G = R/5; $Z_S = R_S$, where 1 - P_1; 2 - P_2; 3 – η; 4 – $\cos\varphi_1$; 5 – $\cos\varphi_2$

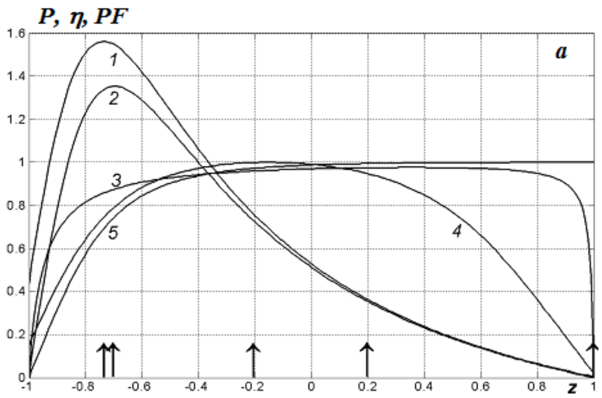

Fig. 11. Dependence on resistance loadings R_S of generated (1) and transferred powers (2), EFFICIENCY (3) and PF source (4) and the receiver (5) at l = 0.0516; R = 0.48; G = R/5; $Z_S = R_S - j/(\omega C_S)$;C_S =1

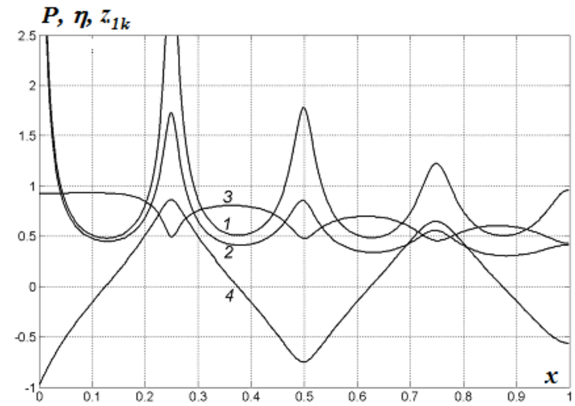

Fig. 12. Dependence on line length x of generated (1), maximum transferred (2) powers EFFICIENCY (3) and critical resistance z_{1k} (4) at R = 0.48; G = R/5.

On fig. 8 and 9 the generalised data about character of power change on input and output ends of line with losses (at various losses) in case of the co-ordinated loading are presented.

It is necessary to notice, that though line losses influence value of transferred power, but there are such points in line for which influence of line losses on value of the power transferred in loading does not come to light. Such modes are possible both in relatively short lines, and in lines comparable with wave length.

On fig. 10 change of generated and transferred power, EFFICIENCY and PF of source and receiver (curves 1-5) depending on parameter *z* is presented at l = 0.0516; R = 0.48 (*a*); 4.8 (*b*); G = R/5; $Z_S = R_S$. These schedules visually illustrate that fact, that maxima of all functions investigated here are reached at various values of loading resistance R_S. With increase in line losses it is observed «run up» of critical resistance for generated and transferred power whereas points of maximum for EFFICIENCY and PF remain practically motionless. Thus, at variation of parameter R_S for any piece of line length it is possible to receive full representation about power overflows that allows to choose an optimum mode of line proceeding from those or other criteria.

The Fig. 11 illustrates dependence of generated and transferred power, EFFICIENCY and PF of source and receiver on parameter *z* at $Z_S = R_S - j/(\omega C_S)$; C_S =1 (17.57mkF)**.** Longitudinal active resistance and active conductivity of line in relative units have values: $R = 0.48$, G = R/5. Longitudinal compensation of loading parameters for this line length increases the maximum transferred power, but reduces EFFICIENCY and $\cos\varphi$.

On fig. 12 dependence of generated and maximum transferred power, EFFICIENCY and critical resistance z_{1k} from line length (curves 1-4) is shown**.**

The increase (reduction) of transferred power in process of change of line length always is accompanied by reduction (increase) in EFFICIENCY. For a quarter wave line the power maximum takes place in mode close to IM (R_S = 13.93 Z_B), and for a half-wave line in mode close to SC (R_S = 0.14 Z_B).

Conclusions

1. Within the frame of the tendency of regional and inter-regional power systems development the urgency of working out of effective methods of modes research in such chains repeatedly increases. Research of influence of various factors what line and loading parameters, waves dissipation and dispersion are on power losses

allows to develop measures on efficiency increase of ETL functioning as a part of regional power connections.

2. The most significant influencing parameter on mode of power transfer on long lines is its length.
3. It is necessary to distinguish line operating modes at the maximum transferred power, EFFICIENCY, PF and the maximum return of energy by the generator of sinusoidal voltage in the given line.
4. Researches in the given direction has not only the scientific importance, but also practical as it is possible is proved to develop the most rational ways of energy transmission on high voltage lines and to solve others problems from area of diagnostics, coordination of insulation, calculation of losses, as in stationary, and non-stationary (transitive) modes.

References

1. In Portugal the world's largest solar power station has opened. http://www.membrana.ru/lenta/index.html?7077.
2. Arizona builds the largest solar power station on the Earth. http://www.membrana.ru/lenta/index.html?8014.
3. Energy from Sahara will "shine" the world. http://www.ecomagazin.ro/energia-din-sahara-va-%e2%80%9elumina%e2%80%9c-lumea-2/
4. Covaleov G.F., Lebedeva L.M. Planetary electropower system. Energy, 2006, №9 p.p. 27-34/ http://courier.com.ru/energy/en0906kovalev.htm.
5. Alexandrov G.N., Le Thani Bak. Reduction of power losses in long transmission lines with controlled reactors. -Electricity, 2007, №3, p.p. 8-15.
6. Vershkov V.A., Nahapetean K.T., Olishevschii O.V., Sovalov S.A., Fotin V.P., Scerbakov V.K. Complex tests of half-wave electricity transmission in 500 кV network of the European part of the USSR.- Electricity, 1968, №8, p.p.10-16.
7. Ziliberman S.M., Samorodov G.I. Possible prospects of electric power import in Republic Moldova from the Tyumen region. Conference works «Power of Moldova 2005», Kishinev: 2005, Printing house of ASM, p.p.104-110.
8. Rimschii V.X., Berzan V. P, Patsyuk V. I, Karcheva N.F., Andros I.V. The wave phenomena in non-uniform lines. Volume 4. Parametrical chains / AS of Moldova. Institute of power. Chisinau: Print house of ASM, 2008.-552p.
9. Rimschii V.X., Berzan V. P, Tirsu M. S. The wave phenomena in non-uniform lines. Vol.1. The theory of potential and current waves distribution. Under edition Rimschii V.X. - Chisinau: Printing house of ASM, 1997. – 298p.
10. Rimschii v.X., Berzan V. P, Patsyuk V. I, etc. How to increase transferred capacity in tens times. – Chisinau: Print house of ASM, 2007. – 178p.
11. Bessonov L.A.. Theoretical bases of electrical engineers. Electric chains /Textbook for The higher technical educational institutions. - M: the Higher school, 1984. – 559p.

О некоторых особенностях режима передачи мощности по длинной линии электропередачи

Berzan V.P., Rimschi V.X., Tirsu M.S., Patsyuk V.I., Uzun M.N.

Институт энергетики Академии наук Молдовы

E-mail: berzan@ie.asm.md

Аннотация. Рассматриваются особенности передачи электрической энергии по длинным линиям, процессы в которых описываются телеграфными уравнениями в системе безразмерных единиц. Граничные условия задаются в виде дифференциально-интегральных уравнений. Использование относительного параметра нагрузки z, позволил получить обобщенные данные о режиме работы длинной линии при изменении ее нагрузки R_S в пределах $-\infty < R_S < +\infty$.

При исследовании режимов длинной линии использован численный метод в конечных разностях, названный авторами метод «Альбатрос». Метод обладает однородной структурой и осуществляет сквозной счет разрывных решений. Фронты волн и другие скачки значений искомых параметров выделяются автоматически и представляются в виде мест больших градиентов волнового поля.

Исследованы режимы передачи мощности в зависимости от значений погонных параметров линии, ее длины и характера нагрузки. Показано, что в электрическом плане длинная линия является неоднородным объектом, который характеризуется особыми точками касательно условий передачи максимальной мощности в нагрузку. Расположение этих точек зависит как от длины электромагнитной волны, так и от параметров потерь линии. В особых точках линий переменного тока активная мощность на ее входе (генераторная) одинакова по значению как в режиме холостого хода (ХХ), так и в режиме короткого замыкания (КЗ) в данной, особой, точки линии.

Длина линии наиболее сильно влияет на режим передачи мощности. Следует различать режимы работы линии при максимальной передаваемой мощности, максимальном значении коэффициента полезного действия (КПД), максимальном значении коэффициента мощности (КМ) и максимальной инжекции энергии в линии генератором синусоидального напряжения.

Представлены характеристики изменения мощностей в начале и в конце линии, коэффициента мощности, коэффициента полезного действия ЛЭП, токов в зависимости от длины, параметров линии и параметров нагрузки.

Ключевые слова: длинная линия, режим, передаваемая мощность.

1. Введение

В настоящее время происходят новые качественные изменения в технике обеспечения энергией, в частности, из-за увеличения доли возобновляемой энергии в балансе потребления. Проблема более широкого вовлечения возобновляемой энергии потребует нового подхода в организации производства и транспорта электрической энергии, поскольку необходимо обеспечить постоянный баланс между производством и потреблением, например, за счет параллельной работы солнечных электростанций, расположенных в различных часовых и климатических поясах.

Возможность производство в больших количествах электроэнергии солнечными электростанциями подтверждается накопленным опытом в этой области. Например, в Португалии (2007 г.) открылась самая мощная в мире солнечная электростанция [1], установленной мощностью 11 МВт. Солнечные PV модули занимают площадь в 60 га. Известны и другие проекты таких электростанций, например, планируемый к реализации в США (штат Аризона) проект, предусматривает строительство и пуск в 2011 г. солнечной электростанции мощностью 280 МВт [2], а также предложение о строительстве солнечной электростанции в пустыне Сахара в Африке [3]. В рамках последнего проекта, мощность источник генерации составит 100 ГВт.

Надежное и устойчивое энергоснабжение при увеличении доли генерации на основе возобновляемых источников энергии возможно при реализации концепции планетарной электроэнергетической системы [4].

Тенденция увеличения мощности источников генерации и дальности передачи электрической энергии характерна для всего периода развития электроэнергетики. Например, напряжение электрических линий увеличилось с 1,5—2 кВ (1882 г.) до 1150 кВ в настоящее время, а расстояние передачи электрической энергии с 57 км до 1500 км и более [1-3, 5-7]. Количественные изменения в структуре, в схемах передачи и распределения электрической энергии сопровождаются и возникновением новых научно-технических проблем, которые не характерны для малоразмерных электроэнергетических систем.

В консолидированных региональных электроэнергетических системах расстояния передачи мощности будут соизмеримы с длинной электромагнитной волны, а при таких размерностях актуальными будут проблемы эффективности и надежности функционирования как системы в целом, так и ее отдельных компонент. Поэтому изучение особенностей передачи электрической мощности на дальние расстояния представляет не только теоретический интерес, но представляет интерес и для практической электроэнергетики.

2. Постановка задачи

Создание больших энергосистем с протяжными электрическими линиями, например, в рамках проекта Запад-Восток, энергетического кольца вокруг Черного моря (региональное объединение энергосистем) или в случае транзита электрической энергии от солнечной электростанции из Сахары в Европу [3] требует более глубокого исследования особенностей передачи энергии на большие расстояния. Кроме того, при создании энергетических коридоров не исключено использование новых технических решений, например таких, как сверхпроводящие ЛЭП или отдельных участков электропередачи на основе эффекта сверхпроводимости, что повлияет на режимы работ таких неоднородных линий.

Количественные изменения в структуре электроэнергетических систем (ЭЭС) порождают ряд вопросов, на которых в настоящее время нет ясных и четких ответов, например таких как:

1. Насколько точны современные методы анализа процессов в длинных линиях и есть ли границы их применимости, например в случае линии без потерь.

2. При каких условиях можно обеспечить наибольшую передаваемую мощность, наибольшее значение КПД линии, в том числе и при компенсации реактивных составляющих нагрузки и линии.
3. Как влияет неоднородность линии, ее длина и значения погонных параметров на характеристики передачи электрической мощности при нормальных и аварийных режимах.

Задача данной работы состоит в анализе влияния масштабного (линейного) и параметрических факторов на эффективность передачи электрической мощности на большие расстояния.

3. Метод исследования

Неоднородность длинных линий и зависимость режима передачи энергии, как от параметров нагрузки, так и от параметров самой линии являются усложняющими факторами при исследовании особенностей их работы в составе ЭЭС.

При анализе особенностей функционирования длинных электрических линий, например, в составе региональных ЭЭС, воспользуемся телеграфными уравнениями.

При анализе будем исходить из положения, что любому установившемуся режиму всегда предшествует нестационарный волновой процесс. Наиболее удобными инструментами для решения задачи в такой постановке являются на наш взгляд метод характеристик и метод конечных разностей «Альбатрос» [8]. Разностная численная схема «Альбатрос» предложена и строго обоснована Институтом энергетики АНМ. Используя этот подход можно легко и просто решать телеграфные уравнения для неоднородных линий и цепей с произвольными потерями, точками ветвления, несколькими генераторными и нагрузочными узлами и другими усложняющими факторами [8].

В методе характеристик необходимо априори выделять и отслеживать конфигурацию волновых фронтов (сильных разрывов), которые значительно усложняются с течением времени. Поэтому метод характеристик целесообразно использовать, в основном, для тестовых расчетов идеальных и неискажающих линий с целью контроля точности численных решений. Метод конечных разностей «Альбатрос» обладает однородной структурой и осуществляет сквозной счет разрывных решений, где фронты волн и другие скачки выделяются автоматически и представляются в виде мест больших градиентов волнового поля. Именно это неоспоримое преимущество, в сочетании с практически абсолютной точностью, позволяет осуществить расчет переходных и установившихся процессов по единообразным формулам типа предиктор–корректор с учетом различного рода неоднородностей без излишней физической и геометрической идеализации исследуемых электрических систем и устройств [8-10].

Благодаря консервативности, нулевой разностной диссипации и минимальной дисперсии численной схемы ошибка вычислений по ней не накапливается, что позволяет рассчитывать нестационарные процессы на больших интервалах времени, соответствующих 300…500 пробегов электромагнитной волны по длине линии вплоть до получения установившегося режима. При этом параметры нагрузок могут внезапно меняться, моделируя, к примеру, аварийные ситуации типа КЗ или разрыва линии.

Метод конечных разностей «Альбатрос» базируется на известных телеграфных уравнениях длинной линии, которые хорошо описывают процессы в двухпроводных, многопроводных и коаксиальных линиях. Эти структуры наиболее широко используются на практике в качестве продольно-регулярных направляющих структур, в которых энергия распространяется в виде поперечных электромагнитных волн (Т-волны). Как известно, поле Т- волны в поперечном сечении совпадает со стационарным полем в той же структуре, а токи в проводниках протекают только в продольном направлении (токи проводимости). Поэтому при анализе особенностей протекания электрических процессов в длинной линии напряжение u и силу тока в проводнике i можно рассматривать в качестве независимых переменных и проводить анализ “волн” напряжений и токов в линии на основе телеграфных уравнений [8-10]:

$$L\frac{\partial i}{\partial t}+\frac{\partial u}{\partial x}+Ri=0;\; C\frac{\partial u}{\partial t}+\frac{\partial i}{\partial x}+Gu=0, \qquad (1)$$

где L, C, R, G – погонные индуктивности, емкости, активные сопротивления и проводимости изоляции.

При анализе этих процессов целесообразно использовать систему безразмерных величин, что позволяет получать обобщенные данные о протекание процессов в длинных линиях в не зависимости от частоты тока (50 или 60 Гц). Рассматриваемая задача относится к классу задач математической физике с начально-краевыми условиями. При решении таких задач переход к безразмерным (нормированным) величинам осуществляется по формулам:

$$u=\frac{u^o}{U^o};\quad i=\frac{i^o Z_B^o}{U^o};\quad t=\frac{t^o}{\Delta^o};$$

$$R=\frac{R^o\lambda^o}{Z_B^o}\quad x=\frac{x^o}{\lambda^o};\; R_S=\frac{R_S^o}{Z_B^o}; \qquad (2)$$

$$G=G^o\lambda^o Z_B^o;\; Z_B^o=\sqrt{L^o/C^o};$$

$$a^o=1/\sqrt{L^oC^o}\;;\; z=\frac{R_S^o-Z_B^o}{R_S^o+Z_B^o},$$

где U – некоторое номинальное напряжение; Z_B – волновое сопротивление идеальной линии; R_S -сопротивление нагрузки; λ = a/f – длина волны на частоте источника электропитания цепи; Δ – время пробега волны по длине линии, равной λ: $\Delta = \lambda/a$; a – скорость распространения электромагнитных возмущений вдоль линии; значок градуса присутствует у размерных величин.

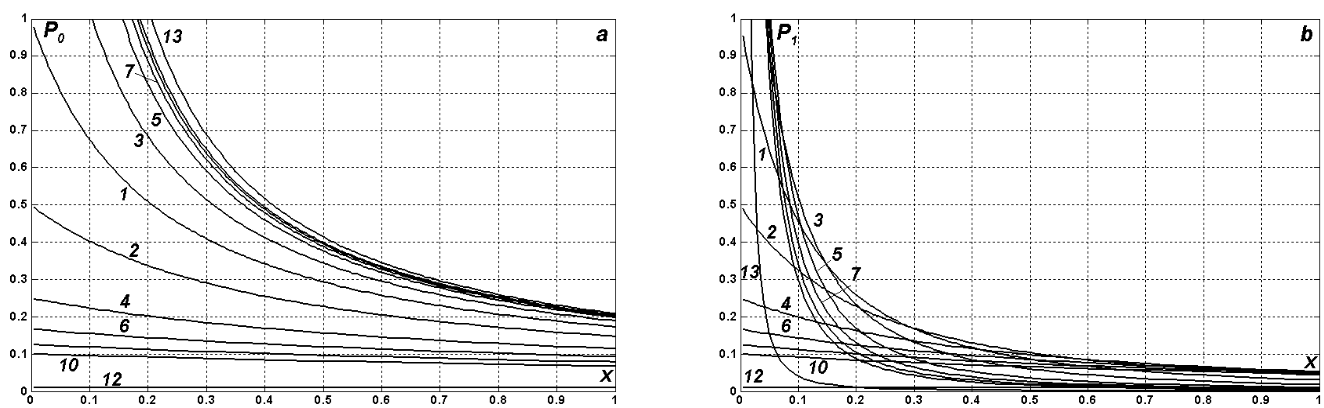

Рис.1. Зависимость генерируемой (a) и передаваемой (b) мощности от длины линии при различных сопротивлениях нагрузки: R_S = 1 (1); 2(2); 1/2 (3); 4 (4); 1/4 (5); 6 (6); 1/6 (7); 8 (8); 1/8 (9); 10 (10); 1/10 (11); 100 (12); 1/100 (13) и R = 4.8, G = 0

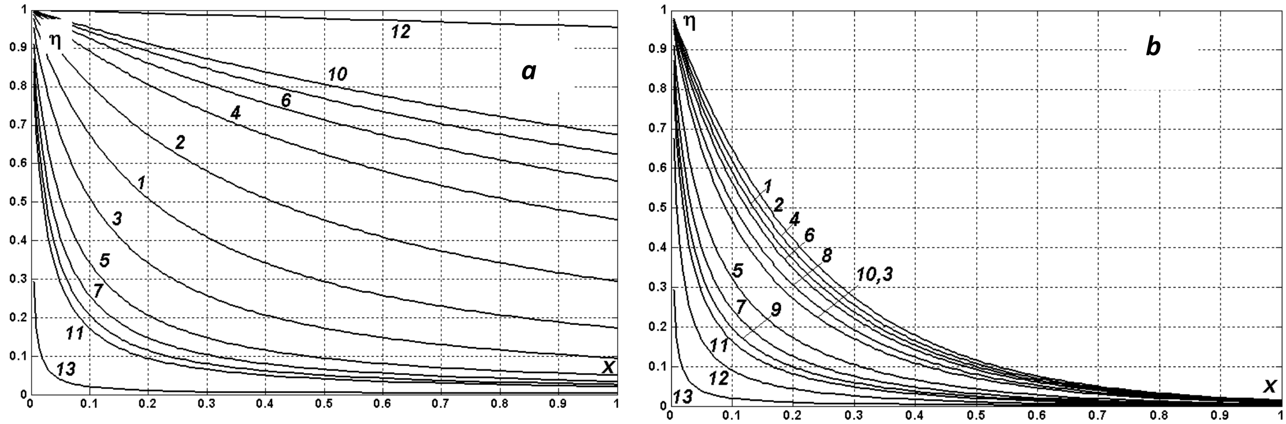

Рис.2. Зависимость КПД от длины линии при различных сопротивлениях нагрузки: R_S = 1 (1); 2(2); 1/2 (3); 4 (4); 1/4 (5); 6 (6); 1/6 (7); 8 (8); 1/8 (9); 10 (10); 1/10 (11); 100 (12); 1/100 (13) при R = 4.8, G=0 (a) и G = R/5(b)

4. Особенности режима длинных линий

4.1.Линия постоянного тока

Пусть однородная линия длиной l, имеющая погонные параметры: R >0; G = 0, подключена к источнику постоянного напряжения: $u = U_0$, а ее приемный конец замкнут на чисто активную нагрузку с сопротивлением $Z_S = R_S$. В этом случае в качестве внутреннего сопротивления генератора напряжения используем полное сопротивление линии: $R_g = lR$. В данной цепи условие передачи максимальной мощности P_1 в нагрузку R_S известно, т.е. $R_S = lR$ [11].

Результаты параметрического анализа показывают (рис.1), что функция мощности генератора $P_0(x)$ достигает предельных значений в режиме, близком к КЗ при $R_S \to 0$, тогда как максимумы функции мощности нагрузки $P_1(x)$ явно зависят от длины линии x.

Коэффициент полезного действия линии постоянного тока монотонно убывает с увеличением длины линии и потерь в ней (рис. 2), причем в случае потерь в изоляции снижение значения КПД линии с ростом ее длины проявляется более сильно.

4.2. Линия переменного тока

Рассмотрим мгновенное включение на переменное напряжение незаряженной линии ($u = i = 0$ при $t = 0$), нагруженной на сосредоточенное сопротивление R_S :

$u = U_0(t)$ при $x = 0$, $t > 0$;

$$u = R_S i \quad \text{при} \quad x = l,\ t > 0. \qquad (3)$$

Очевидно, что при $R_S = 0$ получаем режим короткого замыкания: $u = 0$, а условие $R_S = \infty$ соответствует холостому ходу линии: $i = 0$ (нагрузка отключена). Подобные вырожденные нагрузки (ХХ или КЗ) на практике встречаются сравнительно редко, однако их изучение представляет несомненный интерес как исходная ступень при переходе к реальным (невырожденным) нагрузочным режимам.

Пусть электрическая цепь (рис.3) присоединяется в начальный момент времени $t = 0$ к внешнему источнику напряжения

$u = u_0(t)$ при $x = 0$,

а ее конец замкнут на RLC – нагрузку:

$$u = R_s i + L_s \frac{di}{dt} + \frac{1}{C_s}\int_0^t i(\tau)\,d\tau \ \text{при}\ x = l\,.$$

Очевидно, что при $R_S = L_S = 0$, $C_S = \infty$ получаем режим короткого замыкания: $u = 0$, а условие $R_S = \infty$ соответствует холостому ходу линии: $i = 0$ (нагрузка отключена).

При синусоидальном напряжении $u = U_0 \sin(2\pi f t)$ номинальное значение мощности определяем из соотношения $P = \dfrac{U_0^2}{2Z_B}$ в размерном или $P = \frac{1}{2}$ в безразмерном виде. При постоянном значении амплитуды переменного напряжении на входе линии: $U_m = const = U_0$ получаем $P = \frac{U_0^2}{Z_B}$ или $P = 1$.

На рис. 4 показано изменение средних (безразмерных) значений генерируемой и передаваемой мощности (кривые 1;2), КПД (3), КМ ($\cos\varphi$) источника и приемника (4;5) в зависимости от длины линии *x* при $Z_S = Z_0$ (*a*); Z_B (*b*); $R = 0.48$, *G*=*R*/5, где Z_0 –комплексное волновое сопротивление, при котором линия работает в режиме бегущих волн; Z_B - волновое сопротивление, при котором линия работает в режиме смешанных волн и которое является чисто активным сопротивлением.

Как видно из графиков с увеличением длины линии передаваемая мощность и КПД монотонно убывают, а генерируемая мощность остается практически неизменной, испытывая лишь незначительные (в пределах 1…3 %) флуктуации при $Z_S = Z_B$.

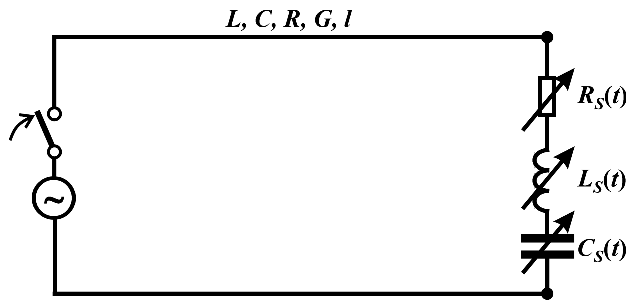

Рис 3. Линия переменного напряжения с RLC–нагрузкой на конце

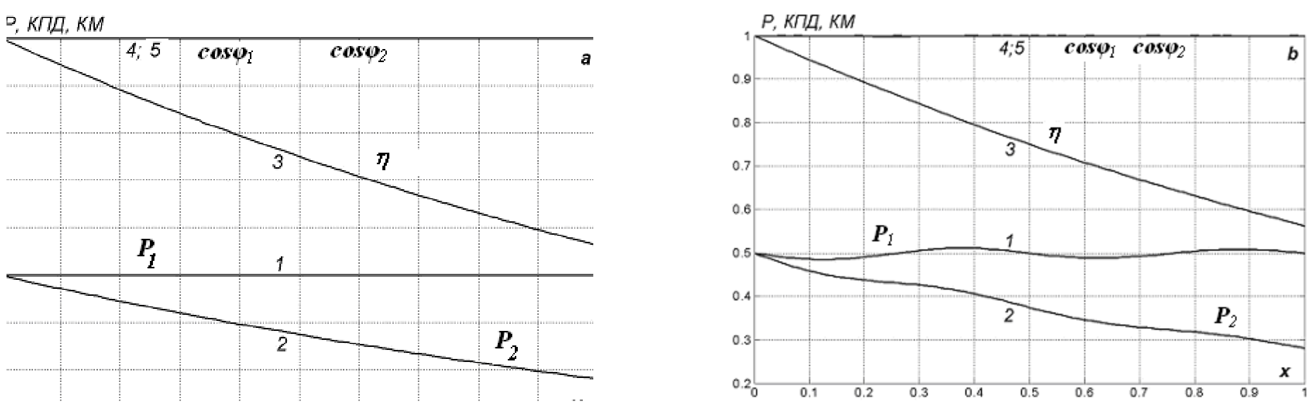

Рис. 4. Зависимость генерируемой и передаваемой мощности, КПД и КМ источника и приемника от длины линии x при $Z_S = Z_0$ (a); Z_B(b); R = 0.48; G = R/5.

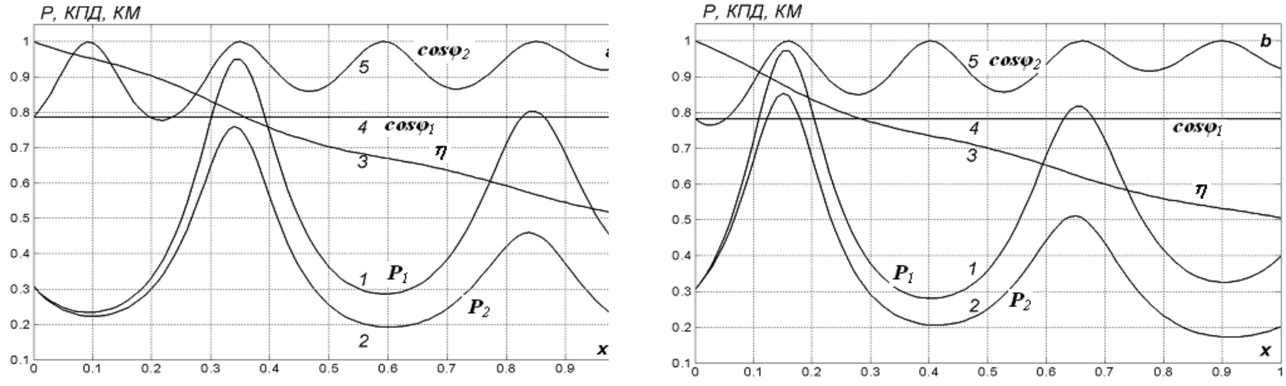

Рис. 5. Зависимость генерируемой и передаваемой мощности, КПД и КМ источника и приемника от длины линии x при ZS = ZB +jω LS (a); ZB –j/(ω CS) (b); LS =1/8; CS =1/5;R = 0.48; G = R/5.

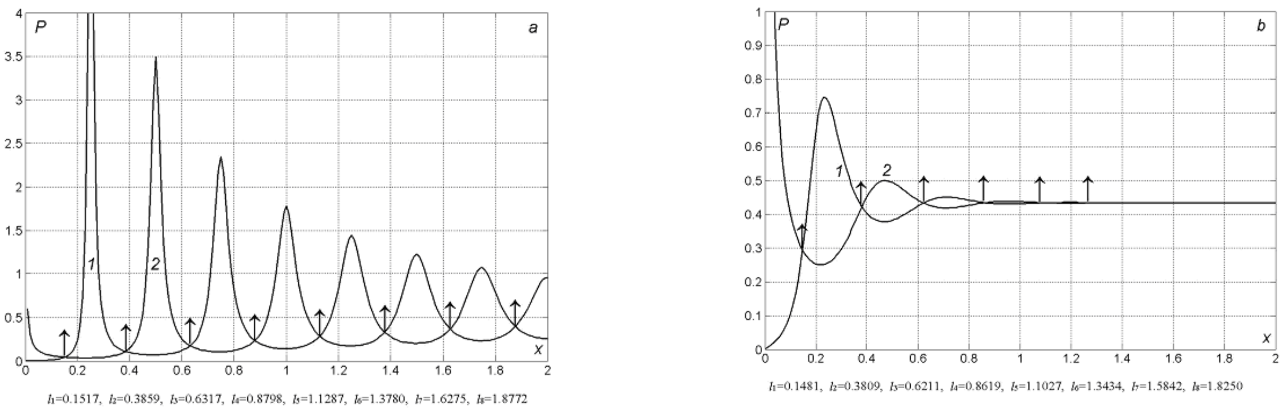

Рис. 6. Зависимость мощности генератора P0 от длины линии x в режиме ХХ (1) и КЗ (2) при R = 0.48 (a); R = 4.8 (b); G = R/5.

На рис. 5 представлена зависимость исследуемых величин от длины линии *x* при $Z_S = Z_B + j\omega L_S$ (*a*); $Z_B - j/(\omega C_S)$ (*b*); L_S =1/8 (0.66 Гн); C_S =1/5 (15.23 мкФ); *R* = 0.48; *G* = *R*/5**.** Наличие реактивных элементов в нагрузочном сопротивлении приводит к резкому изменению входного сопротивления цепи и как следствие все величины, характеризующие процесс передачи мощности переменным током испытывают колебания на десятки процентов. Для полуволновой линии передаваемая мощность и КПД являются максимальными, когда нагрузка на ее приемном конце чисто активная.

В случае линии с потерями (рис.5b) волнообразный характер отдаваемой генератором мощности в сети подобен как для линии без потерь. С увеличением длинны линии, функция мощности генератора быстрее стремится к установившемуся значению при увеличении продольного погонного активного сопротивления этой линии. Вследствие этого происходит ослабление влияния масштабного фактора на процесс передачи в линию активной мощности генератором.

Исследование изменения мощности генератора отдаваемой в линии в режиме ХХ и КЗ показывает, что имеются особые точки (длины линии) для которых эта мощность одинакова по значению как для режима ХХ, так и для режима КЗ линии в данном сечении (рис.6 - особые точки обозначены стрелками). Рост погонного активного сопротивления *R* уменьшает число таких точек. Функция $P_0(x)$ активной мощности генератора, подключенного к линии, при этом условии быстрее достигает установившегося значения при увеличении длины линии. Следовательно, для амплитуды мгновенной мощности генератора выполняется условие $P_{02}(x) < P_{01}(x)$ для $R_2 > R_1$, где R_1, R_2 - погонные сопротивления длинной линии (рис.6).

Установлено также, что в окрестности особых точек линии активное погонное сопротивление не влияет на значение мощности отдаваемой в линии генератором. Например, при увеличении погонного активного сопротивления с 0.48 до 4.8 относительных единиц для длин линии, определяемых координатами расположения особых точек, получены одинаковые значения активной мощности генератора подключенного к такой линии.

В отличие от линии постоянного напряжения, где мощность генератора на холостом ходу всегда меньше, чем при коротком замыкании, здесь имеем по 4 точки пересечения этих кривых на каждом отрезке длины линии, равном λ. Координаты этих точек по длине линии следующие:

$l_1 = 0.1481;\ l_2 = 0.3809;\ l_3 = 0.6211;\ l_4 = 0.8619;$
$l_5 = 1.1027;\ l_6 = 1.3434;\ l_7 = 1.5842;\ l_8 = 1.825$

Параметрический анализ процессов передачи электрической энергии по длиной линии показал в электрическом плане, что линия электропередачи является неоднородным объектом. Режим работы генератора в начале линии зависит от многих факторов, таких как: волновой длины линии, точки подключения нагрузки, характера нагрузки и устройств для компенсации реактивной мощности, схемы подключения компенсирующего устройства трансформаторов для повышения и/или понижения напряжения в линии, схемы подключения нагрузки к лини и в произвольных точках и в особых точках длинной линии.

В качестве примера на рис. 7 показана схема замещения длинной линии с указанием особых точек подключения нагрузок, компенсирующих устройств и трансформаторов, обеспечивающих передачу наибольшей мощности в нагрузке.

Для любой неискажающей линии для которой выполняются условие $RC = GL$, мощности генераторов при ХХ и КЗ совпадают в точках x = λ/8, 3λ/8, 5λ/8 и т.д. Если же выполняется условие $RC > GL$, то вследствие дифракции волн, кривые мощности генератора смещаются несколько вправо: x = 0.15λ, 0.386λ, 0.63λ. Отсюда следует, что максимальный отбор мощности от линии переменного напряжения на участке: 0.15λ ≤ x ≤ 0.386λ возможен в режиме, близком к ХХ, а на участках: 0 < x ≤ 0.15λ и 0.386λ ≤ x ≤ 0.63λ в режиме, близком к КЗ. Такая ситуация повторяется через каждые отрезки волновой длины линии, равные примерно λ/4.

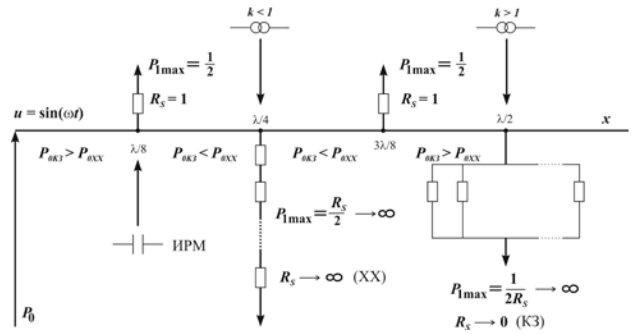

Рис.7. Особые точки длинной линии и рекомендуемые схемы включения компенсирующих устройств, трансформаторов и нагрузок к линии

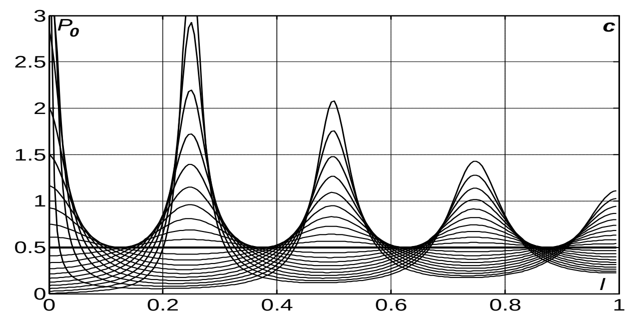

Рис.8. Характер изменения активной мощности на входе линии с потерями в функции от ее длины при согласованной нагрузки

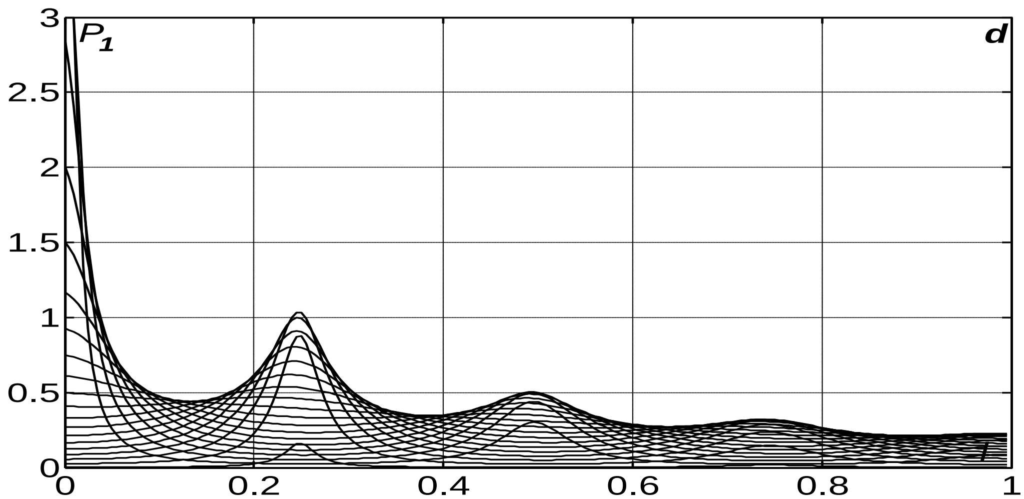

Рис.9. Характер изменения активной мощности (транзитной) на конце линии с потерями в функции от ее длины при согласованной нагрузки

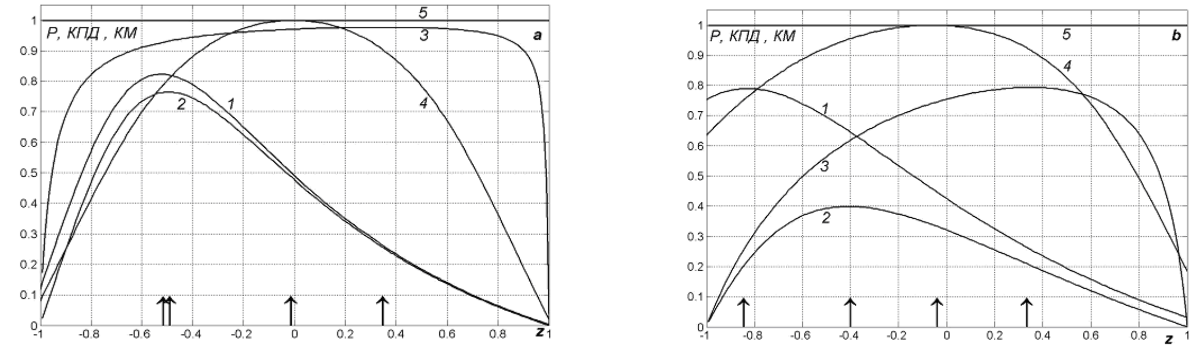

Рис. 10. Зависимость генерируемой и передаваемой мощности, КПД и КМ источника и приемника от сопротивления нагрузки RS при l = 0.0516; R = 0.48(a); 4.8(b); G = R/5; $Z_S = R_S$, где 1 – P1; 2 – P2; 3 – η; 4 – cosφ1; 5 – cosφ2

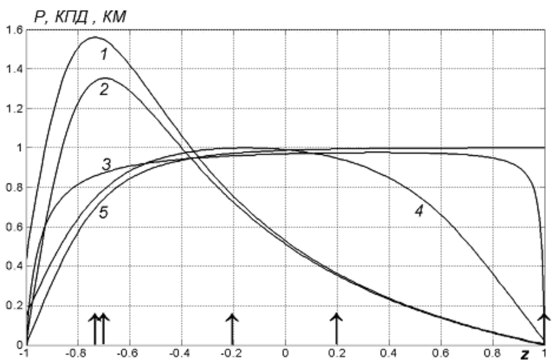

Рис. 11. Зависимость от сопротивления нагрузки RS генерируемой (1) и передаваемой мощности (2), КПД (3) и КМ источника (4) и приемника (5) при l = 0.0516; R = 0.48; G = R/5; $Z_S = R_S - j / (\omega C_S)$;CS =1.

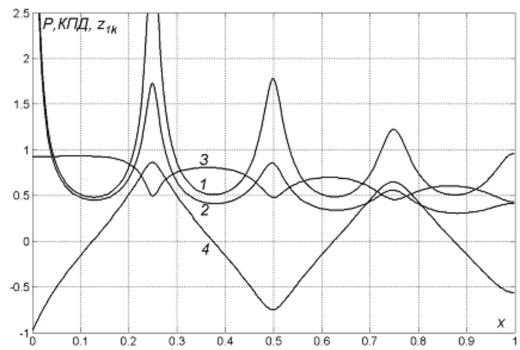

Рис. 12 Зависимость от длины линии x генерируемой (1), максимальной передаваемой (2) мощности, КПД (3) и критического сопротивления z1k (4) при R = 0.48; G = R/5.

На рис. 8 и 9 приведены обобщенные данные о характере изменения мощности на входе и на приемном конце линии с потерями (при различных потерях) в случае согласованной нагрузки.

Следует отметить, что хотя потери линии влияют на значение передаваемой мощности, но имеются такие точки в линии, для которых не выявляется влияние потерь линии на значение переданной в нагрузку мощности. Такие режимы возможны как в линиях относительно коротких, так и в линиях сравнимых с длинной волны.

На рис. 10 представлено изменение генерируемой и передаваемой мощности, КПД и КМ источника и приемника (кривые 1-5) в зависимости от параметра *z* при *l* = 0.0516; *R* = 0.48(*a*); 4.8(*b*); *G* = *R*/5; $Z_S = R_S$. Эти графики

о

щий

достигаются при различных значениях сопротивления нагрузки R_S. С увеличением потерь в линии наблюдается «разбегание» критических сопротивлений для генерируемой и передаваемой мощности, тогда как точки максимума для КПД и КМ остаются практически неподвижными. Таким образом, при вариации параметра R_S для любого отрезка длины линии можно получить полное представление о перетоках мощности, что позволяет выбрать оптимальный режим линии исходя из тех или иных критериев.

Рис.11 иллюстрирует зависимость генерируемой и передаваемой мощности, КПД и КМ источника и приемника от параметра *z* при $Z_S = R_S - j/(\omega C_S)$; C_S =1 (17.57 мкФ**)**. Продольное активное сопротивление и активная проводимость линии в относительных единицах имеют значения: $R = 0.48$, *G* = *R*/5. Продольная компенсация параметров нагрузки для этой длины линии увеличивает максимальную передаваемую мощность, но уменьшает КПД и $\cos\varphi$.

На рис.12 показана зависимость генерируемой и максимальной передаваемой мощности, КПД и критического сопротивления z_{1k} от длины линии (кривые 1–4).

Увеличению (уменьшению) передаваемой мощности по мере изменения длины линии всегда сопутствует уменьшение (увеличение) КПД. Для четвертьволновой линии максимум мощности имеет место в режиме, близком к ХХ ($R_S =$ 13.93 Z_B), а для полуволновой линии в режиме, близком к КЗ (R_S = 0.14 Z_B).

Выводы

1. В рамках тенденции развития региональных и межрегиональных энергетических систем актуальность разработки эффективных методов исследования режимов в таких цепях многократно возрастает. Исследование влияния различных факторов, какими являются параметры линии и нагрузки, диссипация и дисперсия волн на потери мощности позволяет разработать меры по повышению эффективности функционирования ЛЭП в составе региональных энергообъединений.
2. Самым значимым влияющим параметром на режим передачи мощности по длинным линиям является ее длина.
3. Следует различать режимы работы линии при максимальной передаваемой мощности, КПД, КМ и максимальной отдаче энергии генератором синусоидального напряжения в данную линию.
4. Исследования в данном направлении имеет не только научную значимость, но и практическую, поскольку можно обосновано разрабатывать наиболее рациональные способы передачи энергии по линиям высокого напряжения и решать других задачи из области диагностики, координации изоляции, расчета потерь, как в стационарных, так и нестационарных (переходных) режимах.

Литература

1. В Португалии открылась крупнейшая в мире солнечная электростанция. http://www.membrana.ru/lenta/index.html?7077.
2. Аризона строит крупнейшую солнечную электростанцию на Земле. http://www.membrana.ru/lenta/index.html?8014.
3. Energia din Sahara va „lumina“ lumea. http://www.ecomagazin.ro/energia-din-sahara-va-%e2%80%9elumina%e2%80%9c-lumea-2/
4. Ковалев Г.Ф., Лебедева Л.М.Планетарная электроэнергетическая система. Энергия, 2006, №9 сс. 27-34/ http://courier.com.ru/energy/en0906kovalev.htm.
5. Александров Г.Н., Ле Тхань Бак. Уменьшение потерь мощности в дальних линиях электропередачи с управляемыми реакторами.-Электричество, 2007, №3, СС. 8-15.
6. Вершков В.А., Нахапетян К.Т., Ольшевский О.В., Совалов С.А., Фотин В.П., Щербаков В.К. Комплексные испытания полуволновой электропередачи в сети 500 кВ Европейской части СССР.- Электричество, 1968, №8, сс.10-16.
7. Зильберман С.М., Самородов Г.И. Возможные перспективы импорта электроэнергии в Республику Молдова из Тюменского региона. Труды Конференции «Энергетика Молдовы 2005», Кишинев: 2005, Типография АНМ, СС.104-110.
8. Римский В.К., Берзан В.П., Пацюк В.И., Карчева Н.Ф., Андрос И.В. Волновые явления в неоднородных линиях. Том 4. Параметрические цепи/ АН Молдовы. Ин-т энергетики. Кишинэу: TASM? 2008.-552с.
9. Римский В.К., Берзан В.П., Тыршу М.С. Волновые явления в неоднородных линиях. Т.1. Теория распространения волн потенциала и тока. Под ред. Римского В.К. – Кишинев: Типография АНМ, 1997. – 298с.
10. Римский В.К., Берзан В.П., Пацюк В.И. и др. Как увеличить передаваемую мощность в десятки раз. – Кишинев: Типография АНМ, 2007. – 178с.
11. Бессонов Л.А. Теоретические основы электротехники. Электрические цепи /Учебник для ВТУЗов. – М.: Высшая школа, 1984. – 559с.

Assessing the risk for pollution due to abnormal behavior of a hazardous installation

Dr. Julian Argirov

e-mail: argirov@inrne.bas.bg

Address: Institute for Nuclear Research and Nuclear Energy, 1784 Sofia, Bulgaria

Abstract: Our current understanding is that since 18th century many of mankind's activities contribute significantly to the changes in the global climate system. The number of hazardous installations in use and their diversity has dramatically increased during the last 60 years. Each of those technological facilities is a potential source of major accidents with huge or catastrophic impacts on the soil, atmosphere, water quality, ecosystems and directly on human health. The paper briefly comments on an approach for addressing the uncertainty about the unacceptable consequences expected from a particular hazardous facility. The first stage of the approach is discussed in a case study. This part of the methodology is capable to search for and rank those likely abnormal situations having high potential to progress further on into major accidents.

Keywords: Hazardous installation, technological risk, major release scenarios.

1. Introduction

The scientific community works systematically more than 20 years to understand and predict dangerous anthropogenetic interference with the climate system (Hansel et al., 2005), (EEA, 2008), (Rohde, R., et al. 2011). Part of these efforts is to identify and reduce the frequencies and magnitudes of accidents at any engineering system (ES).

Nowadays, natural hazards are not the only threats that affect seriously human live and the global climate system. Modern society relies on various fixed and movable facilities as those of process industries, the energy sector, offshore platforms, etc. It also cannot exist without airplanes and various vehicles for land and marine transport. Many of these ES use, produce and store hazardous materials. Both moving vehicles and fixed installations can be responsible for distinct health effects on their personnel, off-site population and various impacts on ecosystems all over the world.

While operating normally, some installations of the energy sector and process industries emit permanently various substances. In general, observing continuously the dangerous substances, which an ES usually releases, we are able to estimate their quantities with increasing degree of certainty. There is no doubt that the effective techniques for capturing of specific substances, escaping permanently from an ES, may be neither simple nor cheap to implement. However, the uncertainty, about the negative effects on human health and the environment due to persistent emissions, can be reduced just by monitoring the daily production rate of given substances. Thus, efficient protection measures against the continuous pollution of air, the soil and waters are easier to implement than against the harmful impacts, which fixed installations and vehicles can give rise to, in case of occasional abnormal behavior.

Since the industrial era (starting about 1750 A.D.), the "capacity" of ES to utilize diverse hazardous substances in civil and military industries enhances from a day to a day. As a result unexpected releases from hazardous installations (HI) will keep occurring. Part of these undesired events may progress to accidents, associated with shocking impacts of various magnitudes, having the potential to damage smaller or larger regions of the Earth. A list of accidents ending in the past with catastrophic health and environmental effects can be too long. The accidents at: Bhopal chemical plant in 1984 (e.g. Khan & Abbas, 1997), Chernobyl NPP in 1986 (see IAEA, 2006), offshore platform Piper Alpha in 1988 (e.g. HSE, 2004) etc. are only small part of those occurred in the recent 25 years all over the world.

Although major accidents at HI rarely happen, due to their huge or catastrophic immediate and long-term consequences, they are rather risk-significant. On the other hand the accident consequences are too diverse and should be assessed in terms of human deaths and injuries, financial losses, ecological damages etc. Actually, the experience shows that accidents can never be entirely prevented. However, implementing different means to reducee the chance for severe consequences is a reasonable strategy for minimizing the resources that should be spent for post accident activities.

Since ionizing radiation exposure damages living cells and the half-life of a number of radioactive elements is thousands of years, living beings must be protected as effectively as possible from the products of nuclear fission. Specific nuclear legislation and design concepts, applying several levels of defensive barriers, redundant safety systems and various types of emergency procedures, guarantee the high safety of every operating Nuclear Power Plant (NPP) unit.

To keep acceptably low the chance for no adverse impacts on human health and the environment, the radioactive substances at every NPP site must stay isolated, by the installed strictly independent defensive barriers, after any abnormal situation no matter how rarely it can occur. Although, the accidents stemming from non-nuclear HI usually cannot lead to extremely long-lasting consequences, the release of some toxic substances may cause both immediate and long-term damages. The Seveso disaster in 1976, in which the surrounding area near Milan was contaminated with tetrachloro dibenzo dioxin, is such an example.

Taking care about high level of safety for the non-nuclear establishments, the EU Council defines in 1996 the Directive 96/82/EC (known as Seveso II). The Seveso II lists many requirements for installations, operating with big amounts of non-nuclear dangerous substances which the legislation of each of the member states should implement. The philosophy of the Seveso II directive is discussed in many works for instance (Hawksley, 1999), (Kirchsteiger, 1999), (Mitchison, et al, 1999), etc.

From 2002 the first edition of the Bulgarian law for "Environmental protection" is in force. Chapter 6 of the law obliges all individuals and organizations, before starting whatever activities, to obtain special assessment specifying their possible impacts on the environment. The chapter 7 of this law directly applies the Seveso II directive to everyone whose activities in the country pose non-nuclear hazards. It specifies that every operator of a large scale facility must classify it as a unit with low or with high risk potential for the environment. The operator of a highly risky installation needs a safety report that should be periodically updated.

The non-nuclear installations of the energy sector usually contain huge amounts of combustible or flammable materials. Some toxic substances also can be present in those ES. Therefore, if something goes wrong in such installations, it is very likely major accidents, associated with release of large quantities of pollutants, eventually to take place.

Section 2 of this paper briefly presents an approach for identifying those zones at a certain site from which accidental scenarios can emerge. That section also discusses the ranking of likely release scenarios by the release rate of specific hazardous substances. Section 3 comments on a simple case study showing how the method can be applied. In section 4 some conclusions are drawn.

2. Generic features of the approach

A hazardous substance is free to escape in all directions from a given hazardous unit after the defensive barriers, installed to isolate it from its close vicinity, have lost their integrity. The first stage of the approach under discussion quantifies the frequency for occurrence of situations that may go forward into major accidents. This stage of the methodology needs suitable inferential methods by which from the available observations the occurrence frequency of the events, leading even rarely to accidents, to be quantified. Once an undesired event has started proper action of certain mitigating systems and emergency procedures must be applied for preventing the progress of accidental phenomena. The success or failure of these means for fighting accidents determines the chance for harming a target region by dangerous substances escaping from the disabled HI. A number of conditional probabilities estimates the chance for success (or failure) of particular accident fighting means to prevent the occurrence of significant consequences. Finally, correcting the occurrence frequency of the initial abnormal event by these conditional probabilities the frequency of huge consequences in the regions around the stricken HI can be quantified.

The paper comments only on some elements of the entire methodology. It very briefly considers the method for quantifying the frequency of initiators of accidents. Actually, the paper focuses on quantifying the chance that the disturbances with a high risk potential can emerge from each part of a hazardous facility.

The frequency for arising into a given zone X of the HI J of accidents whose risk potential is higher than a given threshold can be formally assessed as:

$F_{J\text{-}x} = F_J * P(Ax|F_J)$, where $A_x \equiv (R_x \cap D_x)$

F_J – Occurrence frequency of specific type of accidents in all zones of the installation J of interest. This entity is considered in many references (e.g. Bier & Yi, 1995; Argirov, 1999) etc., and there is no discussion on it here;

$P(A_x \equiv (R_x \cap D_x)|F_J)$ - The chance that the complex event A_x addresses sufficiently well the uncertainty associated with emerging of accidents of a given type in the zone X of the installation J. Probability theory helps for quantifying this chance;

The event A_x specifies those random and deterministic factors that determine the risk potential of abnormal events in whose further progress hazardous substances escape out of the defensive barriers. The symbols R_x and D_x indicate sets (vectors) consisting of the values of the random parameters and the deterministic variables, respectively. Members of both sets can deviate in space and time and can be complexly related logically with each other. A simple case is considered here in which none of the random parameters varies in time t and each of them is also independent from the deterministic variables. Actually, this is a reasonable assumption if the occurring accident is progressing too quickly for the corrective actions by automatics and operators aimed at preventing the accidental phenomena to be successful thus allowing the hazardous substances to bypass the dedicated defensive barriers.

The set R_x includes values of such random factors that identify how those barriers, which are available at the zone X of the installation J, can fail at the time t=0. The initial values of the deterministic variables, D_x [t=0], should be known to predict how the indicators for severity of the potential accidents vary. The symbol D_x [t]| R_x shows that for the zone X the deterministic variables can also depend on anyone of the random parameters.

Due to the assumptions and conventions mentioned above the following relation can be written:

$P((R_x \cap D_x[t])|F_J)=P(R_x|F_J)P(D_x[t]|F_J, R_x)$ (1)

$P(R_x|F_J)$ – Conditional probability specifying the severity of initial disturbances by using a vector of random parameters whose value R_x falls into a particular region of a corresponding hyperspace. This term identifies the vague damaging potential of this fraction of the likely accidents, which for a unit time arise just at the zone X of the facility J. The values of the random parameters identify "holes" in a barrier inducing particular fractions of accidents;

$P(D_x[t]|F_J, R_x)$ – Conditional probability specifying those abnormal events that, after arising from the zone X with the potential identified by the values of R_x and $D_x[0]$, progress later on in such a way that can overcome the rest of the defense barriers. This means that for this fraction of possible accidents as the R_x so the $D_x[0]$ are known to the accuracy of a small region within their hyper-spaces.

In fact, the final consequences are those indicating how severe an accident scenario is. However, while an abnormal situation progresses from stage to a stage its magnitude can be "measured" by using some "intermediate" indicators. For instance, using the release rate of a hazardous substance as an indicator we can find those potential disturbances, which can develop further on into major accidents. Indicators of every stage take their values depending on what has happened in previous stages of the propagation of accidents. The time variation of the indicators, suggesting that major accidents are possible, depends strongly on the $D_x[t]$. On the other hand for similar scenarios the deterministic variables never accept the same values $D_x[t]$ at the time t. The initial values $D_x[0]$ of deterministic factors change from scenario to scenario since the value of every random parameter is predictable only to the accuracy of a certain range. If the sets of values R_x and $D_x[0]$ plus those deterministic laws of nature that govern the evolution of the dominant accidental phenomena are exactly known, then predictions are obtainable by single values. However, this is impossible in the real word because of the uncertainties which both the parameters and the models introduce. Quantifying the indicators the analyst should consider that random factors are inherently vague and also it is not possible to specify exactly the real initial values of all deterministic variables. Since mathematical expressions for deterministic laws of nature more or less adequately approximate but very rarely entirely reproduce the real progress of the phenomena of interest they also contribute to the uncertainty. Being unable to assess with zero error how the indicators vary in space and time, the best we can do is to address the uncertainty which dominant factors introduce in the investigations.

The formal mathematical relations discussed so far suggest that the uncertainty about the indicators, for arising of high risk abnormal situations, can be addressed varying suitably in their hyperspaces the factors, identifying the potential of the zone X, to induce accidents. It is assumed that the values R_x, which the random parameters take initially, stay unchanged while accidents progress. Also, that the initial values, $D_x[0]$, of the deterministic variables can depend on R_x but the opposite is not true.

The approach here presented supposes that the real world accidental scenarios are expressible sufficiently well by the following logical order: $R_x \rightarrow D_x(0) \rightarrow [D_x(t)=f(R_x, D_x(0))] \rightarrow [{}^{I}M_x(t)=f(D_x(t))]$
- the symbol $f(\cdot)$ shows a function of a number of arguments;

- the symbol ${}^{I}M_x(t)$ points out the value taken by the indicator's vectors, given the initial values of the random and deterministic factors are restricted within small regions of their hyperspaces. The components of the matrix:
$M_x(t) \equiv [{}^{1}M_x(t), 2M_x(t), ... , {}^{Imax}M_x(t)]$ can be calculated altering the values of both type of parameters for all sub-regions they can fall into. (Since I_{max} is usually a big number the analysis is time consuming.)

In order to address the vague potential of the abnormal events, occurring from the zone X of the J, the first step is to define the joint probability distribution – $P_x(R_1, R_2, \dots, R_N|F_J)$, for n=1, 2, …., N, of those N random parameters having dominant contribution. The hyperspace, in which these factors vary, is an ordered N-tuple Cartesian product. An appropriate inferential approach is needed to identify the marginal probability distributions first, and after that their joint probability distribution. Then the likely initial values, $D_x[0]$, which the deterministic variables take into their hyperspace, should be identified. Once the hyperspaces of both types of factors are divided into a reasonable number of sub-regions the components of the matrix $M_x[t]$, are assessable by using corresponding expressions for the deterministic laws of nature. Finally, the fraction of the risk-significant abnormal events can be assessed as the ratio of the number of those values of the matrix $M_x[t]$, which fall outside the safety region of the indicators hyperspace, to the total number of its elements.

There is no more discussion on the generic features of the methodology further in this work. None of the issues related with the model uncertainty are commented on here in order to focus on the methodology's application. Some specific methods that the methodology uses are considered in the next section.

3. Case study

The case specific discussion on the approach

A vertical cylindrical storage tank filled with a liquid flammable fuel is analyzed to identify the land areas around the tank from which huge fires or explosions can occur. Although the tank is no part of an installation processing hazardous substances it is surrounded by other vessels. Thus, at the site in which the tank of study is situated the domino effect is highly possible.

The wall of the vessel is the single barrier separating the fuel form the environment. Therefore, any time when the wall has lost its integrity release scenarios occur and liquid fuel and its vapors will be emitted around the tank. The mass flow rate of fuel through the tank's wall is used as an indicator showing that the wall failures can grow further into huge fires or explosions. The magnitude of velocity through the ruptured place and the cross-section of this hole uniquely determine the mass of fuel released for any given period. The direction of velocity from the hole is also important parameter since contents of both the vulnerable items and the ignition sources in the vicinity of the tank can vary largely from one target area to another. It is well know that the meteorological conditions and local topology dominantly determine how the fuel will disperse first in the air and then onto the land but this stage of accident progression is outside the scope of this work.

The restricted analysis, here presented, aims to identify the most severe release scenarios. The fuel mass that has left the tank for a certain period $[0, t_1]$ is an indicator for those wall's failures, which later on can turn into fires or explosions. The indicator $M[t_1]$ is quantified by the following relations:

$$M[t_1] = \int_0^{t_1} M[t]dt; \quad M[t] = |\mathbf{u[t]}|\,\rho[t]A_h \qquad (2)$$

where,

$|u[t]|$ - the magnitude of the velocity through the hole at the time t - [m/s];

$\rho[t]$ – the density of the liquid fuel leaving the hole at the moment t – [kg/m^3];

Ah – [m^2] the cross-section of the wall's rupture, specified by a circular hole with the same face.

For this study, R_1 identifies the location on the wall surface in which the tank fails and R_2 is the diameter of a circular hole with cross-section of A_h. (To specify the joint distribution of these two random variables their marginal distributions should be obtained first).

Let us suppose that the tank of study stands on the ground and there is no thermal isolation over its metal wall. The tank height is 3 [m] and its diameter is 1 [m]. Neither chemical reactions nor other sources generate or sink heat into the tank but heat fluxes from the outside make the pressure, the temperature and the fuel properties to fluctuate. The tank has no connection with other vessels or pumps also the fuel inside is under stable static pressure and its temperature is almost the same as the ambient one. Thus, when a rupture arises the static pressure is the force pushing the liquid fuel out of the tank. Later on, due to the loss of fuel, the pressure and the density of fuel inside the tank decrease and the mass flow rate through the hole reduces continuously in the time. (The pressure inside cannot change suddenly due to impacts from other vessels or active components like pumps and valves). After the tank fails the pressure and the density inside will change very slowly as only small holes are assumed possible to occur unexpectedly. When the failure of the tank's wall induces a very mild transient the Bernoulli equation is a suffieciently correct deterministinc law for prediciting the quasi-static change in the pressure of fuel inside. Due to the assumpions listed above, for a short time step the average velocity over the hole's cross-section $u_h[t]$ is assessed as:

$$uh[t] = (h[t]g)^{0.5}; \qquad (3)$$

where,

g – acceleration of gravity [m/s^2];

h[t] – the distance between the free fuel surface in the tank and the center of hole at the time t [m].

Identifying the ranges in the hyperspaces of parameters

To estimate uniquely the fuel mass flow rate through the hole at the given time of t_1 we need the initial values of two deterministic parameters - the temperature behind the hole $T_h[0]$ and the distance h[0]. The initial temperature in the whole tank can be supposed almost the same and equal to $T_h[0]$ but its exact value is uncertain because the varying ambient conditions influence on the state of the fuel inside. For this study we assume that $T_h[0]$ varies in the range [5^o, 45^o] degrees Celsius. Due to the uncertainty about the exact value of $T_h[0]$ it falls into a larger range than the range in which the $T_h[t]$ varies during the progress of release scenarios. Thus, for the period $t \leq t_1$ $T_h[t]$ is considered a constant equal to $T_h[0]$. The h[0] falls into the range [0, 3] in [m] and it is a function of the random parameter R_1, which is discussed later on.

The following sequential steps are applicable in the inner cycle of the iteration scheme, given the random factors $\{{}^KR_1, {}^LR_1\}$ are identified to the accuracy of a small region within their space :

1. The values ${}^bu_h(t_i)=f(h[t_{i-1}])$,$\rho[t_{i-1}]=\rho(p_h[t_{i-1}],T_h[0])$, $p_h[t_i]=p_0+g^bh[t_{i-1}]\rho[t_{i-1}]$, for p_0 the atmospheric pressure, and $\Delta^bM[t_i]={}^bu_h[t_i]\rho[t_{i-1}](t_i-t_{i-1})A_h$ are assessed at each time step i first;

2. After correcting the fuel mass in the tank by the lost mass of $\Delta^bM[t_i]$ the new value of ${}^ch[t_i]$ is estimated. Then ${}^cu_h[t_i]$, $\rho[_{ti}]$, $T_h[t_i]$ and $\Delta^cM[t_i]$ are calculated. The time step is reduced if the difference between $\Delta^bM[t_i]$ and $\Delta^cM[t_i]$ is too large. When the error of lost mass at current time step is acceptably small then $\Delta M[t_i]=\Delta^cM[t_i]$ and the calculation goes on;

3. Since the conjugate space of the deterministic variables for the case study is two-dimensional the indicator should be predicted by combining their initial values at least in four couples. The biggest among the calculated values is used as conservative estimate for the fuel mass lost through a particular area over the wall surface. The maximal value of the indicator can be obtained as:

$$\Delta^mM[t_i]=\max(\Delta^{d,d}M[t_i],\Delta^{d,u}M[t_i],\Delta^{u,d}M[t_i],, {}^{u,u}M[t_i])$$

The meaning of the above listed symbols is as follows:

$$T_h(0)\in[{}^JT^d,\ {}^JT^u];h(0)\in[{}^Nh^d,\ {}^Nh^u];\ {}^LR_2\in[{}^LR_2^d,\ {}^LR_2^u];$$

${}^K\mathbf{R_1}$ is radius vector of the space surface;

$\Delta^{d,d}M = f({}^{J}T^{d},\ {}^{N}h^{d},\ {}^{K}\mathbf{R}_1,\ {}^{L}R_2);\ \Delta^{d,u}M = f({}^{J}T^{d},\ {}^{N}h^{u},\ {}^{K}\mathbf{R}_1,\ {}^{L}R_2)$;

$\Delta^{u,d}M = f({}^{J}T^{u},\ {}^{N}h^{d},\ {}^{K}\mathbf{R}_1,\ {}^{L}R_2);\ \Delta^{u,u}M = f({}^{J}T^{u},\ {}^{N}h^{u},\ {}^{K}\mathbf{R}_1,\ {}^{L}R_2)$

The range of the initial temperature of fuel in the tank can be divided on two sub-ranges [5^o, 25^o) and [25^o, 45^o]. The sub-ranges of the initial distance h[0] depend on the sub-regions on which the random parameter R_1 is divided on.

The outer cycle of the iteration scheme includes sequential visiting of all sub-regions into which the entire hyperspace of random parameters is divided for the case of study.

1. The parameter R_1 should identify so small areas on the entire surface of the tank's wall within which the minimal and the maximal value of the indicator do not differ too much. For the case of study a cylindrical coordinate system is suitable to define the radius vector of any part of the wall surface in which the rupture can arise. Also, the point at which the tank axis crosses the land surface is used as the origin of this coordinate system. In order to identify the values of the radius vector ${}^{K}R_1$, corresponding to the area ${}^{K}A_w$ of the wall surface, two parameters are used - height Y and azimuth angle θ:

$$Y \in (0,3);\ {}^{1}Y \in (0,0.6];\ {}^{2}Y \in (0.6,1.3];\ {}^{3}Y \in (1.3,2.1];\ {}^{4}Y \in (2.1,3)$$
$$\theta \in [0^o,360^o];\ {}^{1}\theta \in [0^o,60^o];\ {}^{2}\theta \in [60^o,120^o];\ {}^{3}\theta \in [120^o,180^o]$$
$${}^{4}\theta \in [180^o,240^o];\ {}^{5}\theta \in [240^o,300^o];\ {}^{6}\theta \in [300^o,360^o]$$

By using the listed notations it is easy to find that the couple ${}^{3,5}R_1 \equiv \{{}^{3Y},{}^{5}\theta\}$ corresponds to that part of the wall surface for which the Y and the θ falls into the ranges (1.3, 2.1] and (240^o, 300^o], respectively.

2. The other random parameter the diameter of the hole, specified by the symbol R_2, uniquely identifies the cross-section of the crack location as $A_h = \pi R_2^2$.

A suitable inferential model is required to quantify the marginal distributions of the random factors. Because of the above listed, for the case of interest, at the outer cycle of the iteration scheme 4x6 sub-regions within the conjugate hyperspace of the random parameters should be visited. For each one of those 24 sub-regions the initial values of deterministic parameters are altered at least 4 times and by using the deterministic laws the indicator values varying in time should be found and ranked. The maximal among those 4 figures about the indicator, obtained in the inter cycle of the iteration scheme, specifies the most dangerous release scenario among those emerging from anyone of the specified parts of the tank's wall. The mass of fuel left the tank for the control time t1 shows how likely the given release scenarios are to progress later on into huge fires and explosions. The discussion so far focuses on identifying the significance of release scenarios in terms of deterministic arguments. In the author's opinion the more important question is what is the fraction of release scenarios that for the period t_1 can push out of the tank a fuel mass bigger than given threshold value?

Quantifying the probabilities of the major release scenarios

As it was discussed in section 2 the approach here presented estimates the chance that the possible failures of the tank of study can grow to major releases of hazardous substances. The approach introduces the conditional probabilities $P(D_x[t]|F_J, R_x)$ and $P(R_x|F_J)$. The term $P(D_x[t]|F_J, R_x)$ identifies how probable it is if the rupture has occurred the deterministic variables after falling initially into a certain region of their hyper-space to change later in a particular way, given the random parameters are restricted within a small sub-region of their hyperspace.

For the tank of investigation we should assess the probability of the following complex events:

$$E_{1,1,[1,K2],L} \equiv [{}^{1}T_h[0] \in [5^o,25^o]) \cap ({}^{1}h[0] \in (2.4,3])] \,|\, ([{}^{1}Y,{}^{K2}\theta],\ {}^{L}R_2]$$
$$E_{2,1,[1,K2],L} \equiv [{}^{2}T_h[0] \in [25^o,45^o]) \cap ({}^{1}h[0] \in (2.4,3])] \,|\, ([{}^{1}Y,{}^{K2}\theta],\ {}^{L}R_2]$$

…………………………………………………….

$$E_{1,4,[4,K2],L} \equiv [{}^{1}T_h[0] \in [5^o,25^o]) \cap ({}^{4}h[0] \in (0,0.9])] \,|\, ([{}^{4}Y,{}^{K2}\theta],\ {}^{L}R_2]$$

$$E_{2,4,[4,K2],L} \equiv [{}^{2}T_{h}[0] \in [25^{o},45^{o}]) \cap ({}^{4}h[0] \in (0,0.9])] \mid ([{}^{4}Y,{}^{K2}\theta],\ {}^{L}R_{2}]$$

for K_2 varying from 1 to 6 as first L=1 and then L=2.

We can define the following probabilities:

$$P({}^{1}T_{h}[0]) = 0.5;\quad P({}^{2}T_{h}[0]) = 0.5$$

The term $P(R_x|F_J)$, that the methodology introduces should specify in the case of study the rupture location on the defensive barrier – the tank's wall for this study.

Since the uncertainty about random parameters is expressed by their joint probability distribution let us suppose that the parameters R_1 and R_2 are independent and the following is true:

$$P(R_1 \cap R_2) = P(\mathbf{R_1})P(R_2);\ P(\mathbf{R_1}) = P(\bigcup_{K=1}^{24} {}^{K}\mathbf{R_1});\ P(R_2) \approx P({}^{1}R_2 \cup {}^{2}R_2)$$

The symbol ${}^{d}R_2$ indicates that value of the hole diameter at which the cumulative distribution is equal to some value c_1 or $P(0 < R_2 \leq {}^{d}R_2) = c_1$. The symbol ${}^{u}R_2$ shows the 97.5% quintile of this distribution or $P({}^{d}R_2 < R_2 \leq {}^{u}R_2)=0.975-c_1$ and $P(R_2 > {}^{u}R_2) = 0.025$.

Having no reliable observations about those areas on the tank surface within which the wall's integrity is more often lost, the assumption that rupture is equally likely in each one of the specified 24 parts of the wall surface is a reasonable one or:

$$P({}^{1}\mathbf{R_1}) = \ldots = P({}^{10}\mathbf{R_1}) = \ldots = P({}^{20}\mathbf{R_1}) = \ldots = P({}^{24}\mathbf{R_1}) = 0.04167$$

The distribution about the hole's diameter should be identified first, then the values of ${}^{d}R_2$ and ${}^{u}R_2$ can be assessed. When there is not enough specific data, as usually the situation is, Bayesian statistics can help. It is capable to combine coherently generic information with the limited data coming from identical units.

Identifying the distribution about the hole's diameter

The Bayesian concept on probability is outside the scope of this paper. Many excellent works as (Robert, C., 2004) and many others are dedicated to the Bayesian approach. A parametric Bayesian model is used to specify the distribution for the entity R_2. This inferential model can obtain the posterior density function about the rupture diameter relating it with both its prior distribution and the likelihood function about the available observations.

$$\pi(\varphi \mid \mathbf{O}) = \frac{\ell(\varphi \mid \mathbf{O})\pi(\varphi)}{\Lambda},\ \text{where}\ \Lambda = \int \ell(\varphi \mid \mathbf{O})\pi(\varphi)d\varphi \quad (4)$$

$\ell(\varphi \mid O) = p(O \mid \varphi)$ - likelihood function about the evidence $\mathbf{O}$

$\pi(\varphi),\ \pi(\varphi \mid O)$ - prior and postrior density functions

Λ – normalizing constant

$O \equiv [O_G, O_I]$ – a set of more or less relevant observations about the entity R_2;

The set of observations includes generic data, OG, and more relevant data about ruptures of identical tanks - OI. The source of generic information for the study is the (HSE, 2000) and data here used are listed in the appendix. Due to the lack of reliable data for the size of cracks on identical tanks the set $O_I \equiv [2, 5, 10]$ in [mm] is applied in order to show how the inferential model works.

The Bayesian theorem is applied two times. On the first stage the evidence O_G is used to specify the generic posterior distribution. On the second stage the generic posterior distribution is updated by means of the data set O_I coming from identical units. Hierarchical Bayesian models are used on every one of these stages. A huge number of references are dedicated to the theoretical aspects of Bayesian models with hierarchical structure, like (Browne&Draper, 2000), (Gelman&Pardoe, 2006) etc. The application of Bayesian inference at various practical problems is also considered in many works, for example (Esner et al., 2004), (Argirov, 2006) and so on.

The multilevel model used has the following structure:

$\beta \sim gamma(\alpha_1, \mu_1)$; where α_1, μ_1 are constants

$$\sigma \sim \text{uniform}(\alpha_2, \mu_2);\ \text{where } \alpha_2, \mu_2 \text{ are constants}$$

$$\pi(\varphi) \equiv \pi(\beta, \sigma)$$

$$\ell(\varphi \mid \mathbf{O}_L) \sim \text{Normal}(\beta, \sigma \mid \mathbf{O}_L);\ \text{for } L = G, I \qquad (5)$$

The constants α_1, α_2, μ_1, μ_2 are chosen in such a manner that the distributed parameters β, σ identify our prior believe about the variability of the hole diameter. Then, under the assumption that the likelihood functions for all separate observations belong to the lognormal family, the parameters β, σ are updated by using first the evidence O_G and then the data O_I. Although, the hierarchical model here presented is not the best one, it demonstrates well enough how the uncertainty about the entity R_2 is addressed.

The computer code WinBUGS (Spiegelhalter et al., 2003), (Woodward, 2005) is used to solve this multilevel inferential model. The generic prior, the generic posterior and the tank specific posterior density functions are presented on figures 1, 2 and 3 respectively. Some characteristics of these distributions are listed in table 1. Table 1 shows that as far as the evidence O is relevant to our case we can be 97.5% sure that the hole's diameter is smaller than 14.5 mm.

Therefore, we can specify that $P(0 < R_2 \leq 8.44)=0.75$, $P(8.44 < R_2 \leq 14.5)=0.225$ and $P(R_2 > 14.5)=0.025$.

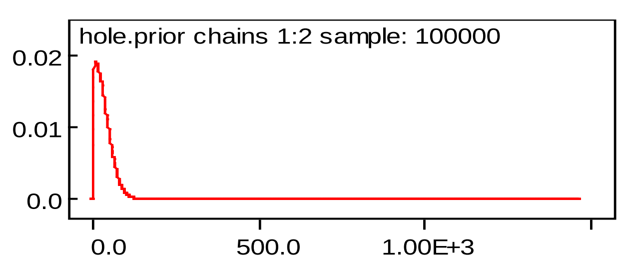

Fig. 1. Generic prior distribution

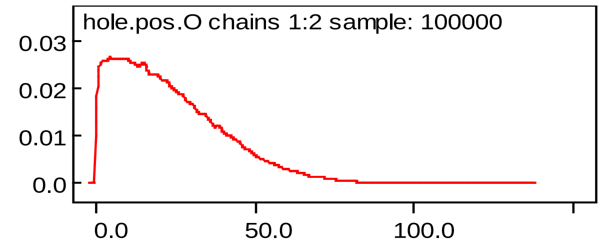

Fig. 2. Generic posterior (specific prior) distribution

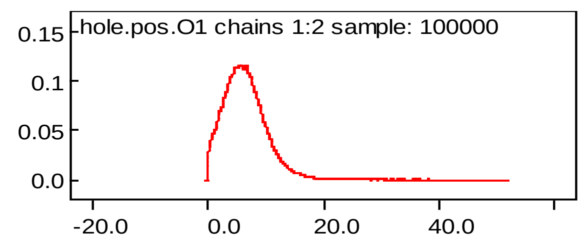

Fig. 3. Specific posterior distribution

Table 1: Distributions about the diameter of the hole

Distribution about the hole diameter in [mm]	2.5%	50%	75%	97.5%
Generic prior (hole.prior)	1.29	27.4	46.6	104.3
Specific prior (hole.pos.O)	0.95	19.8	33.2	63.2
Specific posterior (hole.pos.O1)	0.66	6.04	8.44	14.5

Quantitative characteristics of the release scenarios

For the tank of investigation it is easy to figure out that the bigger accidental release rates are associated with a sub-area of its wall that is closest to the ground. These parts of the wall surface are analyzed by the following events:

$$E_{1,1,[1,K2],L} \equiv ({}^{1}T_h[0] \in [5^o, 25^o]) \cap ({}^{1}h[0] \in (2.4, 3]) \mid ([{}^{1}Y, {}^{K2}\theta], {}^{L}R_2)$$
$$E_{2,1,[1,K2],L} \equiv ({}^{2}T_h[0] \in [25^o, 45^o]) \cap ({}^{2}h[0] \in (2.4, 3]) \mid ([{}^{2}Y, {}^{K2}\theta], {}^{L}R_2)$$

for K_2 varying from 1 to 6 as first L=1 and then L=2.

All of these events, consider release scenarios for which the parameter h[0] varies in the range

[2.4, 3] in [m] and the velocity $u_h[0]$ falls in the rage [4.86, 5.42] in [m/s].

The events $E_{1,1[1,K2],1}$ and $E_{2,1[1,K2],1}$ represent the random occurrence of ruptures in the tank wall with equivalent diameter smaller than 8.44 [mm]. For both events the value of A_h is smaller than $2.24x10^{-4}$ [m^2] and the chance that it is true is about 0.75 - P(0<R2<8.44)=0.75. The couple of events $E_{1,1[1,K2],2}$ and $E_{2,1[1,K2],2}$ identifies release scenarios for which the value of A_h is in the range [$2.24x10^{-4}$, $6.61x10^{-4}$) and also P(8.44<R2<14.5)=0.225. The chance for random occurring raptures with cross-section of about $6.61x10^{-4}$ [m^2] and above is no more than 0.025.

Let us assume that the tank contains flammable methanol at pressure of 1.3 [bar] whose density and the specified temperatures are: $\rho[5^o]$=805.1, $\rho[25^o]$=786.4 and $\rho[45^o]$=767.4 [kg/s], respectively. Having in mind all listed figures we can conclude that the maximal mass flow rate of interest from the tank at the t=0 is 2.88 [kg/s]. Thus, for the study the following is true:

$$P(E_{1,1,[1,K2],2} \cup E_{2,1,[1,K2],2}) = P(\bigcup_{K2=1}^{6} E_{1,1,[1,K2],2}) + P(\bigcup_{K2=1}^{6} E_{2,1,[1,K2],2}) = 0.0563$$

$$P(\bigcup_{K2=1}^{6} E_{1,1,[1,K2],2}) = P(5^o < T_h[0]) < 25^o)P(\bigcup_{1}^{6} {}^{1,K2}R_1)P(8.44 < R_2 < 14.5)$$

$$P(\bigcup_{K2=1}^{6} E_{2,1,[1,K2],2}) = P(25^o < T_h[0]) < 45^o)P(\bigcup_{1}^{6} {}^{1,K2}R_1)P(8.44 < R_2 < 14.5)$$

$$P(T_h[0]) < 25^o) = P(25 < T_h[0]) < 45^o) = 0{,}5;$$

$$P(\bigcup_{1}^{6} {}^{1,K2}R_1) = 0.25;\ P(8.44 < R_2 < 14.5) = 0.225$$

Thus, no more than about 2.25% of the expected release scenarios may originate with release rate bigger than 2.88 [kg/s]. A fraction of 5.63% of all scenarios is associated with an initial mass release rate varying in the range [0.835, 2.88] [kg/s]. For the tank of study the remaining release scenarios occur with mass flow rate smaller than the figure of 2.88 [kg/s].

4. Conclusions

The paper suggests that the possible impacts on the global climate system due to accidental releases of dangerous substances should be quantified and taken into account. Since the magnitude of such releases is associated with huge uncertainty, specific methodology is required. An easy for implementing in practice approach capable to “measure” the potential of release scenarios to progress further into major accidents, is presented. This methodology allows the fraction of those scenarios which can affect badly certain target land areas, situated in particular directions from a hazardous unit, to be identified. The part of the approach presented in this work is applicable to search for those zones over a defensive barrier, separating hazardous substances from their surroundings, within which risk significant release scenarios can emerge. The information, that even the first stage of the approach here presented finds, can help in ranking by quantitative criteria the areas, in the surroundings of a hazardous unit, which may be polluted seriously. By predicting conservatively the most likely amounts of dangerous substance entering in certain regions around the failed unit the uncertainty about the consequences of likely accidents for people and the environment can be reduced.

References

Argirov, J., 1999, “Estimating the Frequency of Fire Scenario by Means of Improved Apportionment of the Frequency of Fires Associated with Engulfed Ignition Sources”. PSA99 (International Topical Meeting on Probabilistic Safety Assessment, vol. II, held in Washington, DC, USA

Argirov, J., 2006, “Assessing the uncertainty rage about the time to occurrence of a key event based on observations” Proceedings of the 8-th International Conference on Probabilistic Safety Assessment and Management, held in New Orleans, USA

Bier, V., Yi, W., 1995, “The Performance of precursor-based estimators for rare events frequency”. Reliability Engineering and Safety Systems, v.50 p 241-251

Browne, W., Draper, D., 2000, “Implementation and performance issues in the Bayesian and likelihood fitting of multilevel models”. Computational Statistics v.15 p 391-420

Esner, J., Jagger, T., 2004, A Hierarchical Bayesian Approach to Seasonal Hurricane Modelling”. Journal of Climate, v.17 p 2813-2827

EEA, 2008, “Impacts of Europe’s changing climate – 2008 indicator bases assessment”. Joint EEA-JRC-WHO report, EEA report No 4/2088, 248 pages

Gelman, A., Pardoe. I., 2006, “Bayesian Measures of Explained Variance and Pooling in Multilevel (Hierarchical) Models”. Technometrics, 2006, v.48 No. 2 p 241-251

IAEA, 2006, “Environmental Consequences of the Chernobyl Accident and their Remediation: Twenty Years of Experience”. Report of the Chernobyl Forum Expert Group “Environment”

HSE, 2000, ”Offshore technology report OTO 1999-079, Offshore Hydrocarbon Releases”

HSE, 2004, “A critical review of post Piper-Alpha developments in explosion science for the Offshore Industry”. prepared by Firebrand International Ltd.

Hawksley, J., 1999, “Developing a Major Accident prevention policy”. Journal of Hazardous Materials, v.65 p 109-121

Hansel, J. et al. 2005, “Earth’s Energy Imbalance: Confirmation and Implication”. Science, v.308, p 1431-1435

Kirchsteiger, C., 1999, “Trends in accidents, disasters and risk sources in Europe”. Journal of Loss Prevention in the Process Industries v.12 p 7-17

Khan, F., Abbasi, S., 1997, “Accident Hazard Index”. Process Safety and Environmental Protection. v.75 p 217-224

Mitchison, N., Papadakis G., 1999, “Safety management system under Seveso II: Implementation and assessment”. J. of Loss Prevention in the Process Industries, v.12, p 43-51

Robert, C., 2004, “The Bayesian Choice, From Decision-Theoretic Foundations to Computational Implementation”. Second ed. Springler

Rohde, R., et al. 2011, “Berekely Earth Temperature Averaging Process”. report Available at:

http://berkeleyearth.org/pdf/berkeley-earth-averaging-process.pdf

Spiegelhalter, D., et al. 2003, “WinBUGS Version 1.4 Users Manual”. MRC Biostatistics Unit, Cambridge

Woodward, P., 2005, “Bugs: Bayes for the Common Man”. J. of Statistical Software, v.14, N.5, p 1-15

Appendix

Generic evidence - OG for failures of units operating with liquids (based on HSE, 2000)

No (year)	System	Equivalent hole [mm]
1 (92-93)	Utilities Oil; Heat transfer Oil	3
2 (93-94)	Gas Compressor lubricating Oil	25
3 (93-94)	Gas Compressor lubricating Oil	1
4 (92-94)	Gas Compressor lubricating Oil	1
5 (93-94)	Condensate methanol	50.8
6 (93-94)	Processing Methanol	20.4
7 (93-94)	Dehydration of Glycol	10
8 (93-94)	Dehydration of Glycol	12.7
9 (93-94)	Power gen. turbine, Diesel released	6.7
10 (93-94)	Utilities, Oil, diesel	25.4
11 (93-94)	Utilities, Heat transfer oil	9.53
12 (93-94)	Power gen. turbine, Oil released	1.0
13 (93-94)	Separation, Oil test	12.7
14 (93-94)	Flare, Condensate released	76.2
15 (93-94)	Processing, LPG released	12.7
16 (94-95)	Export, Oil released	1.0
17 (94-95)	Gas Compression, Lub. Oil released	12.7
18 (94-95)	Gas Compression, Lub. Oil released	1.0
19 (94-95)	Gas Compression, Lub. Oil released	1.0
20 (94-95)	Gas Compression, Lub. Oil released	1.0
21 (94-95)	Processing, Glycol released	2.0
22 (94-95)	Dehydration of Glycol	1.0
23 (94-95)	Dehydration of Glycol	1.0
24 (94-95)	Dehydration of Glycol	1.0
25 (94-95)	Power Gen. turbine, Diesel released	5.0
26 (94-95)	Utilities Oil, Heat transfer Oil	1.0
27 (94-95)	Utilities Oil, Heat transfer Oil	1.8
28 (94-95)	Utilities Oil, jet fuel	1.0
29 (94-95)	Power Gen. turbine, Diesel released	11.8
30 (94-95)	Power Gen. turbine, Diesel released	11.8
31 (94-95)	Power Gen. turbine, Oil released	25.4
32 (94-95)	Treatment of (H2S/CO2), Condensate	25.4
33 (95-96)	Gas Compression, Lub. Oil released	1.0
34 (95-96)	Gas Compression, Lub. Oil released	2.7
35 (95-96)	Dehydration of Glycol	1.0
36 (95-96)	Power Gen. turbine, Diesel released	1.0
37 (95-96)	Utilities, Diesel released	2.3
38 (95-96)	Heat transfer Lub. Oil released	1.0
39 (95-96)	Heat transfer Lub. Oil released	38.1
40 (96-97)	Export Lubrication Oil	1.0
41 (96-97)	Power Gen. turbine Lub. Oil released	5.4
42 (96-97)	Power Gen. turbine, Diesel released	1.0
43 (96-97)	Utilities, Diesel released	1.0
44 (96-97)	Utilities, Diesel released	1.0
45 (96-97)	Utilities, Diesel released	12.7
46 (96-97)	Utilities, Diesel released	12.7
47 (96-97)	Utilities, Diesel released	12.7
48 (96-97)	Utilities, Diesel released	1.0
49 (96-97)	Utilities, Diesel released	1.0
50 (96-97)	Utilities, Diesel released	1.0
51 (96-97)	Import, Condensate released	1.0
52 (97-98)	Utilities, Diesel released	1.0
53 (97-98)	Utilities, Diesel released	3.0
54 (97-98)	Utilities, Diesel released	1.0
55 (98-99)	Gas Compression, Lub. Oil released	5.0
56 (98-99)	Dehydration of Glycol	1.0
57 (98-99)	Power Gen. turbine, Lub Oil released	1.0
58 (98-99)	Power Gen. turbine, Lub Oil released	1.0
59 (98-99)	Power Gen. turbine, Lub Oil released	5.0
60 (98-99)	Power Gen. turbine, Oil released	3.2
61 (98-99)	Power Gen. turbine, Lub Oil released	1.0
62 (98-99)	Utilities, Diesel released	1.0
63 (98-99)	Utilities, Diesel released	1.0
64 (98-99)	Utilities, Diesel released	1.0
65 (99-00)	Utilities, Diesel released	1.4
66 (99-00)	Utilities, Diesel released	1.0
67 (99-00)	Utilities, Diesel released	1.4
68 (99-00)	Power Gen. turbine, Lub Oil released	1.9

ценивая Риск Загрязнения из-за Ненормального Поведения Опасной Установки

Др. Джулай Argirov

e-mail: argirov@inrne.bas.bg

Адрес: Институт Ядерных Исследований и Ядерной Энергетики, 17 84 София, Болгария

Резюме: Наше нынешнее понимание, заключается в том, что с 18-го века многие виды деятельности человека способствуют многозначительно изменениям в глобальной климатической системе. Количество опасных установок в использовании и их разнообразие резко увеличилось в течение последних 60 лет. Каждый из этих технологических объектов является потенциальным источником крупных несчастных случаев, с огромными или катастрофическими воздействиями на почву, атмосферу, качество воды, экосистемы и непосредственно на здоровье человека. В статье кратко комментируется подход к решению неопределенности в отношении неприемлемых последствий которые ожидаются от особенного опасного объекта. Первый этап подхода обсуждается в исследовании конкретного случая (кейс стади). Эта часть методологии способна искать и классифицировать те, вероятно, ненормальные ситуации с высоким потенциалом к дальнему прогрессу в несчастных случаях.

Ключевые слова: Опасные установки, технологический риск, сценарии основного выпуска.

A POD model for the concentration fluctuations of gases instantaneously released in the atmosphere

Anastasios ANTYPAS (corresponding author)

Tel. and fax: (210)8991372, e-mail: t_antypas@yahoo.com

Address: 4, Pringipos Petrou St. 16673 Voula, Attiki, Greece

John BARTZIS

Address: University of West Macedonia, Dept. of Mechanical Engineering,

Salvera & Bakola St., 50100 Kozani, Greece

Abstract: In this work, the concentration signal of repeated instantaneous releases of hazardous gases into the atmosphere is decomposed into its principal components by means of the Proper Orthogonal Decomposition (POD) with the dual purpose of reconstructing it from its first (most energetic) components and predicting it in cases sharing common features with the cases from which those features were extracted by applying the POD. The analysis showed that a model can be constructed by interpolation in the range of varied parameters. The important issue of the uncertainty associated with the proposed POD model is discussed and a measure of uncertainty is provided.

Keywords: concentration, dispersion, prediction.

1. Introduction

In cases where a polluting substance is released into the environment, the need for assessing the consequences of its release arises. The question of the extent of the impact caused may be posed by governmental agencies or private operations administrations, relating the extent of the impact to regulatory directives or legal actions or both. In particular, referring to the case of hazardous (toxic or flammable) gases being released into the atmosphere, in order to quantify the environmental impact of such releases, mathematical models are constructed and employed that describe the physical process of dispersion of the released substances into the atmosphere, as well as the chemical processes involved.

Such models have been introduced decades ago and since then are being continuously improved as research carries on. The aim is to improve the accuracy of the model performance by taking into account the factors that affect it. Such factors include the fundamental physics and chemistry associated with the phenomenon of the dispersion of the released substance, as well as the mathematical and statistical techniques applied to describe the phenomenon.

1.1. *Physical and mathematical - statistical background*

In this study no chemical reactions will be considered, so the concentration of the pollutant in question will be treated as a passive scalar. In such a case, the concentration $\Gamma(\boldsymbol{x},t)$ at position $\boldsymbol{x}$ and time t

is determined by two processes: advection by a turbulent flow with velocity field Y(x,t), and molecular diffusion with constant diffusivity k. Γ obeys the equation

$$\frac{\partial \Gamma}{\partial t} + Y.\nabla\Gamma = k\nabla^2\Gamma \qquad (1)$$

where Y satisfies the Navier-Stokes equations with the incompressibility condition ∇.Y = 0 (Monin & Yaglom vol.1, 1971).

Since all the flows encountered in the real world are turbulent, Y and hence Γ, are random (or *stochastic*) fields. That means that their values at a given location x and at a given time instant t cannot be predicted and vary from realisation to realisation, in antithesis to predictable quantities like time or space averages or *rms* concentration values often considered in practical applications. Hence, a probabilistic approach should be followed.

The probability density function (PDF) of the concentration field Γ($\mathbf{x}$,t), denoted by $p(\theta;\mathbf{x},t)$, is defined by

$$p(\theta;\mathbf{x},t)=\frac{d}{d\theta}\{P[\Gamma(\mathbf{x},t)\leq\theta]\} \qquad (2)$$

for all $\theta\geq 0$. The variable θ ranges over all the possible values Γ($\mathbf{x}$,t) can take.

P[Γ($\mathbf{x}$,t) ≤ θ], the probability that Γ($\mathbf{x}$,t) ≤ θ is the proportion of realisations forming the *ensemble* of realisations for which Γ($\mathbf{x}$,t) ≤ θ. Being a probability measure, $p(\theta;\mathbf{x},t)$ satisfies

$$\int_0^\infty p(\theta;\mathbf{x},t)d\theta = 1 \qquad (3)$$

Then, the expected value (or ensemble mean) and the variance of Γ($\mathbf{x}$,t) are defined in the usual way, by

$$\mu(\mathbf{x},t)=E[\Gamma(\mathbf{x},t)]=\int_0^\infty \theta p(\theta;\mathbf{x},t)d\theta \qquad (4)$$

and

$$\sigma^2(\mathbf{x},t) = \mathrm{var}[\Gamma(\mathbf{x},t)] = \int_0^\infty [\theta - \mu(\mathbf{x},t)]^2 p(\theta;\mathbf{x},t)d\theta = \int_0^\infty \theta^2 p(\theta;\mathbf{x},t)d\theta - [\mu(\mathbf{x},t)]^2 \qquad (5)$$

respectively. The square root of the variance denoted by $\sigma(\mathbf{x},t)$ is the standard deviation of the concentration, otherwise known as the *rms concentration fluctuation.* Higher central moments are defined in analogy to eq.(4) with a suitable choice of the exponent. The time evolution equations of the PDF, mean and variance of concentration are given by Chatwin (1990).

The true values of these parameters are unknown, therefore in practice, in order to estimate them one must draw a random sample from the *ensemble* of realisations and compute statistics to be used as estimators of the aforementioned parameters.

1.1.1. *The mean concentration*

From a sample of n realisations $\Gamma_i(\mathbf{x},t)$ one may compute the sample mean,

$$\overline{\Gamma}_n(x,t) = \frac{1}{n}\sum_{i=1}^{n}\Gamma i(x,t) \qquad (6)$$

defined as the arithmetic mean of the data (the subscript n is often omitted). This is itself a random variable (it varies as the sample is varied with respect to its size as well as with respect to the experimenter's choice of values of the varied parameters). When used as an estimator of $\mu(\mathbf{x},t)$, it possesses the property of *unbiasedness,* as well as that of *least variance,* hence being referred to as the *best unbiased estimator* of the mean (Arnold, 1990; p.264). Notably, in the limit as $n\to\infty$, eq. (5) provides

$$\mu(\mathbf{x},t)=\lim_{n\to\infty}\overline{\Gamma}_n(\mathbf{x},t) \qquad (7)$$

Often, when data are not available, the mean concentration is modelled with a Gaussian, which provides a reasonably good approximation some time after release (Hanna and Drivas, 1987).

However, although the sample mean suggests itself as an important measure in estimating concentrations of harmful substances dispersing in the atmosphere under realistic conditions, it does not *per se* establish a panacea in that regard. The reason is that a predictive concentration model should also incorporate concentration fluctuations, measured by the concentration *rms* as defined above, since in many cases the standard deviation of concentration is as large as its mean or even larger (Chatwin, 1982).

1.1.2. The variance of concentration

The sample variance of the concentration field, defined by

$$s_n^2 = \frac{1}{n-1}\sum_{i=1}^{n}[\Gamma i(x,t) - \overline{\Gamma}_n(x,t)]^2 \qquad (8)$$

is an *unbiased* estimator of the ensemble concentration variance, not possessing though the property of least variance (Arnold, 1990; p. 266). Further, the statistical noise it contains (being a random variable) is likely to be greater than that of the sample mean.

A very important contribution in the direction of modelling the concentration variance in the context of turbulent diffusion was the introduction of the Chatwin – Sullivan collapse theory (Chatwin and Sullivan, 1990), which states that a simple quadratic relationship between the mean and the variance exists, namely

$$\sigma^2 = \beta^2 \mu(\alpha\mu_0 - \mu) \qquad (9)$$

where β and α are scalar non-dimensional parameters and μ_0 is a scale for μ (e.g. its maximum).

The above equation fits well data taken from steady continuous sources for which the statistical properties of the concentration field are stationary. In these cases α and β must both be constants satisfying $1<\alpha$ and $0<\beta<1$. For instantaneous releases though, for which the statistical properties of the concentration field are non-stationary, α, β and μ_0 must be functions of downwind receptor position and time. More on mathematical models for α and β can be found in Sullivan (1990), Moseley (1991), Mole (1995), Mole *et al*. (1997) as well as in Mole *et al.* (2007).

1.2. Stochastic concentration models – motivation for use of Principal Components Analysis

The development of mathematical models predicting, ideally the PDF, or less ambitiously, the mean and variance of the concentration field has been and carries on being a major area of research as already pointed out by Chatwin and Sullivan (1994).

The main reason is that such models are much less costly than most deterministic ones, exhibiting at the same time a very good performance, often superior to that of deterministic ones that need vast computing power (unavailable in the reasonably near future) for the large number of direct numerical simulations required. They also tend to replace Gaussian models which due to the many unrealistic assumptions they include are becoming obsolete. Mole, Chatwin and Sullivan (1993) provided a detailed account on different modelling approaches, as well as methods for assessing model performance.

Hanna and Drivas (1987) also declared emphatically the need for development of concentration fluctuation models in their detailed synopsis, adding the imperative requirement of inclusion of the uncertainty assessment that should accompany the model, without which use of the model should be avoided.

Here, the less ambitious direction will be followed, i.e. the proposed model will restrict itself to describing the variance of the concentration field, with the mean being estimated by eq. (6). The methodology proposed is based on the decomposition of the covariance matrix of the concentration field into its principal components. It has been used to identify and describe the coherent structures of turbulent flows by analysing the velocity field Y into a series of orthogonal functions (principal components) possessing the property of *optimal convergence* with success (Berkooz *et al.*, 1994; Kevlahan *et al.,* 1994; Holmes *et al.,* 1996). The term "optimal" means that only a few of these functions suffice in order to reproduce the original signal, thus playing a key role in the identification of coherent structures. Following an analogous way of thinking, the method is applied here with the hope of extracting from data sets common features characterising the process of turbulent dispersion of a passive scalar, in particular the concentration field. In such a case it would be possible to reconstruct the concentration field or make predictions based only on a few orthogonal functions whose shape would bear the common features mentioned above.

2. The problem and the proposed methodology

The problem addressed here is stated as follows:

Given as input

(a) the dimensions of a gaseous pollutant source with finite dimensions e.g. the cylinder radius R_0 and the cylinder height L (which is taken to be the length scale of the problem), in the case of a cylindrical source;

(b) the initial gas density $\rho_{gas} \Rightarrow g' = g\Delta\rho/\rho = g(\rho_{gas} - \rho_{air})/\rho_{air}$,

(c) the mean wind speed U at source height,

(d) the mean concentration field;

describe and predict the temporal evolution of the concentration of the instantaneously released gas in the atmosphere, at some position downstream.

The proposed methodology is the Proper Orthogonal Decomposition (POD), or Principal Components Analysis, presented in Holmes *et al*. (1996), the basis of the analysis of the velocity field into its principal components that provides an optimal, low-dimensional model.

2.1. POD of concentration field

Consider an ensemble $\{\Gamma_i(t)\}$ of concentration fields, each being defined in the domain $0 \le t \le T$ and thought of as a point in an infinite dimensional Hilbert space L^2 $([0,T])$ with inner product

$$(f,g) = \int_0^T f(t)g(t)dt \quad (10)$$

The evolution in time of such a concentration field is, as already mentioned, governed by eq.(1).When the Reynolds number Re=UL/ν >> 1 (U is the mean wind velocity, L is the characteristic length scale and *ν* the molecular viscosity), the flow is turbulent (Monin & Yaglom vol. 1, 1971), so **Y** and, consequently, Γ_i are random variables.

Hence, a statistical description of the physical phenomenon of turbulent diffusion is necessary, as discussed in the introduction.

To that end, the non-dimensional *concentration fluctuation* is defined as

$$F_i(t) = \frac{\Gamma_i(t)}{\Gamma_0} - \mathrm{E}\left[\frac{\Gamma_i(t)}{\Gamma_0}\right] = C_i(t) - \mathrm{E}[C_i(t)] \quad (11)$$

where Γ_0 is a typical concentration scale so that the value of *C(t)* is a non-dimensional concentration representing the data set, and $\mathrm{E}[.]$ denotes an "ensemble" average.

Thus *F(t)* is non-dimensional with E[*F(t)*]=0. The purpose here is "to find a basis $\{\varphi_j(t)\}_{j=1}^{\infty}$ for L^2 that is optimal for the data set in the sense that finite-dimensional representations of the form

$$F^{(N)}(t) = \sum_{j=1}^{N} a_j \varphi_j(t) \quad (12)$$

describe typical members of the ensemble better than representations of the same dimension in any other basis" (Holmes *et al*., 1996).

In this context, the optimality problem is stated as:

$$\text{find} \max E[|(F(t),\varphi(t))|^2]$$

subject to $\|\varphi\|^2 = 1$

where $\|.\|$ is the standard norm in L^2,

$$\| f\| = (f,\ f)^{\frac{1}{2}} = [\int_0^T f^2(t)dt]^{\frac{1}{2}} \qquad (13)$$

from eq. (10).

Introducing a Lagrange multiplier λ, the functional

$$J[\varphi] = E[|(F,\varphi)|^2] - \lambda(\|\varphi\|^2 - 1) \qquad (14)$$

is constructed and the extremum condition

$$\frac{d}{d\delta} J[\varphi + \delta\psi]\ |_{\delta=0} = 0 \qquad (15)$$

is imposed, where $\varphi + \delta\psi \in L^2([0,T]), \delta \in R$, is a variation of φ.

Solving the extremisation problem it is found that the optimal basis is given by the eigenfunctions $\{\varphi_i\}$ of the covariance of concentration (Holmes *et al.*, 1996). In the finite dimensional case, where the observations $\{C_i\}$ are m-vectors (where m is the number of sampled time points), the eigenvectors $\{\varphi_i\}$ are the principal components of the mxm concentration covariance matrix. Furthermore, the eigenfunctions φ_j are mutually orthogonal in L^2 being basis vectors:

$$\int_0^T \varphi_i(t)\varphi_j(t)dt = 0, i \neq j \qquad (16)$$

Assuming no degeneracy of the eigenvalues, that is:

(i) $\lambda = 0$ is not an eigenvalue;

(ii) no multiple eigenfunctions for a given eigenvalue;

and from $\lambda_j \geq 0$, we may order the eigenvalues:

$$\lambda_j > \lambda_{j+1}. \qquad (17)$$

Then, F(t) may be reproduced by a modal decomposition based on the eigenfunctions $\{\varphi_j(t)\}_{j=1}^{\infty}$:

$$F(t) = \sum_{j=1}^{\infty} a_j \varphi_j(t) \qquad (18)$$

where

$$a_j = \int_0^T F(t)\varphi_j(t)dt \qquad (19)$$

Equation (18) is called the POD, $\{\varphi_j(t)\}$ are the empirical orthogonal functions (EOF), $\{\lambda_j\}$ are the empirical eigenvalues and the (random) constants a_j are the expansion coefficients with the following statistical properties:

$$E[a_j] = \int_0^T E[F(t)]\varphi_j(t)dt = 0 \qquad (20)$$

and

$$\text{cov}[a_i, a_j] = E[a_i a_j] = \lambda_i \delta_{ij} \qquad (21)$$

Thus, the expansion coefficients a_j are uncorrelated and

$$\text{var}[a_j] = \lambda_j$$

Also,

$$\text{var}[F(t)] = \frac{1}{\Gamma_0^2}\text{var}[\Gamma(t)] = \sum_{i=1}^{\infty} \lambda_i \phi_i^2(t) \qquad (22)$$

If eq. (16) can in practice be strengthened to $\lambda_j >> \lambda_{j+1}$, in which case only a few modes will suffice to reproduce the original signal accurately, so that eq. (18) can be replaced by eq. (12), the model will be of great value for describing the data and possibly for making predictions.

Finally, when the domain of $\{\Gamma_i(t)\}$ is not bounded, as in the case of open flows considered here, it will be assumed that $\Gamma_i(t)$ decays rapidly to zero outside some bounded domain [0,T], when no measurements exist for $t>T$, where T is the length of the record of the experiment, so that the above analysis is still valid.

3. The experiments and the data

The data used here to carry out the POD were collected in the course of the experiments of Hall *et al*. (1991) which modelled the Thorney Island (UK) trials at 1/100 scale. The experiment corresponds to the sudden release of a heavy gas in the neutrally buoyant atmospheric boundary layer over a flat terrain. The apparatus used consisted of a cylinder of *height L=13cm and diameter 14cm that collapsed* upon release of its content, a dense contaminant gas, in a wind tunnel. The Richardson number R_i, characterising the gas, is defined by $R_i = g\Delta\rho L/\rho U^2$, where $\Delta\rho/\rho$ is the relative to air gas density and U the mean air velocity at the top of the cylinder. The values of *Ri* were 0, 0.5, 1, 2, 5, 10. Values of *Ri* close to zero indicate a neutrally buoyant gas, while higher values characterise heavier (denser-than-air) gases. 50 releases were made with the two highest values of R_i and 100 with the rest. Four sensors were used to record the gas concentration signal, located at 70 and 200cm along the centre-line, at heights of 0.4 and 2.4cm above the ground. In this paper, the four measuring positions are denoted by X1(70,0,0.4), X2(70,0,2.4), X3(200,0,0.4), X4(200,0,2.4). The near-field sensors at positions X1 and X2 monitored gravitational effects dominating close to the source, while the far-field sensors located at positions X3 and X4 captured atmospheric turbulence effects at a further downwind location where the gas concentration was 2% of the initial concentration upon release. Typical release plots with R_i=0 are provided in Hall et al. (1991).

The POD is applied here to the time series obtained from the experiments of Hall *et al.* described above, with the purpose of investigating the possibility of obtaining a universal model for the description of the data, as well as a predictive tool with varying parameters R_i, downwind distance from the source and height from the ground.

4. Data analysis

4.1. Comments on eigenfunctions

The sequence of resulting eigenvalues λ_i (shown in Table 1) of the concentration covariance matrix appears to satisfy $\lambda_i >> \lambda_{i+1}$ in agreement with the discussion in section 2.1. The first eigenfunction, corresponding to the largest eigenvalue, resembles a typical replication

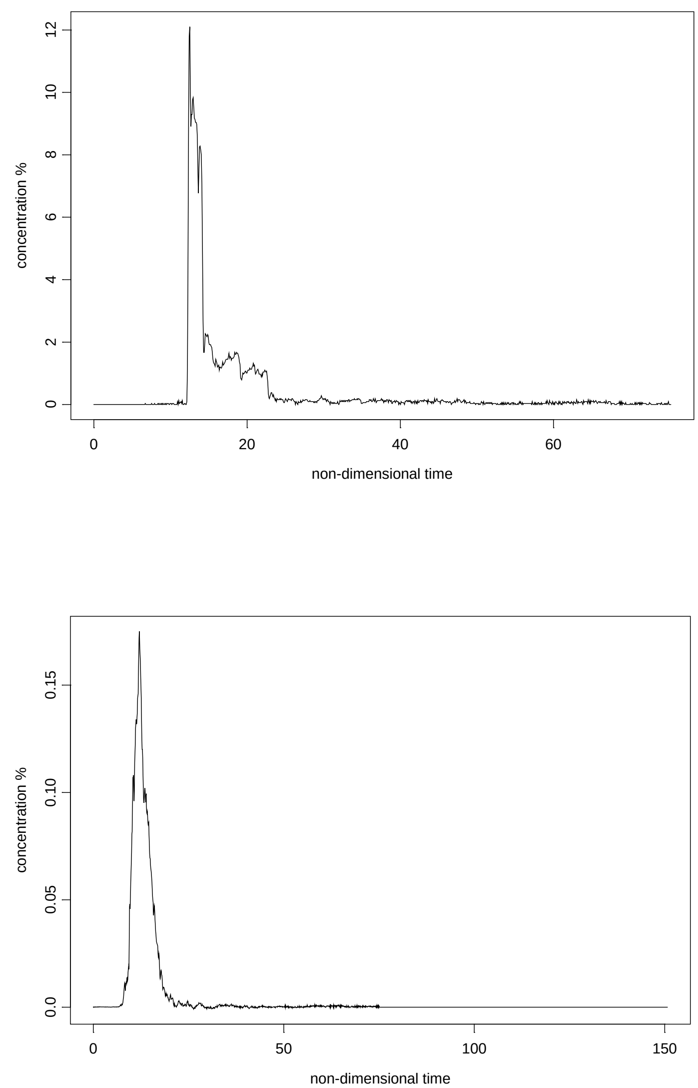

Fig. 1. Typical release (top) and first concentration eigenfunction (bottom) with Ri=0; position X.

(see Figure 1) since it carries the largest variance proportion because

$$\text{var}[F(t)] = \sum_{i=1}^{\infty} \lambda_i \phi_i^2(t) \approx \lambda_1 \phi_1^2(t) \quad (23)$$

from eqs. (12) & (22), and since the plot of concentration standard deviation against time resembles that of mean concentration. Also, the fact that the plot of concentration standard deviation against time resembles that of mean concentration more with decreasing Richardson number, and particularly so for R_i=0 (Robinson, 1996), suggests that it may be possible to obtain a universal POD model for neutrally buoyant gases.

Table 1: Normalised concentration eigenvalues (relative variance proportion) corresponding to the first four eigenfunctions (modes).

R_i	Station	Normalised Eigenvalues			
0	**X**1	0.438	0.142	0.090	0.066
	X2	0.220	0.150	0.130	0.080
	X3	0.397	0.205	0.074	0.057
	X4	0.213	0.148	0.080	0.070
0.5	**X**1	0.458	0.159	0.089	0.059
	X2	0.198	0.127	0.085	0.059
	X3	0.481	0.195	0.079	0.043
	X4	0.289	0.129	0.065	0.051
1	**X**1	0.389	0.152	0.072	0.044
	X2	0.146	0.103	0.079	0.063
	X3	0.516	0.172	0.080	0.044
	X4	0.257	0.121	0.078	0.054
2	**X**1	0.475	0.171	0.093	0.045
	X2	0.207	0.156	0.083	0.054
	X3	0.609	0.126	0.057	0.027
	X4	0.202	0.076	0.056	0.040
5	**X**1	0.322	0.178	0.120	0.070
	X2	0.463	0.131	0.082	0.048
	X3	0.504	0.249	0.076	0.033
	X4	0.091	0.074	0.059	0.056
10	**X**1	0.325	0.149	0.099	0.080
	X2	0.117	0.090	0.067	0.062
	X3	0.550	0.290	0.039	0.025
	X4	0.140	0.066	0.056	0.048

The first eigenfunction tends to zero as time tends to infinity, while the long right tails observed in some cases and dealt with in section 4.2 not only do not represent actual concentration measurements (they should be attributed to instrument noise) but may potentially distort the true shape of the eigenfunction, contributing unwanted fluctuations to consequent calculations.

The first eigenfunction's smoothness decreases with Richardson number at the higher measuring stations consistent with the larger degree of intermittency in those cases.

The initial peak characterising measurements of concentration at the three highest Richardson numbers, 2, 5 and 10, at the measuring stations close to the source is exhibited by the first eigenfunction, displaying the existence of a gravity current head at the edge of these gas clouds.

The first eigenfunction's shape widens as the Richardson number increases closer to the ground, indicating that heavier gases spend a larger proportion of time near the ground, again consistent with the gravity current motion induced by these gases.

The shape of the eigenfunction is not affected when reducing the length of record down to 2/3 of the original length. The eigenvalues are almost the same, with small differences in the 3rd decimal. When the record length was reduced to 1/2 the original length, in one case (R_i =10, X3), the first eigenfunction changed slightly and in another case (R_i=5, X4) even less. In these cases, eigenvalues differ to the second decimal. In all cases, eigenvalues are not affected by truncation of record length, when rounded to one decimal. All of the above provides evidence that the shape of eigenfunctions is invariant under record length truncation when the main part of the cloud has passed, so that further measurements do not contribute. Record length appears to have an effect only when the cloud is truncated.

4.2. Normalisation and scaling

In order to be able to transfer results to another scale, so that a universal model can be obtained, the problem of normalisation and scaling of the first eigenfunctions of concentration covariance is addressed:

By applying an appropriate transformation to the eigenfunctions defined in section 2.1, it is hoped that their shapes will collapse to a common universal shape, thus removing the dependence on varied parameters. Then, by inverting the transformation, it would be possible to reproduce an eigenfunction based on the universal shape obtained, thus enabling one to transfer to another scale. That would lead to a simple model for describing the data and for making predictions. The eigenvectors φ_i ,i=1,…,N of the concentration covariance matrix defined in section 2.1 are normalised as

$$\int_0^T \phi_i^2 dt = 1 \qquad (24)$$

To obtain a common universal shape produced by the first (most energetic) eigenfunctions $\varphi_1(t)$, start by defining

$$\mu_t = \int_0^T t\varphi_1^2(t)dt \Big/ \int_0^T \varphi_1^2(t)dt = \int_0^T t\varphi_1^2(t)dt \qquad (25)$$

$$\sigma_t^2 = \int_0^T (t-\mu_t)^2\varphi_1^2(t)dt \Big/ \int_0^T \varphi_1^2(t)dt = \int_0^T (t-\mu_t)^2\varphi_1^2(t)dt \qquad (26)$$

$$\psi_1(s) = \sigma_t \phi_1(t) / A \qquad (27)$$

$$s = \frac{t-\mu_t}{\sigma_t} \qquad (28)$$

$$A = \int_0^T \phi_1 dt, \qquad (29)$$

$$\int_{t=0}^{t=T} \psi_1(s)ds = \int_0^T \varphi_1(t)dt / A = 1 \qquad (30)$$

where the last equality in both eqs. (25) and (26) is obtained by virtue of eq. (24).

Then, apply the scale transformations under which all scaled eigenfunctions have area equal to 1: where $dt=\sigma_t ds$ from eq. (28) .

The reason for the unusual definition of μ_t and σ_t^2 in eqs. (25) and (26) is that choosing $\varphi_1^2(t)$ as the weight in the definition of μ_t and σ_t^2 , effectively removes the small fluctuations about zero in the long right tail of $\varphi_1(t)$ in experiments which measured much further into the tails, thus resulting in obtaining comparable functions as desired.

The statistics μ_t and σ_t can be interpreted as estimators of the mean signal time and its standard deviation (rms), respectively. In particular, σ_t may be regarded as a measure of the cloud width. Below is provided a physical description of the variation of μ_t and σ_t with Richardson number and spatial position.

a. The variation of μ_t

μ_t gives a central time for the cloud at the measurement position. Therefore this time is the sum of the time the cloud takes to arrive at that point and roughly half the time it takes to pass over that point. The latter contribution will be roughly proportional to σ_t , which measures the spread of the cloud.

Regarding the former contribution, it can be pointed out that comparing values of μ_t with 90%iles of cloud arriving time reported by Hall *et al.* (1991), in principle there is a direct analogy in variation. As Ri increases though, there is a disproportionate decrease of μ_t from the low near to the high near station. Also, for the three heavier gases (R_i=2,5,10) a similar decrease of μ_t is observed from low far to the high far station, which for R_i=5 and 10 is reported for the 90%ile of cloud arriving time too, suggesting that the variation pattern reported is not greatly altered.

Regarding the latter contribution now, as far as variation of μ_t with respect to height is concerned, for the three higher values of R_i (R_i=2,5,10), the cloud spends more time at the lower stations than at the higher ones due to the gravity current-like motion being more pronounced in these cases (heavier gases) and causing velocity shear stress layers between the cloud and the surrounding air (Hunt *et al.*, 1983).

As R_i decreases, this effect is attenuated and particularly for R_i=0, μ_t is almost the same at the lower and higher stations, because a neutrally buoyant gas will diffuse faster than a heavier one that will settle on the ground due to negative buoyancy.

Concerning now the variation of μ_t with respect to downwind distance, for the three lower values of R_i (R_i=0,0.5,1), the cloud spends about twice as much time at the far stations than at the near stations as a result of the larger travel time to the downwind stations. For the three higher values of R_i (R_i=2,5,10), the time the cloud spends at the lower stations is almost tripled going from near to far stations for the same reason as above, the effect being more pronounced for heavier gases though. Also, for all values of R_i>0, one may explain the larger times spent at the downwind stations as a result of the decoupling of the cloud from the ambient flow and its motion downwind at a rate slower than the ambient wind speed.

At the higher stations now, as the cloud moves from the position close to the source (near field) to that away from the source (far field) the amount of time spent is about four times as much because upward diffusive flux dominates over downward flux produced by the mean sinking motion of the cloud (Hunt *et al.*, 1983).

b. The variation of σ_t

In the case of a neutrally buoyant gas (R_i of 0), from near to far stations σ_t increases (more than double) because spreading from turbulent dispersion as well as gravity current spreading has occurred as it moves downstream. As R_i increases, σ_t increases at the stations near the source, which, acting as near-field monitors, record fluctuations occurring during the gravity slumping phase. Thus, heavier gas clouds exhibit a wider profile in time.

At the far stations, σ_t is also increasing with increasing R_i.

A general (all stations), but not striking, exception in the increasing trend of σ_t with R_i is observed when Ri changes from 0.5 to 1. Referring to the Appendix of Hall *et al.* (1991) though, it is seen that plots of typical repetitions also possess this feature. A possible physical explanation is that these values of R_i represent the threshold of the transition from neutrally buoyant to heavier gas behaviour. A notable exception is the decrease of σ_t at position X2 when R_i is changed from 1 to 2. It should also be pointed out that in that case (R_i=2, X2), the first principal component was swapped with the second principal component (its shape resembled the shape of the second principal components produced by the POD).

4.3. Towards a universal model

Application of the normalisation procedure described above gave the normalised first eigenfunctions, which were then matched. The results are summarised in the following plot in the Figure 2, which depicts clearly the most successfully matched first eigenfunctions.

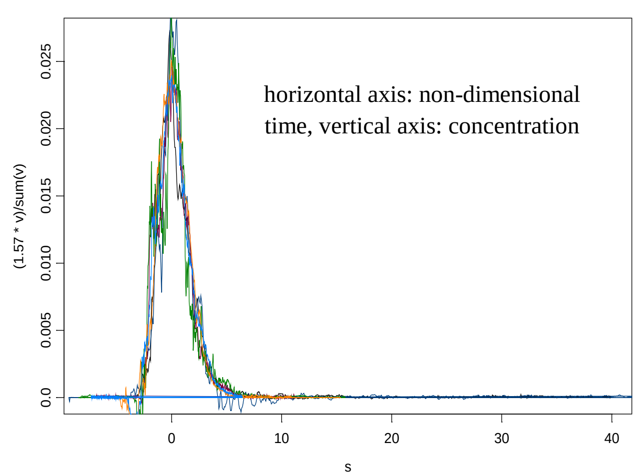

Fig. 2. Matched normalised and scaled first concentration eigenfunctions in cases with R_1=0; all stations and R_1=0.5; lower stations.

Inspection of the collapse of the shape of the first normalised eigenfunctions in Figure 2 suggests that it might be possible to describe the first eigenfunction with R_i=0 at all measuring positions and R_i=0.5 at the two lower positions by a common universal shape, so that one would be able to transfer to another downwind distance or height or Richardson number by inverting the transformations (27) and (28):

$$\phi_1'(\sigma_t s+\mu_t)=\frac{A}{\sigma_t}\psi_1(s) \quad (31)$$

where the left hand side is a predicted first eigenfunction from a given scaled eigenfunction ψ_1.

4.4. Reconstructing the signal

The first eigenfunction (principal component or mode) carries the more coarse features of the signal, since it resembles a typical repetition, the finer details being carried by the next (higher) eigenfunctions.

More specifically, the first eigenfunction, carrying most of the variability represents the largest scale of the fluctuations caused by the biggest eddies. The next eigenfunctions with less and less energy content represent smaller scale fluctuations due to smaller size eddies. According to the “energy cascade” theory (Batchelor, 1953; Tennekes and Lumley, 1972), bigger eddies supply energy to smaller ones in a hierarchical order, until in the final stage of the dispersion process all the energy will have dissipated to heat.

As provided by the theory in section 2.1, the signal can be reconstructed using only a few principal components (eq. (12)) when the sequence of the eigenvalues converges sufficiently rapidly, a condition that is generally satisfied here.

Next, a measure of the accuracy of reconstruction of the concentration signal is provided.

Since the data are conceptualised as vectors in an L^2 space (section 2), it would seem natural to choose an error formula that incorporates the L^2 norm:

The relative error (RE) in the L^2 space is defined as

$$RE_i=\frac{(\sum(C_t-Cr_t)^2)^{1/2}}{(\sum C_t^2)^{1/2}},\, i=1,\ldots,n, \quad (32)$$

where C_i is the observed concentration signal and Cr_i the reconstructed concentration signal from the principal components of the covariance matrix at sampling time *t*.

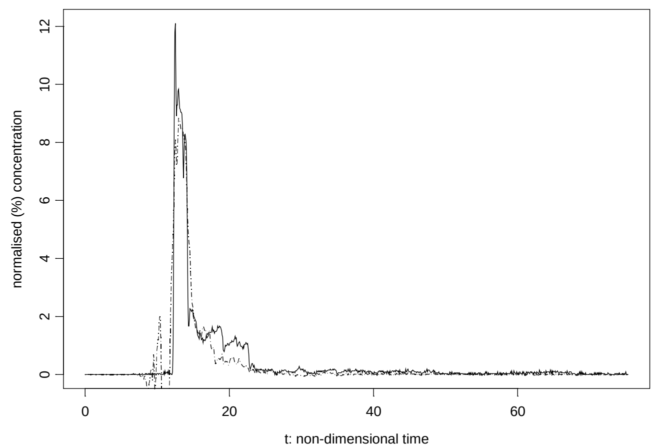

Fig. 3a. Observed (solid line) and reconstructed from first 4 eigenfunctions (dashed line) concentration signal with R_i=0 at position X1. Randomly chosen release.

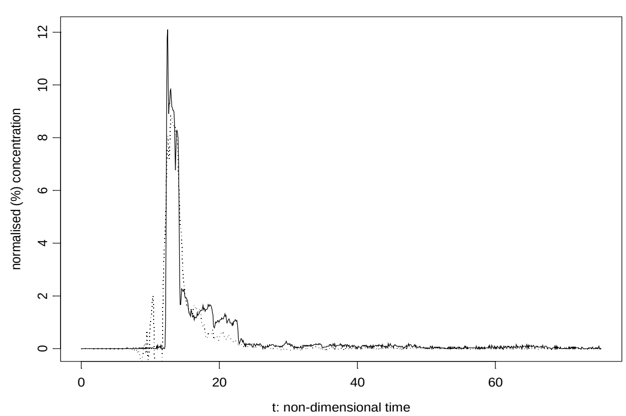

Fig. 3b. Observed (solid line) and reconstructed from first 4 eigenfunctions (dotted line) concentration signal with R_i=0 at position X1. Randomly chosen release.

Table 2: Mean relative error between observed and reconstructed signal using 2 and 4 modes.

R_i	Station	No of modes	MRE
0	X1	2	.41
		4	.34
	X2	2	.50
		4	.42
	X3	2	.32
		4	.26
	X4	2	.48
		4	.43
0.5	X1	2	.33
		4	.27
	X3	2	.60
		4	.50

The mean relative error (MRE) is the sample mean value of RE over all *n* replications:

$$MRE = \frac{1}{n}\sum_{i=1}^{n} RE_i \qquad (33)$$

The reason for choosing RE as the appropriate measure of accuracy of reconstruction of a concentration signal is that from the point of view of the end user of the model, knowing that the MRE is 10 percent means a great deal more than knowing that the mean absolute error is 123 for example (Makridakis *et al.*, 1983, p.47).

Now, from the concentration eigenvalue sequence (see Table 1) is provided an indication that initially the MRE converges relatively fast. This was verified by computing MRE, shown in Table 2, with 2 and 4 modes. When more modes (5 to 12) were included in the reconstruction of the concentration signal, differences in the MRE occurred only in the 3rd decimal place or above, indicating that the rate of convergence of the MRE is much slower beyond the 4th mode.

In the cases where the MRE is small and almost the same (or the same within 1 decimal place) when 2 or 4 modes are used, it is clear that the signal can be reconstructed using the first 2 modes only as discussed also by Kevlahan *et al.* (1994). In those cases the contribution of small scale fluctuations is negligible in the sense that the amount of energy contained in the first 2 eigenfunctions representing the larger scales of motion is sufficient to reproduce the signal fairly well.

The mean relative error (MRE) computed over all replications, between observed and reconstructed signal is shown in Table 2.

In Figure 3, the reconstructed signal from the first four modes is plotted together with the original signal, portraying the good approximation expected from the theory.

4.5. *The distribution of the expansion coefficients*

It is also of interest to discuss the distribution of the coefficients (eq.(19)) in the expansion (18) of the concentration field, and particularly the distribution of a_1 used in the prediction model presented in section 5.

In Figure 4, histograms (with estimated density lines) of the first expansion coefficients are shown in all cases with R_i=0. The sample means are almost zero and the sample variances are almost equal to the respective eigenvalues. The small differences observed between these statistics and the theoretical values of the respective parameters provided by the theory should be attributed to the fact that a finite sample of gas releases was used to produce these results.

Next, the hypothesis that the expansion coefficients come from a normal distribution is tested. The reason behind this particular choice is that normality might be a desirable property related to the practical application of the model, although no such property is prescribed by the theory.

The setting is:
Null hypothesis
H_0:True PDF of coefficients is normal
vs.
Alternative hypothesis
H_1:True PDF of coefficients is not normal.

To carry out this test, an appropriate test statistic and a test criterion must be chosen.

Kolmogorov and Smirnov have developed a normality test in which estimates of the parameters of the normal distribution from the data are used. This test is rather conservative though, in the sense that lower p-values than those computed by the Kolmogorov-Smirnov test can be achieved (Lilliefors, 1967). A more powerful normality test has been proposed by Shapiro and Wilk (Shapiro and Wilk, 1965), based on a variance ratio, that will reject the null hypothesis more often than the more conservative Kolmogorov-Smirnov test.

Carrying out both tests it was found that the more powerful Shapiro-Wilk test rejected the null hypothesis concerning the first expansion coefficient a_1 in the following cases:R_i=0, station X3 (p-value=0.0094); and R_i=0.5, station X1 (p-value=0.0082), while the Kolmogorov-Smirnov test never did.

Further, regarding the question of independence of the first expansion coefficient α_1, Pearson's χ^2 -criterion was employed in order to carry out two hypothesis tests according to the following setting:

(a) Null hypothesis

H_0: α_1 independent with respect to measuring position vs.

Alternative hypothesis H_1: α_1 not independent with respect to measuring position;

(b) Null hypothesis

H0: α_1 independent with respect to Richardson number vs.

Alternative hypothesis H1: α_1 not independent of Richardson number.

In all cases the tests rejected the null hypotheses of independence, thus providing evidence that the first expansion coefficients are not independent with respect to measuring position or Richardson number.

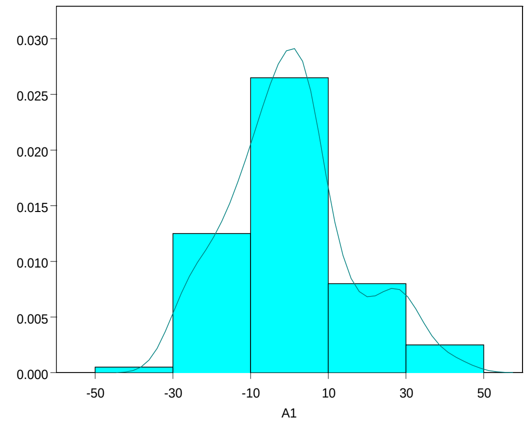

Fig. 4. Histogram with estimated density line of first expansion coefficients α1 for Ri=0 at position X1.

5. Predictive model validation

In this section, a predictive model for the concentration fluctuation field is proposed, based on the results found in the previous sections.

The model is built based on the assumption that the true mean-corrected concentration curve is closely approximated by the first eigenfunction of concentration, given that the first eigenfunction carries most of the variability.

Furthermore, the universal shape of the first eigenfunction obtained in section 4.3 suggests the feasibility of constructing a POD–based prediction model for the case of neutrally buoyant gases (Ri=0 and Ri=0.5).

5.1. The predictive model

The proposed model is

$$F'(t) = a_1'\phi_1'(t) \qquad (34)$$

or, from the definition (eq.(11)) of the concentration fluctuation *F(t),*

$$C(t) = \mu(t) + a_1\phi_1(t) + \varepsilon(t) \quad (35)$$

where dashes denote predictors and

$C(t)$ is the concentration field,

$\mu(t)$= E[$C(t)$] is the mean concentration field,

$\varphi_1(t)$ is the normalised first (most energetic) eigenfunction of concentration,

a_1 is the first expansion coefficient chosen from the PDF of coefficients given and discussed in section 4.5, and

$\varepsilon(t)$ is the POD model error.

Now, since $C(t)$ is a random variable, because of the nature of the phenomenon of turbulent dispersion, any prediction of it would be a prediction of one member of the ensemble of realisations considered. It is more sensible therefore to predict the mean and standard deviation of the ensemble instead, as discussed in the introduction of this work, where the standard deviation is approximated by the square root of $\lambda_1\varphi_1^2(t)$.

Given that the collapse of the first concentration eigenfunction occurred at all measuring stations for R_i=0, and at X1 and X2 for R_i=0.5 (see section 4.3), predictions for the mean concentration (and dose) field can be obtained by means of linear interpolation between values of the varied parameters.

As discussed in the introduction (section 1.1), the sample mean curve is the *best unbiased* estimator of the true mean concentration curve.

The sample mean concentration defined by eq. (6) at a measuring position is computed as

$$\bar{C}(t) = \frac{1}{n}\sum_{i=1}^{n} C_i(t) \qquad (36)$$

where n is the number of repetitions of the experiment.

To assess convergence of the statistic, the data sets were split in half and the sample mean was recalculated with $n/2$ observations. The resulting mean curves were indistinguishable from the ones found using all n observations in agreement with Schopflocher and Sullivan (1997), thus providing evidence that convergence of the statistic was attained.

Furthermore, the proposed model predicts the mean concentration when the *best* estimator of the coefficient a_1 is chosen to be the expected value of the distribution of coefficients - which is found to be zero in agreement with the theory (see section 2.2).

To predict the variance of concentration now, the first eigenvalues and squared first eigenfunctions of concentration must be predicted, so as to form their product as the concentration variance predictor. The method of linear interpolation can be used again as discussed above.

Regarding the question of estimating the first eigenfunction independently of the data, the Chatwin-Sullivan collapse theory (eq. (9)) in combination with the first comments in section 4.1 suggests that the mean concentration (which is easily modelled with a Gaussian) can be used as the predictor of φ_1, thus providing a theoretical predictive model.

5.2 Model uncertainty

As far as the predictive uncertainty is concerned, this is due to three factors:

One is the data input and observations factor, which is not dealt with in this work; the second factor is the mean estimation error and the third one is stochastic or random atmospheric (turbulent) fluctuations characterising the natural phenomenon of dispersion of a pollutant substance (Mole *et al*, 1993).

It is mandatory that any predictive model claiming reliability and completeness must incorporate its uncertainty in the output so as to assist end users in the decision making process.

Since the second and third uncertainty components are uncorrelated by virtue of eq. (20), the total uncertainty of the model is given by the following equation (*mean squared error*; Papoulis, 1965), when data input and observations errors are ignored (Hanna and Drivas, 1987):

$$E\{[C(t)-C'(t)]^2\} = E\{[\mu(t)-\mu'(t)]^2\}$$
$$+E\{[C(t)-\mu(t)]^2\}$$
$$= E\{[\mu(t)-\mu'(t)]^2\} + E\{[a_1\varphi_1(t)]^2\} + E\{[\varepsilon(t)]^2\}$$
$$= [l(t)/2]^2 + \lambda_1\varphi_1^2(t) + Var\{\varepsilon(t)\} \quad (37)$$

where

l(t) is the expected length of the confidence interval for the mean, λ_1 the first eigenvalue,

$\phi_1(t)$ the first normalised concentration eigenfunction and

$\varepsilon(t)$ the POD model error.

The total model uncertainty is reduced when

(a) the expected length of the confidence interval for the mean is minimised;

(b) the first (normalised) eigenvalue approaches 1 so that $\varepsilon(t)$ approaches 0 (see section 4.4).

Regarding (a), the classical approach of the construction of a large sample confidence interval (see for example Arnold, 1990; Roussas, 1973), gives large expected lengths. However, a non-parametric approach that makes no assumptions about prescribed form distributions of the concentration mean, described by Frangos and Antypas (2001), leads to a dramatic reduction of the confidence interval expected lengths.

Regarding the POD model error now, $\varepsilon(t)$, using the definition of the relative error (RE) in the L^2 space introduced in section 4.4 (eq. (32), where C_t is the observed concentration signal and Cr_t the predicted concentration signal now from the POD model at sampling time *t*, it is possible to obtain a measure of $\mathrm{var}\{\varepsilon(t)\}$ by computing the variance of *RE* when Cr_t is "predicted" by eq. (35) for values of the parameters for which C_t has been observed:

$$VRE = \frac{1}{n-1}\sum_{i=1}^{n}(RE_i - MRE)^2 \qquad (38)$$

where *MRE* is given by eq. (33).

Here, of course, the model employs only the first (most energetic) principal component.

The following table (Table 3) summarises the results concerning the model predictors variance in all cases exhibiting common features, that is, the cases with corresponding collapsing first eigenfunctions (R_i=0, all stations and R_i=0.5, low-height stations – see section 4.3).

Table 3: Variance of POD model predictors a_1' *and* $F'(t)=a_1'\varphi_1'(t)$.

R_i	Station	Variance of a_1'	*VRE* of $F'(t)=a_1'\varphi_1'(t)$
0	X1	0.438	0.037
	X2	0.220	0.014
	X3	0.397	0.033
	X4	0.213	0.013
0.5	X1	0.458	0.031
	X3	0.481	0.039

6. Discussion of results and conclusions

In this paper is provided a model for the description and prediction of concentration fluctuations of gases dispersing in the atmosphere. The model describes turbulence fluctuations that charactrerise the physical phenomenon of dispersion of contaminants in the atmosphere (Chatwin, 1981, 1982). Initially it was hoped that by applying the POD method of analysis, a model unifying the common features of neutrally buoyant and heavy gases would be obtained. The research provided in the previous sections did not prove to be all that fruitful, nevertheless:

The proposed model claims *universality* for neutrally buoyant gases with respect to downwind distance and height, as well as for gases close to the threshold between neutral buoyancy and heaviness, with respect to downwind distance.

For these gases predictions can be made, that is, the end user of the model is in position predict the mean concentration with the associated POD model uncertainty will be at a fixed time instant, downwind location, height and Richardson number, the varied parameters taken into account by the model. As far as heavier gases are concerned, physical modelling (box models, as discussed by Andronopoulos (1992) can be employed so as to provide predictive results extending thus the proposed model for the neutrally buoyant gases case.

An important advantage of the model is its *simplicity* in the sense that only a few modes (sometimes only one) suffice so as to describe and predict the concentration field. This is in agreement with the findings of Kevlahan *et al*. (1994).

Among the limitations of the model, except for its inability to incorporate heavier gases, one notes that predictions are limited within the range of the values of the varied parameters because of their small sample sizes; extrapolation beyond these values being thus performed via physical modelling as mentioned above.

Regarding now the estimation of population parameters in the model, the sample mean lends itself as a reliable estimator of the true mean being *unbiased*, while the first eigenfunction's shape can be estimated by the mean concentration. Rice and Silverman (1991) propose smoothing the first eigenfunction via the choice of a smoothing constant by the method of cross-validation, thus counteracting its tendency to track high frequency components not present in the population eigenfunction. This may result in a predictor with smaller expected mean squared error. No attempt was made in this work to apply the smoothing method, for it could be argued that smoothing the first concentration eigenfunction might lead to loss of valuable information concerning turbulence phenomena.

Acknowledgements

This work was supported partially by a grant from the University of Sheffield, UK. The authors would like to thank N. Mole and C. Anderson for useful discussions and comments. The work is dedicated to the memory of P. Chatwin and D. Zafiropoulos.

References

Andronopoulos S. (1992): "A review of vapour cloud dispersion models" Report EUR 143 29 EN

Arnold S.F. (1990): "Mathematical Statistics". Prentice – Hall.

Batchelor G.K. (1953): "The theory of homogeneous turbulence". Cambridge University Press.

Berkooz G., Elezgaray J., Holmes P., Lumley J., Poje A. (1994): "The proper orthogonal decomposition, wavelets and modal approaches to the dynamics of coherent structures". Applied Scientific Research, 53, 321-338.

Chatwin P.C. (1981). The Statistical Description of the Dispersion of Heavy Gas Clouds. Report on Contract No 1189/01.01, Health and Safety Executive, Sheffield, UK.

Chatwin P.C. (1982). The use of statistics in describing and predicting the effects of dispersing gas clouds. J Haz Mat 6:213-230.

Chatwin P.C., Sullivan P.J. (1990): "A simple and unifying physical interpretation of scalar fluctuation measurements from many turbulent shear flows". J. Fluid Mech. 212, 533-556.

Chatwin P. (1990): "Statistical methods for assessing hazards due to dispersing gases" Environmetrics, 1(2): 143-162.

Frangos C., Antypas A. (2001): "Jackknife interval estimation of air pollutant concentrations from road traffic". Proc. 14th Conference of Hellenic Operational Research Soc.

Griffiths R.F. (1991): "The use of probit expressions in the assessment of acute population impact of toxic releases" J. Loss Prevention in Process Industries, 4, 49-57.

Hall D.J., Waters R.A., Marsland G.W., Upton S.L., EMMOTT M.A. (1991): “Repeat variability in instantaneously released heavy gas clouds – some wind tunnel experiments”. Report LR 804 (PA), Warren Spring Laboratory, Department of Trade and Industry, U.K.

Hanna S.R. and Drivas P.J. (1987): “Guidelines for use of vapour cloud dispersion models”. Center for Chemical Process Safety, AIChE, N.Y.

Holmes P., Lumley J.L., Berkooz G. (1996): “Turbulence, Coherent structures, Dynamical systems and Symmetry”. Cambridge University Press.

Hunt J.C.R., Rothman J.W. and Britter R.E. (1983): “Some physical processes involved in the dispersion of dense gases”. IUTAM Symposium on Atmospheric Dispersion of Heavy Gases and Small Particles, Deift, The Netherlands, August 1983.

Kevlahan N.K.–R., Hunt J.C.R., Vassilicos J.C. (1994): “A comparison of different analytical techniques for identifying structures in turbulence”. Applied Scientific Research 53, 339-355.

Lilliefors H.W. (1967): “On the Kolmogorov – Smirnov test for normality with mean and variance unknown”. American Statistical Journal,6, 99-402.

Makridakis S., Wheelright S.C., McGee V.E. (1978): “Forecasting: Methods and Applications”. J. Wiley & Sons.

Mole N., Chatwin P.C., Sullivan P.J. (1993): "Modelling concentration fluctuations in air pollution". Modelling Change in Environmental Systems (ed. Jakeman, Beck and McAleer), J. Wiley & Sons Ltd.

Mole N. (1995): "The α-β model for concentration moments in turbulent flows". Environmetrics, 6, 559-569.

Mole N., Clarke E.D., Rietzler E. (1997): "Modelling concentration fluctuation moments for spherically symmetric mean concentration". Il Nuovo Cimento, 20c, N.3

Mole N. (2001): "The large time behaviour in a model for concentration fluctuations in turbulent dispersion". Atmospheric Environment, 35, 833-844.

Mole N., Schopflocher T.P., Sullivan P.J. (2007): “High concentrations of a passive scalar in turbulent dispersion” under consideration for publication in JFM.

Monin A.S., Yaglom A.M. (1965), “Statistical Fluid Mechanics: Mechanics of turbulence” Volume 1, The MIT Press.

Moseley D.J. (1991) M.Sc. dissertation, University of Western Ontario.

Papoulis A. (1965): “Probability, random variables, and stochastic processes”. McGraw – Hill.

Rice J.A., Silverman B.W. (1991): “Estimating the mean and covariance structure non-parametrically when the data are curves” J. R. Statist. Soc. B 53, No 1 pp.233-243.

Robinson C. (1996): “An overview of gas dispersion with fences”. University of Sheffield.

Roussas G.G. (1973): “A first course in Mathematical Statistics”. Addison – Wesley.

Schopflocher T.P., Sullivan P.J. (1997): “Spectral analysis of heavy contaminant clouds”. Environmetrics, 8, 603-612.

Shapiro S.S., Wilk M.B. (1965): “An analysis of variance test for normality (complete samples)”. Biometrika, 52, 591-611.

Sullivan P.J. (1990): "Physical modelling of contaminant diffusion in environmental flows". Environmetrics 1(2), 163-177.

Tennekes H., Lumley J.L. (1972): “A first course in turbulence”. MIT Press.

Venables W.N., Ripley B.D. (1999): “Modern applied Statistics with S-PLUS” Springer.

Zimmerman W.B., Chatwin P.C. (1995) Boundary Layer Meteorology, 75, 321.

СОД Модель для Концентрации Флуктуаций Газов Мгновенно Выпущенных в Атмосферу

Анастасиос ANTYPAS (соотвествующий автор)

Тел. и факс: (210)8991372, e-mail: t_antypas@yahoo.com

Адрес: 4, Ул. Пригипос Петру 16673 Вула, Атика, Греция

Джон BARTZIS

Адрес: Университет Западной Македонии, Департамент Машиностроения,

Ул. Салвера & Бакола, 50100 Козани, Греция

Резюме: В этой работе, разлагается сигнал концентрации повторяющихся мгновенных выбросов опасных газов в атмосферу на свои основные компоненты с помощью Собственной Ортогональной Декомпозицией (СОД) с двойной целью, его восстановления от первых (самых энергичных) компонентов и его прогнозирования в случаях имеющих общие особенности со случаями из которых ети особенности были извлечены с применением СОД. Анализ показал, что модель может составляться интерполяцией в диапазоне варьируемых параметров. Важный вопрос о неопределенности, связанной с предлагаемой модели СОД, обсуждается и предоставляется масштаб неопределенности.

Ключевые слова: Концентрация, дисперсия, прогноз.

Barriers on the propagation of renewable energy sources in Greece

Sofia - Natalia Boemi[1]**, Agis M. Papadopoulos**

Laboratory of Heat Transfer and Environmental Engineering School of Mechanical Engineering, Faculty of Engineering, Aristotle University of Thessaloniki,

54006 Thessaloniki, Greece

[1] Corresponding author: E-mail: boemi@aix.meng.auth.gr,

Tel +30 2310 996011, Fax: +302310996012

Abstract: Renewable Energy Sources (RES), excluding big hydroelectric plants, covered in 2010 7,6% of total electricity production in Greece. According to the current European and national legislation, Greece targets to a 40% share of renewable energy sources (RES) in electricity production by 2020, which is a major challenge. The potential, though, does exist; so does a series of barriers. National legislation is trying to support the development of a "green" electricity market, by means of supply-side policies like subsidies for renewable electricity production and attractive feed-in tariff rates. However, socio-economic and public awareness problems are still met in the planning and implementation of RES projects, together with the lack of a completed national cadastre and a spatial development master plan, specifying areas eligible for RES development. A consolidated study of this broad set of barriers will be discussed in this paper.

Keywords: Renewable energy sources; energy policies; barriers;

1. Introduction

Since the early 1990s the demand for a change in energy policies became a major issue of discussion around the world, driven by economic, environmental, security of supply and social concerns. Political and legislative changes occurred, having a profound influence on the development of Renewable Energy Systems (RES), directly or indirectly. On a European level changes were expressed i.a. by a series of Directives dealing with renewable energy matters, including the Directive on the promotion of electricity from renewable energy sources (Directive 2009/28/EC; 2001/77/EC) and the Directive on the promotion of biofuels (Directive 2003/30/EC) which aimed at the elimination of existing barriers. Within this process, the Directive 2009/28/EC, regarding the promotion of use of energy from renewable sources, sets the mandatory national targets for their overall share in gross final consumption of energy and in transport by 2020. It is a far-reaching package of measures that falls within the line of the European Union's ambitious commitment to fight climate change and promote renewable energy up to 2020 and beyond. Moreover, it establishes a common framework for promoting energy from RES regarding statistical transfers between Member States and third countries, guarantees of origin, administrative procedures, information, training and access to the electricity grid from RES.

In Greece, the first national renewable energy allocation plan foresaw an initial aim of 18%, as determined by the aforementioned Directive 2009/28/EC; it increased to 20%, corresponding to 40% of the total national electricity production in

2010 (Law 3851/2010, NREAP, 2010; Kambezidis et al., 2011). The share of renewable energy sources, with the non-interconnected islands included is depicted in table 1.

When referring in real terms, the overall share of RES in the Greek final energy consumption shows a notable positive trend during the last two decades, rising from 4.5% in 2008 to 7.6% in 2010. Hydropower still represents the dominant renewable energy source; its development has been relatively steady during the last years mainly due to the introduction of other emerging technologies such as wind and solar. Thus, given the present state of market progress on RES and especially on wind power and solar-photovoltaic (PV) applications in Greece (table 1), the target offset for 2020 is rather realistic, under the condition that specific developments will be realized, like removing certain bureaucracy barriers or strengthening the existing legislative frameworks, and persistence or even improvement of the existing policy instruments will be ensured (Kaldellis, 2012).

2. The Greek policy framework

The Greek policy framework is related to the development of a common European energy policy, refers to an integrated strategic objective known as the ‘‘20-20-20’’ target. In this line of approach a series of supplementary laws and ministerial decisions were introduced, to create the framework for an efficient implementation of the aim.

Specifically, Greek legislation incorporated the aforementioned directives in a series of successive laws.

The Law 3468/2006 on “Production of Electrical Energy form RES and combined heat and power in the gross electricity production and other”. The law simplified licensing procedures, whilst it provided a feed-in tariff guarantee for 10 years, which could be extended by 10 years following a producer's unilateral declaration towards the Transmission System Operator. That was made in order to expanse the electrical power market and to provide long term stability. The 20 years period is one element of best practice for national support schemes because it provides stability and support of long term mechanisms.

The Law 3851/2010 on accelerating the development of Renewable Energy Sources in order to deal with Climate Change and other regulations (Governmental Gazette 85/4-6-2010) integrates Directive 2009/28/EC into the national legislation and sets the following national targets until 2020: 40% RES penetration in gross electricity production, 20% RES share in gross energy consumption for heating/cooling and 10% RES share in the transport sector. It is an extension of Law 3468/2006 and it also includes issues regarding the simplification of licensing procedures for RES-E units and establishment of a RES agency under the Ministry of Environment, Energy & Climate Change (MEECC) for advising RES-E investors. Additionally to this law the Ministerial Decision on Physical planning and allocation of RES has been issued (Governmental Gazette B 2464/3-12-2008).

Finally, a series of supplementary presidential decress ministerial decisions were issued to enable the effective implementation of the laws.

3. The barriers for RES in Greece

Greece is, considering its morphology, climate and spatial development, a rather clustered country, as it incorporates mountainous areas and islands, high income touristic places and low income rural areas as well as highly urbanized cities and sparsely populated remote areas. Despite this fact, a series of studies have proven that there are drivers and barriers common in the whole country. Administrative and procedural decoupling of conflicting interests characterizes most of the barriers. Eurostat (2007) used socioeconomic indicators in order to categorize the RES barriers in Greece. The five major types are:

(1) technological barriers;
(2) environmental barriers;
(3) social/public opinion barriers;
(4) economic barriers;
(5) regulatory, administrative and legislative barriers.

The present study, the main finding of which were based on the DEPOIR consolidated Hellenic – Canadian research project, adopts that approach and attempts to identify the existing barriers.

3.1. Technological barriers

There are different needs for the use of RES on the mainland, compared to the islands. It is obvious that, when it comes to the needs of the mainland, the infrastructure network is much more suited to absorb the electrical energy produced by RES in areas with increased potential. The insular electrical connections are, at best, limited to absorb or to store the whole some of the power produced by wind parks (Oikonomou et al, 2009a).

Concerning the wind energy Papadopoulos et al (2007) presented the limited capabilities of absorbing RES-generated power. The need of upgrading existing grids, a time consuming and expensive procedure, especially in the case of high-voltage nets. These problems occur mainly in the regions of Thrace, Evoia and Lakonia, where there is a high interest for investments due to the very favourable wind potential. The seasonal fluctuation of the energy demand, especially on Greek islands, underlines the weakness of the network's infrastructure. There is an problem of concurrency between the demand and the offer of energy and this is, in an insular system, a significant drawback.

3.2. Environmental barriers

The problem with the Greek energy market, at least in its current shape, is that environmental costs are not adequately internalised. While the production of fossil energy is combined with the greenhouse gas emissions as well as with environmental degradation, the costs of these external factors are poorly reflected in the pricing of energy and therefore in the operation of the market. Even thought there has been an effort to reflect environmental costs through the national transmission fees, this reflects only to a small extent on the eco-system (Stangeland, 2007).

According to Oikonomou et al (2009b) the effects on environmental barriers can be recognised on the ecosystems, on the landscape and on the change of land use. More analytically, fauna and flora can change until a RES work completion. Especially, minimal interventions should be made in order for the side to return to its original environmental state as close as possible upon completion of all works.

Also, the upgraded levels of dust and noise during infrastructure works, such as road opening, cables of electric current transport, may lead to an environmental devaluation of the environment. Finally, special attention should be given after completion of all works in order to minimize the intervention with the environment and return the site as close as possible to its original environmental state. The necessary measures include the plantation of trees where new roads need to be constructed, so that the former land use around a wind park does not change.

3.3. Social / public barriers

This is probably the most important underlying factor, because it refers to the public acceptance of the RES. During the last years, a significant number of large-scale RES-based projects have been installed or planned in many places all over Greece, with the public opinion being generally in favour of them. But, moving from global to local, the aforementioned positive view for RES may change considerably (Walker et al., 2010). It should be noted that the public concern often originates from the fact that environmental advantages of RES projects are perceived on a global or national level, whereas, environmental impacts of such systems only affect the local environment and habitants.

This has been also the case in Greece. Deploying a renewable energy project, such as a wind farm, a hydro or, to a lesser extent, a PV plant, close to a community sometimes causes the local population to react, mainly owed to the local habitants' suspicion and negative expectations about this type of applications in their neighbourhood (Kaldellis et al., 2012). Specifically, levels of public acceptance and reactions are usually considered among the primary indicators for implementing a RES project, comprising at the same time a matter of political interest (Elliott, 1994) for all bodies involved (e.g. government, developers, etc.). In some cases, environmental concerns become important enough to affect negatively, or even hinder, the implementation of such projects. Public opposition often focuses on the environmental impacts caused by the installation and operation of wind farms, like the visual impact , the impact on birds' populations and migration, the noise emission, the change in land use, the moving shadows in the nearby vicinities etc.

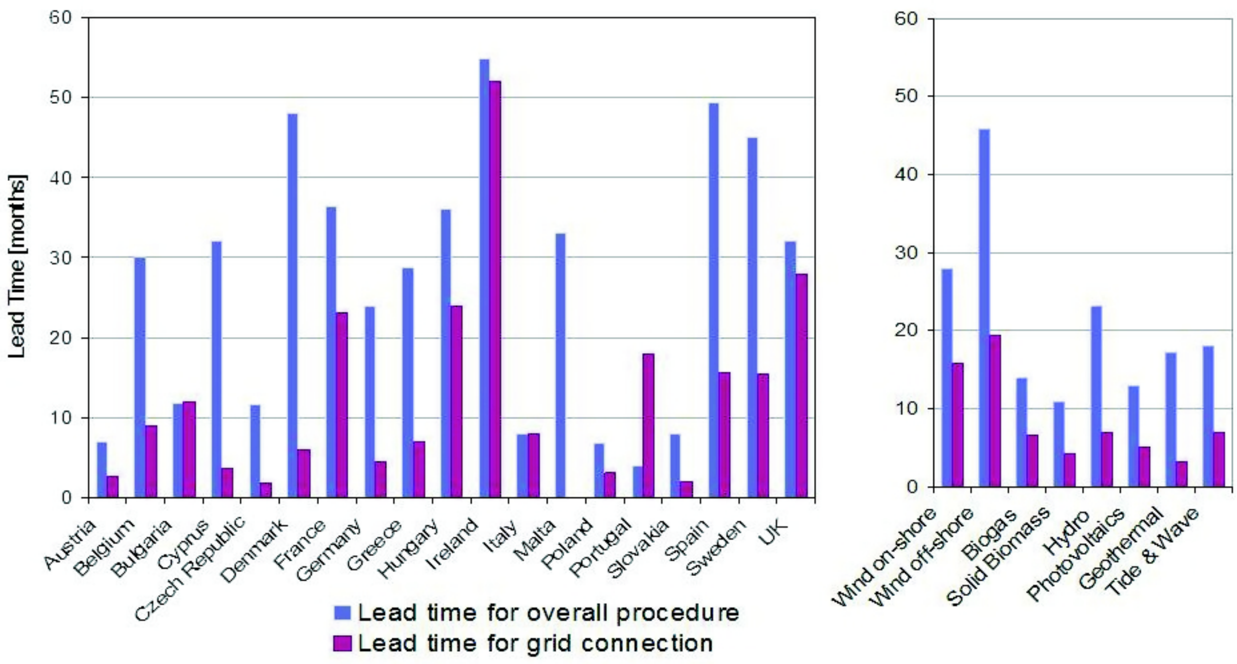

Fig. 1. Average lead time for overall authorisation procedure and grid connection
Source: "Promotion and growth of renewable energy sources and systems" COM 2009

3.4. Economic barriers

Significant economic incentives, together with other forms of stimulus have been launched for propagating the implementation of RES systems in the field and in buildings. Efforts were made on the Greek market to reduce the final price of PVs, but the initial cost is still high, both for commercial and domestic use, to make them attractive without any form of subsidies. Even where feed-in tariffs were attractive, almost excessively so, as in the case of photovoltaics in field, progress is slow and tedious (Papadopoulos et al, 2009).

Referring to the use of wind energy, market distortion and competition exists and unequal distribution of the subsidies' allocation can be monitored between RES and other competitive activities like tourism. Also, an important obstacle for the infiltration of wind energy is the lack of a tax-free income against the expenditure for purchasing small domestic wind turbines (Oikonomou et al., 2009b).

3.5. Regulatory, administrative and legislative barriers

Government procurement policies aim to promote sustained and sustainable commercial development of renewable energy, but bureaucracy still creates obstacles.

One of the major barriers is the overall authorisation procedure together with the grid connection process. As depicted in Figure 1, with respect to the average lead time for overall licensing procedure in Europe, Greece ranks in the last third of the countries.

This is mainly because there is a rather complicated licensing procedure for RES. Concerning the construction of a wind park the duration of the entire procedure can take more than 3 years (Figure 4).

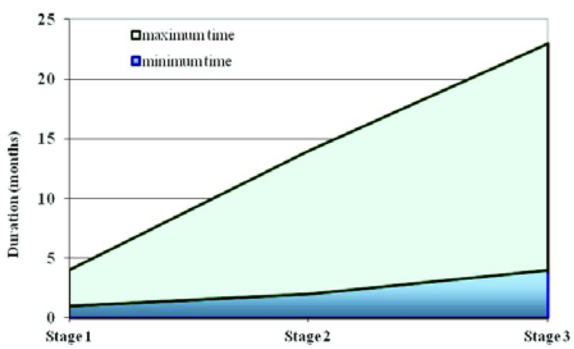

Fig. 4. Stages of development and operation of a PV park - Source: DEPOIR 2007

The first stage, which lasts 3-6 months, is planning and includes site selection and all the required studies.

One of the criteria that should be taken into consideration during the planning phase is, fairly obviously, the wind potential of the selected area. Still, it was not until 2006 that adequate data were available. Other parameters that have to be considered are:

- The distance form transmission networks
- The distance from similar installation;
- The distance from residential areas;
- The distance from archaeological areas;
- The distance from airports and areas protected by international agreements like NATURA, RAMSAR, etc.

The next stage involves the authorization of the wind park project, which lasts from 9 to 18 months, which includes the approvement of a series of detailed studies considering the installations, the construction works and the electrical connections

Finally, the construction of the wind farm, its connection to the grid and a test operation phase are part of the last stage of implementation prior to the plant's commercial operation.

Concerning the construction of a PV park more than ten essential documents are needed in order to start (Figure 5).

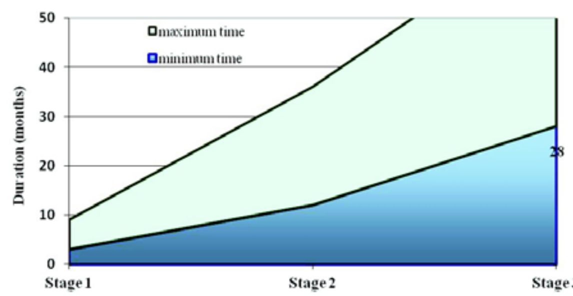

Fig. 5. Stages of development and operation of a wind park - Source: DEPOIR 2007

The first stage for implementing a PV park is the planning. It includes the selection of the suitable area for the installation and the selection of PV frameworks and other system installation based on the best financial deals. The duration of this stage is one to three months.

The next stage includes all the bureaucratic process and lasts from two to nine months. The third and final stage of a PV park project includes (1) ordering and purchase of the equipment [0- 3 months, depending on the availability of materials], (2) installation of PV frames and equipment (not required in buildings), (3) connection to the network. This stage can last from 1 to 7 months depending on the size of the park.

Finally, a problem that cannot remain unaddressed concerns the fact that the same projects are monitored concerning their operation and performance by different authorities simultaneously. The turn-key cost of wind parks is monitored by the Ministry of Development, which is granting the production licences and is also responsible for managing the funding from European Union sources, if applicable. The monthly and annual energy output is monitored by the Hellenic Transmission System Operator (HTSO) which is responsible for the payment of energy producers. The Regulatory Authority of Energy is monitoring the producers' compliance with the terms of the production licences, as well as the evolution of the electricity market as a whole. Although both HTSO and RAE are supervised by the Ministry of Development, this fragmentation does not enable a rundown of the data needed for the evaluation of the wind parks' energy performance and economic efficiency (Papadopoulos et al, 2007). Finally, the Ministry for Finance is monitoring the cash flows from national funding sources.

The implementation of the national spatial master plan for RES is another barrier. In 2007 was published the spatial plan specifically for RES, but its implementation has shown that there are many question to be answered before it actually contributes to speeding up the whole procedure.

4. Conclusions

Price-setting policies in order to reduce cost and pricing related barriers will give a boost to the development of RES. Also, proper dissemination of knowledge on the level of local communities will help in overcoming the social reactions even though the negative social impacts have reduced significantly the last years. Also, a wide variety of policies are designed to explicitly to promote renewable energy and a rise is to the MW produced from RES is obvious Greece need more effective measures to achieve the 20-20-20 target.

Finally, policymakers should provide 'smart' targeting policies in order to boost the RES in early market stages with a view to overcome the institutional barriers to commercialization, to encourage the development of appropriate infrastructure and provide the local markets paths for technologies that require intergraded technical, infrastructure and regulatory changes.

Acknowledgements

The authors wish to acknowledge the General Secretariat for Research and Technology and also to the Hellenic Ministry of National Education and Religious Affairs for partly funding the bilateral research Greek Canadian project DEPOIR (contract No.9387/05). Also, we would like to thank Prof. Karagiannidis and phd candidate Kontogianni Matina for their contribution in completing the DEPOIR report.

Table 1: Mainland's primary energy production for the period 2005–2010 and the demand for 2020
Source: NREAP, 2010; Kambezidis et al., 2011

	2005	2006	2007	2008	2009	2010	2020
Wind	943.8 MW	1199.4 MW	1333.1 MW	1661.2 MW	1908.3 MW	2061.7 MW	7.5 GW
Hydro	164.2 MW	220.4 MW	223.2 MW	324.9 MW	657.2 MW	753.5 MW	3.5 GW (including large hydropower plants)
Solar (photovoltaic and concentrating solar power (CSP) plants	–	-	0.1 MW	5.1 MW	45.1 MW	132.0 MW	2.2 GW and 250 MW
Biomass–biogas	98.1 MW	91.9 MW	155.9 MW	176.7 MW	181.9 MW	193.9 MW	250 MW and biofuels 10% of final con- consumption in the transportation sector
Geothermal energy (including GHP)	14.4 MW	9.1 MW	34.0 MW	34.8 MW	144.1 MW	114.6 MW	120 MW 880 MW of pumped storages systems - concerning exclusively the non-interconnected (NI) islands
RES in total	2.7 %	3.4%	3.5 %	4.5 %	6.5 %	7.6 %	

Table 2: Drivers and barriers for RES and projects in Greece.
Source: DEPOIR, 2007

Barriers	**Renewable Energy Systems**
Technological	Lack of trained human resources.
Environmental	Incorporation costs for RES High cost of grid connection.
Social and political	There is no maturity in the recognition and realistic assessment of the RES potential .
Economic	Lack of funds. Participation in EU funding projects in public-private partnerships.
Legislative and administrative	Delays in the overall procedure. Lack of special spatial design for RES. Ineffective control mechanisms and administrative structures.

References

Boemi, S.N. , Papadopoulos, A.M., Karagiannidis, A., Kontogianni, M., (2010). Barriers on the propagation of renewable energy sources and sustainable solid waste management practices in Greece. Waste Management and Research, Issue 11, p 967-976

Developing practical guidelines for an observatory center on the progress of Implementing projects on Renewables and waste/ wastewater, (2007). General Sectarteriat for Reaserch and Technology. Thesalaloniki

Elliott, D.A., (1994). Public reactions to wind farms: the dynamic of opinion formation. Energy and Environment, Volume 5, p. 343–362.

Eurostat data 2006 (normalised hydro).

Eurostat (2007). www.eurostat.com

Eurostat/Fraunhofer ISI: Electricity Eurostat/Fraunhofer ISI: Electricity from renewable energy sources 2006 breakdown of normalised renewable electricity in 2006

Kaldellis, J.K. , Kapsali, M., Katsanou Ev., 2012. "Renewable energy applications in Greece—What is the public attitude?". Energy Policy, Volume 42, http://www.sciencedirect.com/science/journal/03014215/42pages 37–48

Kambezidis, H.D., Kasselouri, B., Konidari,P., (2011). Evaluating policy options for increasing the RES-E penetration in Greece. Energy Policy, Issue 9, p 5388–5398

Oikonomou, V., Becchis, F., Steg, L., Russolillo, D. (2009a). "Energy saving and energy efficiency concepts for policy making". Energy Policy, Issue 11, p 4787–479

Oikonomou, E.K., Kilias, V., Goumas, A., Rigopoulos, A., Karakatsani, E., Damasiotis, M., Papastefanakis, D., Marini, N., (2009b). "Renewable energy sources (RES) projects and their barriers on a regional scale: The case study of wind parks in the Dodecanese islands, Greece". Energy Policy, Issue 11, p 4874–4883

NREAP, NationalRenewableEnergyActionPlan,2010. /http://ec.europa.eu/ energy/renewables/transparency_platform/doc/national_renewable_ener gy_action_plan_greece_en.pdfS

Papadopoulos, A.M., Glinou, G.L., Papachristos, D.A., (2007). "Development in the utilisation of wind energy in Greece". Renewable Energy, Issue 1, p 105 – 110.

Papadopoulos, A.M. and Karteris, M. (2009). "An assessment of the Greek incentives scheme for photovoltaics". Energy Policy. Issue 5, p 1945 - 1952

Regulatory Authority for Energy (RAE), (2008). www.rae.gr

Stangeland, A., (2007). The potential and barriers for Renewable Energy, The Bellona Foundation,

The Renewable Energy Progress Report, COM(2009) 192 final , (24.04.2009). Commission staff working document, Brussels.

Walker, G.P., Hunter, S., Devine-Wright, P., Evans, B., High, H., (2010). Trust and community: exploring the meanings, contexts and dynamics of community renewable energy. Energy Policy, Volume 38, p. 2655–2663.

Барьеры для Распостранения Возобновляемых Источников Энергии в Греции

София – Наталья Boemi, Агис M. Papadopoulos

Лаборатория Теплопередачи и Экологической Инженерии, Отдел. Машиностроения, Факультет Инженерии, Университет имени Аристотеля в Салониках, 54006 Салоники, Греция

1 Соотвествующий автор: E-mail: boemi@aix.meng.auth.gr, Тел. +30 2310 996011,

Факс: +302310996012

Резюме: Возобновляемые источники энергии (ВИЭ), без учета больших гидроэлектростанций, покрыли в 2010 году 7,6% общего производства электроэнергии в Греции. В соответствии с действующим европейским и национальным законодательством, Греция нацелена на 40% долю возобновляемых источников энергии (ВИЭ) в производстве электроэнергии к 2020 году, что является серьезной задачей. Потенциал, хотя, действительно существует, так же и серия барьеров. Национальное законодательство пытается поддерживать развитие «зеленого» рынка электроэнергии с помощью производственно-сбытовой политики, как субсидии на производство возобновляемой электроэнергии и привлекательные льготные тарифы. Однако, социально-экономические и проблемы общественной информированности, до сих пор встречаются в планировании и реализации проектов, указывают вместе с отсутствием совершенного национального кадастра и пространственного генерального плана развития, области имеющие право на развитие ВИЭ. В этой статье, будет рассматриваться консолидированное изучение этого широкого спектра барьеров.

Ключевые слова: Возобновляемые источники энергии; энергетические политики; барьеры;

The impact of diesel fuels' combustion in cars on the urban air SO_2 pollution in Tirana, Albania

Edlira F. MULLA[1*]; Angjelin SHTJEFNI[2]; Andonaq Lamani (LONDO)[2]

[1] Department of Chemistry. Polytechnic University of Tirana.

[2] Department of Energetics. Polytechnic University of Tirana.

*Corresponding author: Universiteti Politeknik i Tiranës, Sheshi "Nënë Tereza", Tirana, ALBANIA

Tel / Fax: +355 4 222 3707

Email: edimulla@gmail.com

Abstract: Albanian vehicle fleet is composed of 80% diesel vehicles, which use diesel with very high sulfur content and are relatively "old". This article addresses an important aspect: comparison of sulfur concentrations of diesel fuels traded within Albania with diesel fuels traded in an EU country, Greece, and the impact of the diesel combustion in cars on the urban air SO_2 pollution in Albania.

This research showed that: i) diesel D2 has an average S concentration of 1020 ppm for the imported fuel, and 1600 ppm S for the fuel produced in the country; ii) Diesel D1, although a relatively higher quality fuel, has great differences regarding S content: the average S concentration for Diesel D1 imported in Albania was 210 ppm, whereas the average S concentration of Diesel D1 used by the vehicles in Greece was 27 ppm.

On the other hand, although the SO_2 concentrations in the air of Albanian cities continue to respect the Albanian norm of 60 $\mu g/m^3$ a significant increase of SO_2 concentrations in the urban air is observed. SO_2 higher concentrations and trends of annual increase are very well correlated with the annual increase in the number of cars and mainly with the traffic density in certain cross-roads in Tirana city.

Keywords: diesel, sulfur content, SO_2 air pollution.

1. Introduction

1.1 Vehicle Fleet in Albania

The Albanian vehicle fleet is composed of about 80% of diesel cars which are mostly second hand vehicles imported from neighboring countries during the last 20 years. In particular, the number of private cars, has significantly increased during the last 16 years (Figure 1), comprising slightly more than 70% of the total number of registered vehicles in 2009. The number of "0 km" cars at the moment of purchase is very small. For the period 2006-2009 the registered as brand new cars that were purchased during these years is less than 5% of the total number of vehicles (MTTPW, 2010).

Due to the improved living conditions and the higher standards of living in Tirana compared to other districts, the number of cars per 1000 inhabitants has almost doubled in the capital compared to that of the whole country during the last decade. The trends show a significant and constant annual increase, as presented in Figure 2.

The number of cars per 1000 inhabitants presented in Figure 2 shows an even more dramatic increase of this parameter compared to year 1990, as illustrated from data of Table 1 (MTTPW, 2010; INSTAT, 2010). It is worth mentioning that till 1991 the private ownership of any vehicle was not permitted by the Socialist Government in power up at that time.

1.2 Diesels consumed in Albania

The reports regarding the State of Environment which are published every 2 years by the Ministry of Environment, for the time period 1997-2009 attribute the "bad urban air quality" to the fact that vehicles in Albania are "very old" and that the fuel they use is not of good quality (SoE 1999; SoE 2001; SoE 2003; SoE 2005; SoE 2008; SoE 2009). It was also noticed that these reports do not provide figures to illustrate the "bad quality" of fuels used by these vehicles.

Although there is a State Institution, the Central Technical Inspectorate, that is responsible for the fuel analysis, no official reports are published by it until now regarding the fuel quality in the country. Therefore it was necessary for the authors of this paper to conduct this research for the time period 2008-2009 in order to observe the quality regarding sulfur content in diesels traded in Albania and their impact on the SO_2 urban air pollution. The city of Tirana was selected for the observation of the SO_2 air concentrations because: i) over 36 % of the total vehicles in Albania circulate in Tirana District (MTTPW, 2010); ii) 23% of the population of the country lives in this city (INSTAT, 2010) and iii) SO_2 is one of the indicators of the urban air quality.

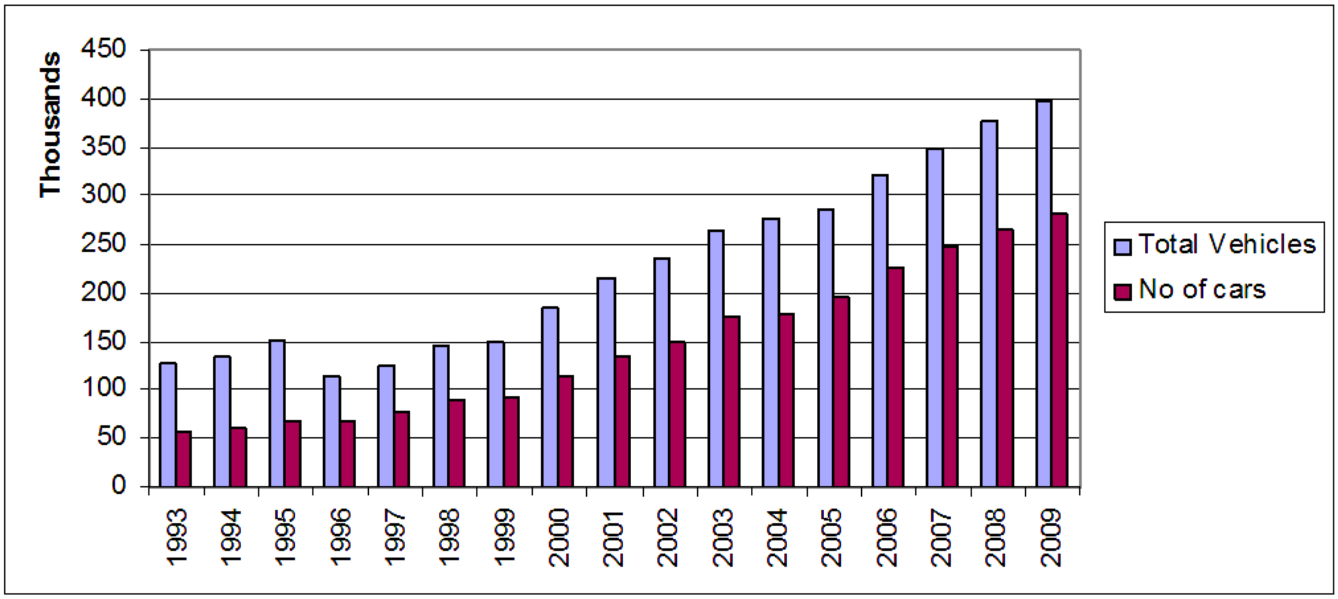

Fig. 1: Number of cars compared to the total number of registered vehicles in Albania during the last 16 years. (Source: MTTPW, 2010).

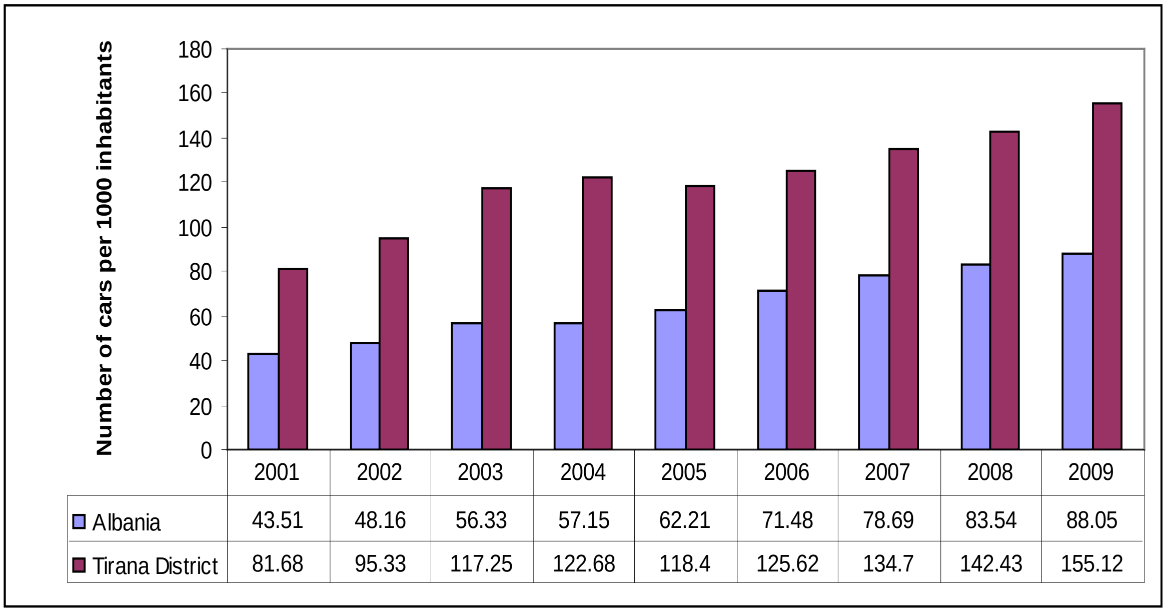

Fig. 2: Number of cars per 1000 inhabitants in the Republic of Albania and in Tirana district for the period 2001–2009. (Source: MTTPW, 2010; INSTAT, 2010).

Table 2: Number of vehicles and cars / 1000 inhabitants for the year 1990

Population of Albania	Total no. of vehicles	No. of cars	vehicles / 1000 inhabitants	cars / 1000 inhabitants
3,273,131	20200	2400	6.171	0.733

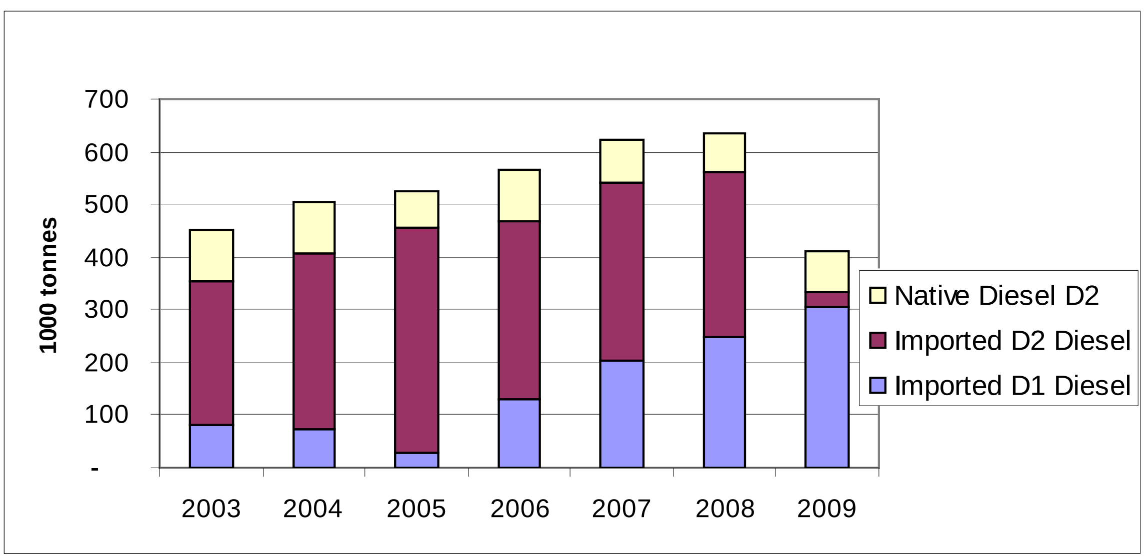

Fig. 3: Quantity of diesels consumed by the Albanian vehicle fleet during the last 6 years (Source: METE, 2010; NICC, 2010).

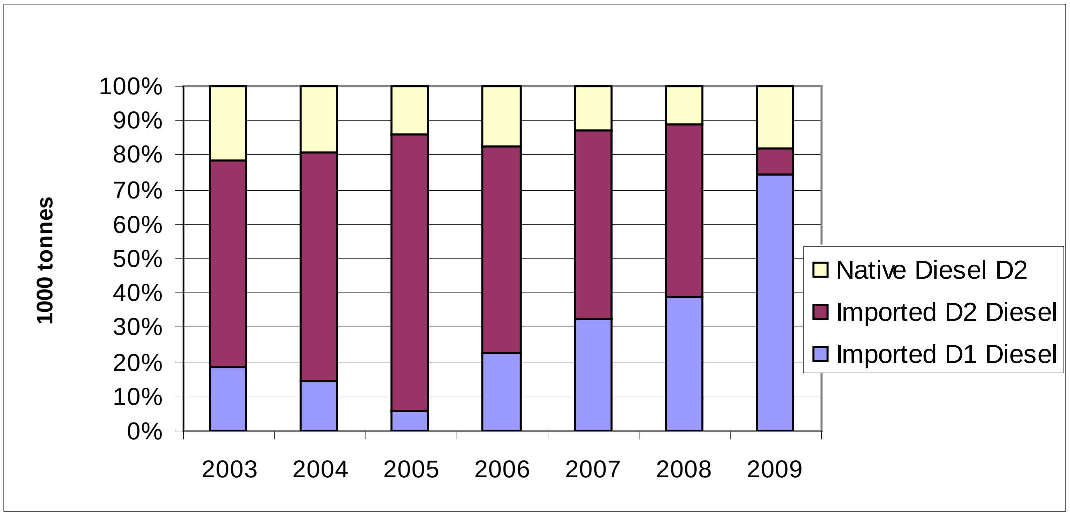

Fig. 4: Shares of Albanian D2, imported D2 diesel and imported D1 Eurodiesel during the last 6 years in the Albanian fuel consumption market (Source: METE, 2010; NICC, 2010).

In Albania up to 2009, the diesel vehicles used Diesel D2 which contained sulfur in the range of 0.05 – 0.2 % in mass and Diesel D1, named “Eurodiesel”, which contains less than 0.05 % (in mass) sulfur, according to the customs’ classification. The diesel produced in Albania up to 2008 was of the type D2 due to its high sulfur content and the lack of a desulphurization plant in the country. The quantity of diesels consumed by the Albanian market has increased annually during the last decade, as Figure 3 shows. However, there was an exception of this trend in year 2009, due to the import banning of Diesel D2 type by the Government, and also due to the effects of the world financial crisis on fuel consumption in Albania.

During the last decade, 85–90 % of fuels in Albania were imported mainly from Greece and Russia. For year 2008 the percentages were respectively 61 % and 32 %, of the whole fuel quantity imported in Albania (NICC, 2010). In average during the last decade only 10-15 % of the fuel market in Albania is being supplied by ARMO, the Albanian Oil Refining company [Figure 4] (METE, 2010).

1.3 Sulfur dioxide concentrations in Tirana

To show the tendency for the period 2002-2009, Figure 5 was produced with annual average SO_2 concentrations in 5 monitoring stations in Tirana (MEFAW, 2009; IPH 2010).

The EU standard for the SO_2 air concentrations is 50 μg/m^3 (annual arithmetic average), whereas the Albanian standard is 60 μg/m^3 (AEF, 2009). Concentrations of SO_2 measured in Tirana respect the Albanian standard in all monitoring stations, nevertheless they show an annual increase especially in the “heavy traffic” cross road named “21 December”. For the year 2008 in this monitoring site, the EU norm was passed for SO_2.

The relationship between the number of vehicles passing by a road and the SO_2 concentrations is shown by comparing Figure 5 with Figure 6. The much higher SO_2 concentrations in the Tirana 4 monitoring point are explained by the much higher number of vehicles passing daily in this monitoring point, based on the traffic numbering in Tirana’s roads during the morning rush hour in 2007 (MT, 2008).

For the period April 2008 – June 2009, in Tirana's heavy traffic section of the crossroad "21 December", the average monthly SO_2 concentration resulted 20.8 μg/m^3 (AEF, 2009), as presented in Figure 7.

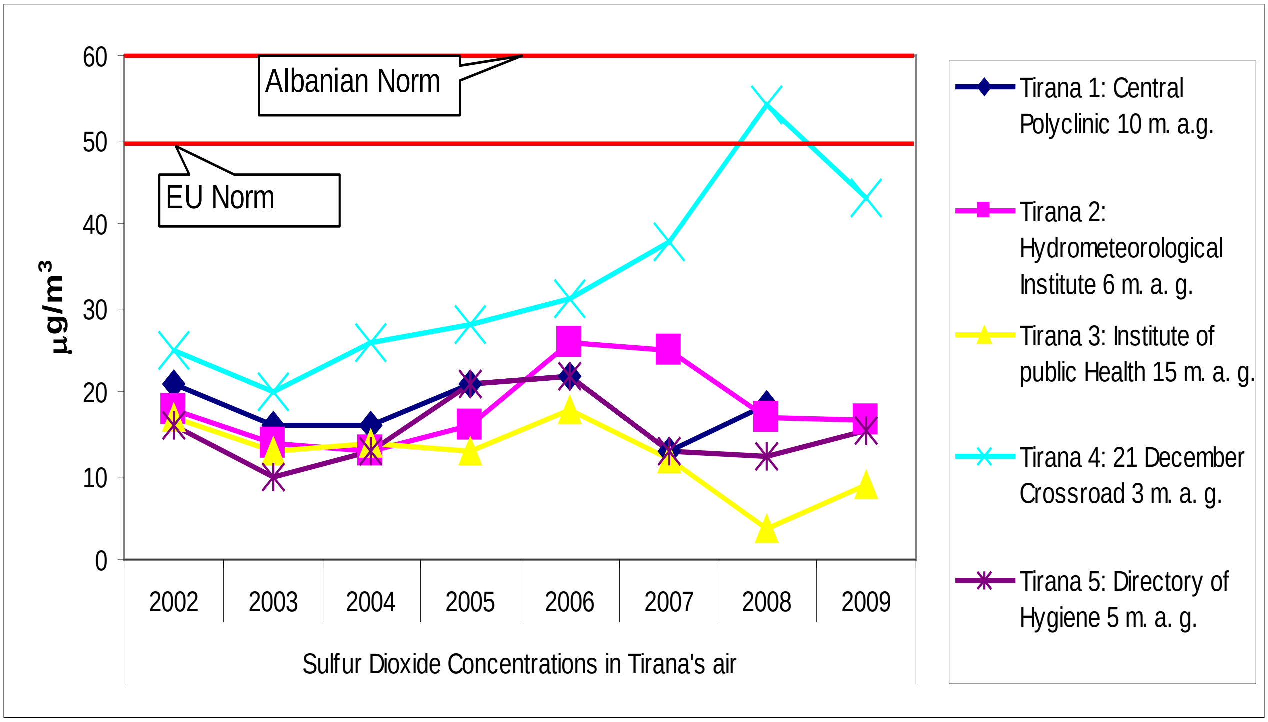

Fig. 5: Average SO_2 annual air concentrations in Tirana at 5 monitoring points carried out by IPH for the period 2001 – 2009 (Source: MEFAW, 2009; ISHP, 2010).

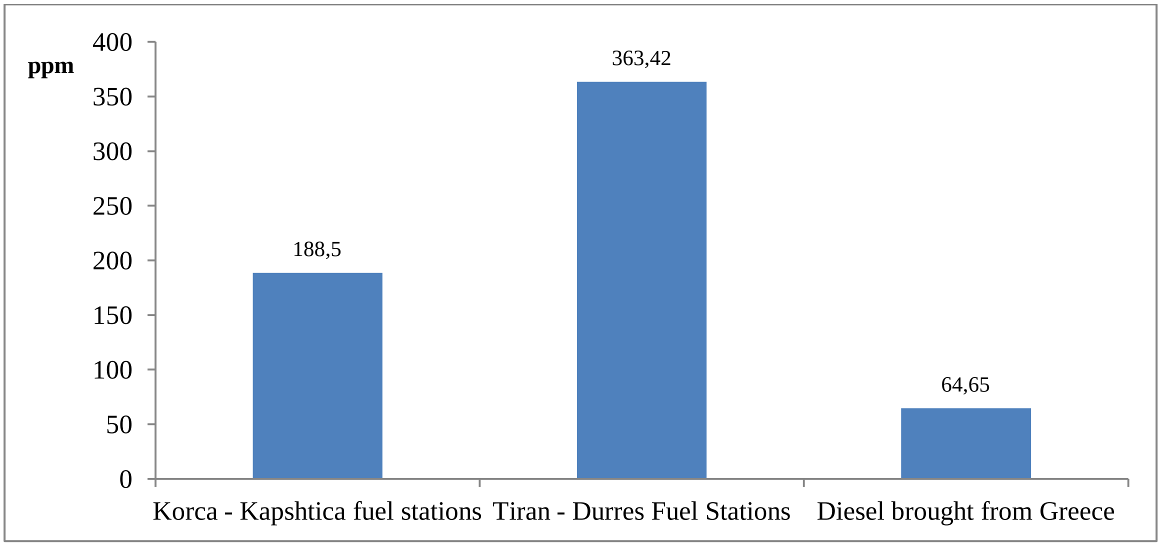

Fig. 6: Total number of vehicles passing by each Air Quality Monitoring Site in Tirana, during year 2007 (Source: MT, 2008).

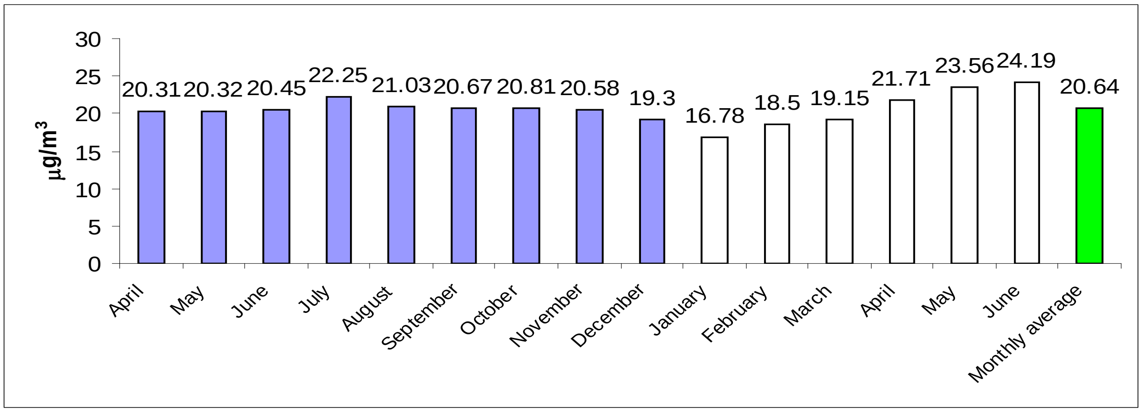

Fig. 7: SO_2 air concentrations in Tirana for the period April 2008 – June 2009 (Source: AEF, 2009).

2. Material and methods

Due to the lack of published data about the fuel quality in Albania and in order to complete this research, information was obtained from Governmental Institutions, such as Ministries, Agencies and Directorates, as presented in references and Source of data for each case. Data was used as it was or combined with data from several Institutions so as to compile certain graphs.

For the experimental part, diesel samples of one liter were taken in sterile plastic bottles from various fuel stations along Tirana- Durres and Korça – Kapshtica highways. For a reference of the fuel used in an EU country, diesel brought from Greek fuel stations was analyzed regarding its sulfur content at the same time and with the same equipment that the other diesel samples were analyzed.

The equipment used to analyze the sulfur content in Diesel fuels is Multi EA 3100 Analytik Jena. Pyrolysis is used for the breakdown of the substances in the Multi EA 3100, with subsequent thermal oxidation of the pyrolysis products. The apparatus was operated in the vertical mode for the analysis of our Diesel samples.

With a syringe of 50 µl capacity, an exactly 20 µl diesel sample was taken and injected manually directly into the evaporation zone of the combustion tube. There the sample was subjected to pyrolysis in the stream of argon. After this, the gases from the pyrolysis were completely oxidized in the stream of oxygen. Reaction taking place can be summarized as below:

$$R\text{-}S + O_2 \rightarrow SO_2 + CO_2 + H_2O \qquad (1)$$

R – represents the organic substances containing carbon in the diesel to be analyzed.

The average S concentration is displayed on the screen on the computer linked to the Multi EA 3100 Analytic Jena apparatus for each analysis based on the calibration function that has been determined before hand and automatically calculates the amount of total sulfur in the fuel sample analyzed (CL, 2009).

For diesels containing 0–50 mg/l sulfur the linear calibration curve was used. For the ones containing 51-500 mg/l sulfur the quadratic calibration curve was used. For the Diesels that contain much more than 500 mg/l sulfur, dilution takes place with the solvent iso-octane. Iso-octane is used as a diluent because it is used to “zero” the apparatus and it does not contain sulfur in it, thus not interfering with the results.

The proportion of dilution depends on the result of the first trial experiment: if it resulted in 1 g/l sulfur, the dilution is 1 part in volume fuel: 3 parts in volume iso-octane. If the result was 1.5 g/l the dilution is made in the proportion 1:4 and if it resulted in 2 g/l the dilution was made in the proportion 1:5 respectively. Dilution is made in order for the S concentrations to be within the boundary of 51-500 mg/l calibration curve, thus resulting in more accurate measurements. For each sample one trial measurement and three other measurements were carried out in order to define an average value of the total sulfur content in the diesels analyzed.

3. Results and discussion

Samples of diesel were collected in the period August – December 2008. Their analysis was carried out at the Laboratory of Petrochemicals in the Customs Directory of Laboratories by the first author of this article, in the period March - April 2009. The summary of analysis' results is presented in Tables 2-6 according to the diesel types analyzed and it is grouped by the place where the diesel samples were taken.

Compared to previous research regarding the sulfur content in Albanian fuels in 1996 (Mulla and Dhimitri, 2002) and 2003 (Mulla and Norbeck, 2005) the diesels' quality in Albania in 2008 has improved significantly compared to their quality in 1996 when their S content did not even respect the Albanian standard of less than 0.2 % S for both the native and the imported Diesel (Mulla and Dhimitri, 2002). In 2003 most of the Diesel used in Albania was D2 with more than 500 ppm Sulfur in it, but all of the imported Diesel samples met the Albanian Standard, whereas the Albanian Diesel D2 [Ballshi Naphta] passed this standard significantly (Mulla and Norbeck, 2005). Five years latter, in 2008, the authors noticed a diversification of the diesel fuel types used in the country, and all the samples meet the Albanian standard, even the Diesel produced in Ballshi Refinery.

Depending on their quality and their sulfur content the prices of Diesels vary. Native Diesel is cheaper and Eurodiesel is the most expensive in the market. The economic situation of the people determines the type of car (new or old), the frequency of service that they will do to their cars and, most importantly, the type of fuel (the expensive or the cheap one) they will use on daily basis.

Based on data from Table 6, the pie charts of Figures 8 and 9 are compiled in order to give a more visual representation of different types of Diesels' contribution in the SO_2 quantity in the air of Albania for the year 2008. The proportions for S content in the fuels and SO_2 released in the urban air are the same because the molar mass of SO_2 is double than the atomic mass of sulfur.

From the graphs in Figure 8 and 9 it is easily noticeable that for the year 2008, although the Albanian D2 Diesel contributed with only 11 % of the total fuel quantity, due to its very high S content, it contributed with 23 % of the total S contained in the Diesels used, and consequently with 23 % of the total SO_2 released in the urban air, due to the Diesels combustion in vehicles' engines. On the other hand, the imported Diesel D1, or the EuroDiesel, contributed with 39 % of the total quantity of fuels, but only with 11 % of the total S in the fuels, and 11 % of the total SO_2 was released in the urban air due to its combustion.

In this research it was concluded that the Diesels D2 used in Tirana District contained less S than the ones used in Korça District. As expected, and as it is illustrated in Figure 10, the samples of Diesel D2 from Ballshi Refinery contained much more S than all the samples of Diesel D2 imported in Albania.

By comparing the S content in the Diesel samples taken in Albania with the ones taken in an EU country, Greece, it is noticeable that the average S content in Diesel D1 used in Albania is nearly 8 times more than the average S content in the Diesels used in Greece as demonstrated by the Graph in

Figure 11. The variation of S content in the Diesel D1 samples taken in Albania is great, from 4.81 ppm to 562.55 ppm, whereas for the samples taken from Greece, the variation of S content is much smaller, from 2.75 to 64.65 ppm.

For many years, meeting the fuel standards regarding sulfur content has been a challenge. Up to early 2009, the Albanian Standard of sulfur content was the same as the one of 1987 (STASH, 1987) thus it allowed the import of fuels with less than 0.2 % (in mass) of sulfur. By the Decision of the Council of Ministers No. 52 dt. 14 January 2009 the Diesel produced in the Refinery of Ballshi would be allowed to be in the fuel market up to the end of 2009 and after that date the ARMO fuel company is obliged to produce and sell Diesel which will respect the EURO standards on this schedule:

Diesel needs not to contain more than:

1) 350 ppm S from 1 Jan. 2010 2) 150 ppm S from 1 Jan. 2011, 3) 10 ppm S from 1 Jan. 2012 (DCM, 2009).

*Table 2**:** Results for the sulfur content in the Diesel D2 samples.*

Place taken	Korca – Kapshtica highway fuel stations			Tirana fuel stations			Diesel D2 from Ballshi, native fuel		
Sample name	diesel 1	diesel 5	diesel 7	diesel 8	diesel 9	diesel 19	diesel 25	diesel 26	diesel 27
S concentration average (mg /l)	865	1257	981.9	866.6	552.7	622.5	1325.1	1349. 2	1408.9
Standard deviation (mg / l)	5.2	5.78	8.56	25.11	4.97	9.15	24.7	16.6	32
Variation coefficient (%)	0.6	0.46	0.87	2.9	0.9	1.47	1.89	1.24	2.04
Quadratic regression [μg]	$C = (k_2 \cdot I^2_{net} + k_1 \cdot I_{net} + k_o) / V$ $k_0 = - 0.055513$ $k_1 = 7.651E – 6$ $k_2 = 1.115 E – 12$								
Density at 15 ^{oC} (kg/l)	0.845	0.838	0.834	0.840	0.833	0.850	0.855	0.854	0.854
S content calculated in ppm = Csulfur average (mg/l) / d15^{o}C (kg/l)	1023	1499.28	1178.04	1031.5	663.90	732.01	1550	1580	1650
S content in mass % = Sppm : 10000	0.102	0.1499	0.118	0.103	0.066	0.073	0.155	0.158	0.165

Table 3: Results for the sulfur content in the Diesel D1 samples with S concentration more than 50 mg/l and less than 500 mg/l.

Place taken	Korca – Kapshtica highway		Tirana	brought from Greece	Tirana – Durres highway					
Sample name	diesel 2	diesel 3	diesel 10	diesel 11	diesel 12	diesel 13	diesel 14	diesel 16	diesel 20	diesel 21
S concentration average (mg/l)	156.8	353.5	298.8	54.33	218.9	386.2	463.6	81.68	46.12	54.93
Standard deviation (mg/l)	1.1	2.02	946.4	0.833	1.07	2.65	5.62	1.92	1.24	1.09
Variation coefficient (%)	0.7	0.57	0.32	1.53	0.49	0.69	1.21	2.35	2.69	1.98
Quadratic regression [μg]	$C = (k_2 \cdot I^2_{net} + k_1 \cdot I_{net} + k_o) / V$ $k_0 = - 0.055513$ $k_1 = 7.651E – 6$ $k_2 = 1.115 E – 12$									
Density at 15 ^{o}C (kg/l)	0.832	0.837	0.822	0.840	0.839	0.840	0.824	0.826	0.836	0.8359
S content calculated in ppm = Csulfur (mg/l) / d15^{o}C (kg/l)	188.5	422.29	363.42	64.65	260.78	459.49	562.55	98.95	55.20	65.71
S content in mass % = Sppm : 10000	0.019	0.042	0.036	0.007	0.026	0.046	0.056	0.010	0.006	0.007

Table 4: Results for the sulfur content in the Diesel D1 samples with S concentration less than 50 mg /l

Place taken	Tirana	Brought from Greece		Tirana – Durres highway		Brought from Greece		
Sample name	diesel 4	diesel 6	diesel 15	diesel 17	diesel 18	diesel 22	diesel 23	diesel 24
S concentration average (mg /l)	24.45	30.85	2.75	4.02	8.25	22.92	22.85	2.3
Standard deviation (mg / l)	6.06	0.12	0.052	0.067	0.086	0.191	0.084	0.064
Variation coefficient (%)	24.78	0.39	1.9	1.67	1.05	0.83	0.37	2.79
Linear regression [µg]	$C = (k_1 \cdot I_{net} + k_0) / V$ $k_0 = - 0.052299$ $k_1 = 8.182$ E - 6							
Density at 15^{o}C	0.832	0.842	0.835	0.836	0.837	0.834	0.834	0.835
S content calculated **in ppm** = Csulfur (mg/l) / d15^{o}C (kg/l)	29.37	36.62	3.29	4.81	9.86	27.50	27.41	2.75
S content **in mass %** = Sppm : 10000	0.003	0.004	0.0003	0.0005	0.001	0.003	0.003	0.0003

Table 5: Summary of the average sulfur content (in mass percentage) of the fuels traded in Albania in 2008, according to their categories.

Diesel D1 imported	12 samples	0.021
Diesel D2 imported	6 samples	0.102
Albanian D2 diesel	3 samples	0.160
Diesel brought from Greece	6 samples	0.003

Table 6: Average amount of S and SO_2 per inhabitant in Albania in 2008.

	S mass %	Diesel quantity in kg in 2008 (10^6)	Total S in Diesels in kg
Diesel D1 imported	0.021	246	51660
Diesel D2 imported	0.102	316	322320
Albanian D2 diesel	0.16	71	113600
Total amount of Sulfur in Diesels in kg			487580
Average amount of SO_2, supposing that S is oxidized 100 % in SO_2 M_{SO2} = 64 g/mol whereas A_S = 32 g/mol			975160
Number of inhabitants in 2008			3170048
Average amount of S per inhabitant / year 2008 in kg			0.154
Average amount of SO_2 per inhabitant / year 2008 in kg			0.308

Source: Table 6 calculations are based on data received from NICC, 2010; METE, 2010; INSTAT, 2010

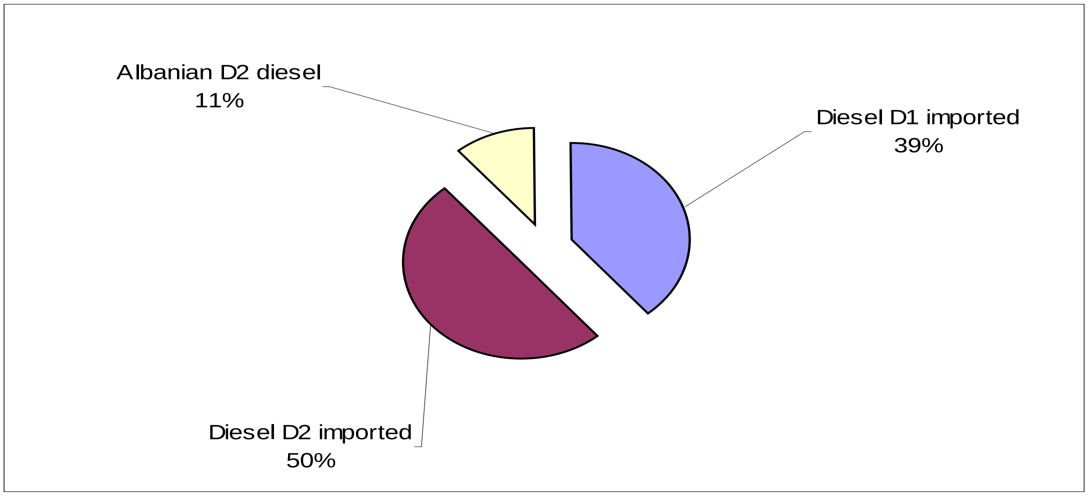

Fig. 8: Share of different types of Diesels traded in Albania for year 2008 (Source: NICC, 2010).

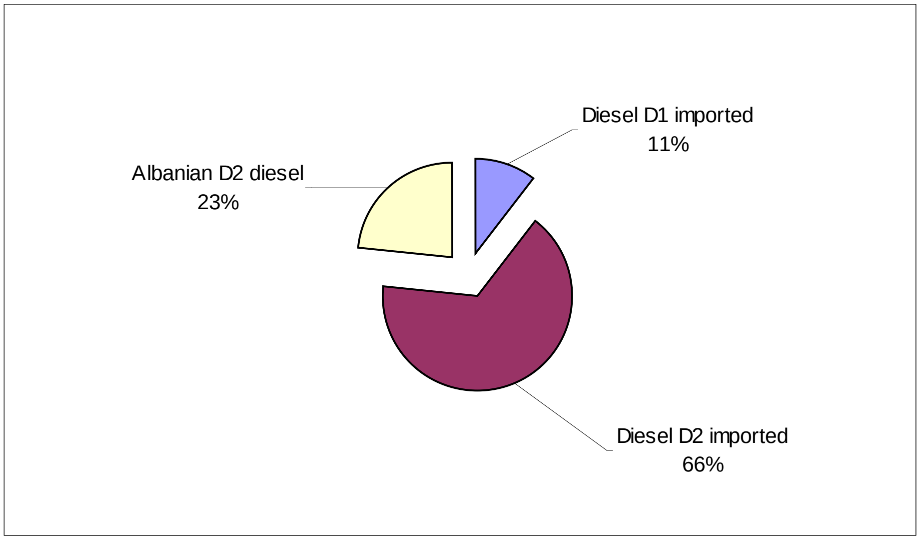

Fig. 9: Share of the total amount of Sulfur contained in different types of diesels traded in Albania in the year 2008.

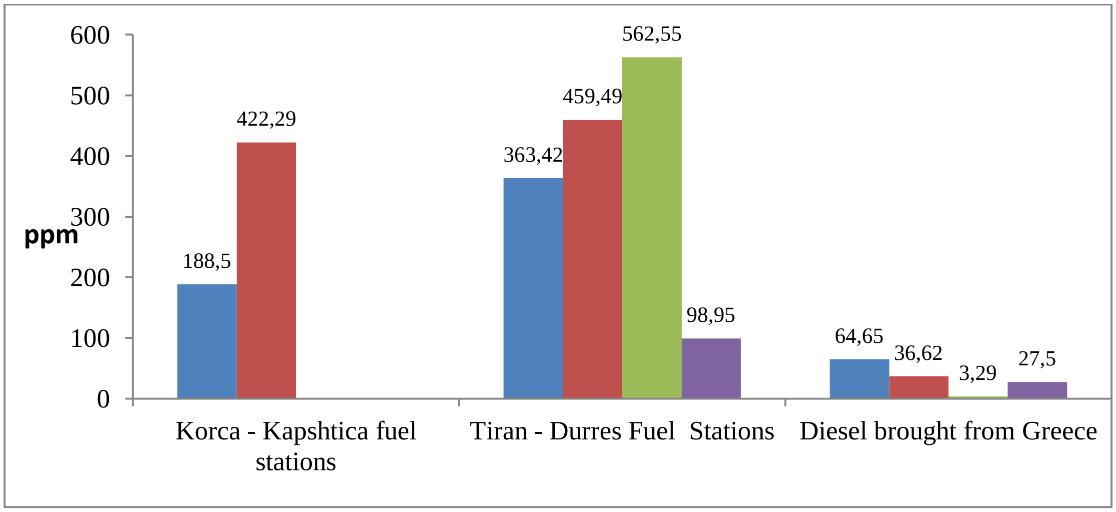

Fig. 10: Sulfur content in diesel D2 samples.

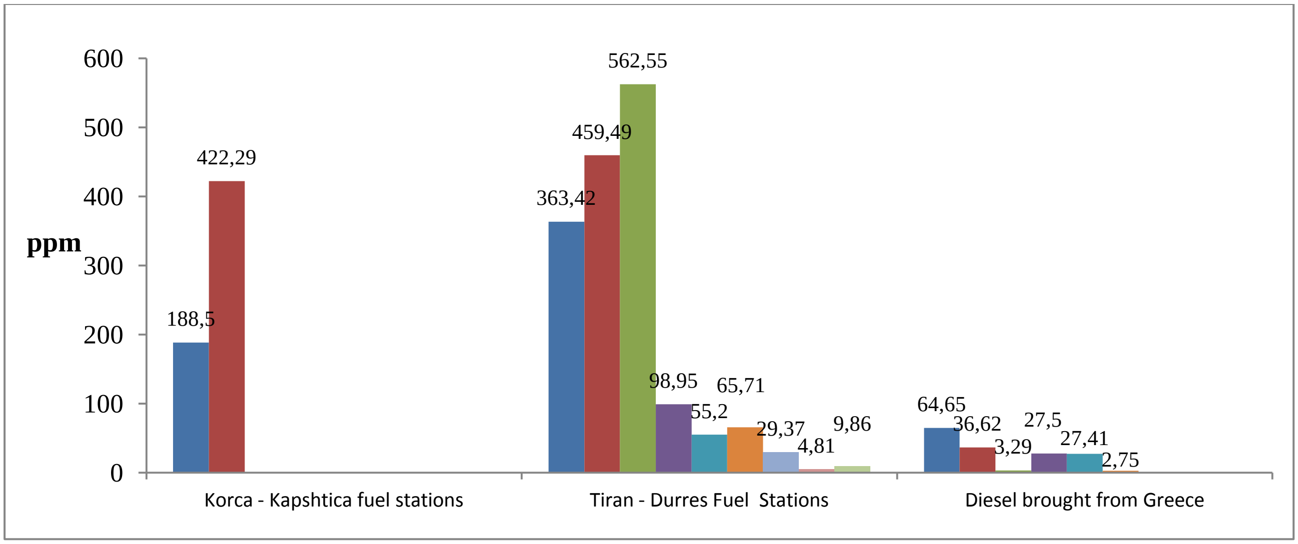

Fig. 11: Sulfur content in Diesel D1 samples.

From Figure 4, it is noticed that in the last seven years the quantity of Eurodiesel consumed in Albania has increased annually, comprising 74 % of the total quantity of the Diesel consumed in 2009, compared to the 18.5 % of the total quantity of Diesel consumed in 2003. This is a good indication of the pressure by the Government to the fuel importers to provide a good quality Diesel for the Albanian drivers. Even within the D1 category of Diesel there are fuel stations which sell Euro 5 Diesel with less than 10 ppm of sulfur in it, thus enabling the drivers to care not only about their cars but also about the environment.

Although SO_2 air concentrations respect the Albanian and EU standards, the SPM (Suspended Particulate Matter) and PM_{10} (particulate matter less than 10 mikrons) concentrations in the urban air in Albania continue to be much higher even than the present Albanian SPM and PM_{10} standard in all the monitoring points not only in Tirana, but in all the monitored cities in Albania (SoE, 2009). An explanation for this is based on research findings from other Universities, that although sulfur is oxidized mostly to SO_2 on combustion in Diesel car engines, sometimes, besides in SO_2, it is oxidized in sulfate ions, SO_4^{2-}, which can assist in the nucleation of particles and therefore give rise to SPM and PM_{10} air concentrations (Colvile et. al. 2001; Placentino et al., 2008; Bader, 2007; Wahlin et al., 2001; Sterner, 2003; Elsom, 1996) For Tirana the SPM and PM_{10} air concentrations correlate very well with the total number of cars passing by the 5 monitoring points (Mulla E. 2008; Mulla E. 2009).

4. Conclusions and recommendations

In conclusion,

1) The analyzed Diesel samples were found to meet the Albanian Standard regarding the sulfur content, but in general they failed to meet the EU standards of Euro 5 type of Diesel. There were a few fuel stations that provided good quality Diesel comparable to the Diesel that was currently traded in Greece.

2) The air quality in Tirana generally does respect the Albanian standard and the EU standard regarding the SO_2 concentrations in the 5 monitoring points, but the trends of these concentrations being increased annually in heavy traffic sections show that the respect of these standards will not last indefinitely. With the significant reduction of Diesel D2 consumption in 2009, a slight decrease of the SO_2 air concentrations was measured at the Tirana 4 station as the monitoring results of 2009 showed.

As a recommendation, out of this research, the Government needs to refresh the Standard regarding the sulfur content. At least, the import of only Euro 5 Diesel (with less than 10 ppm S) must be the first amendment of the Revised standard, in order not only to meet for a very long time the SO_2 air concentrations standard, but also the SPM and the PM_{10} standard.

Because Albania produces its own Diesel which has always resulted in a very high S content, it is recommended that in the near future the Government finds the proper economical and legal mechanisms so that the private company which runs the Oil Refinery of Ballshi provides only Euro 5 Diesel for the Albanian car drivers and becomes a good competitor in the Diesel market in Albania.

References

AEF 2009: Agency of Environment and Forests. / Directory of Air Quality Monitoring. Unpublished data used with permission. Tirana, May 2009.

Bader, J. 2007: Single Fuel Policy. Compatibility with EURO 4 Diesel Engines. - NATO RTO AVT ET-073 Spring Meeting 2007. Florence, Italy. Pp. 3.

CL – 2009. Customs Laboratory. Operation Manual multi EA 3100. Edition of 06/2005. Analytic Jena AG. Pgs. 25-29.

Colvile, R.N., Hutchinson, E.J., Mindell, J.S., Warren, R.F., (2001). *The transport sector as a source of air pollution.* Atmospheric Environment 35, 1537–1565.

DCM 2009: Decision of the Council of Ministers. Fletorja Zyrtare e Republikes se Shqiperise. Botim i Qendres se Publikimeve Zyrtare. No. 5. 29 Jan. 2009. Pg. 82-83.

Elsom, D. 1996: Smog Alert – Managing urban air quality. - Earthscan Publications limited. London. 220 pp.

INSTAT 2010: National Institute of Statistics. Unpublished data used with permission. Tirana, March 2010.

IPH 2010: Results of the Monitoring of Urban Air Quality for the year 2009 in Albania. - Institute of Public Health, Ministry of Health. Tirana 2010. Pp. 2, 6-8.

MEFAW 2009: Ministry of Environment, Forests and Administration of Waters / Directory of Information. Unpublished data used with permission. Tirana, April 2009.

METE 2010: Ministry of Economy, Trade & Energetics. General Policies Directorate. [Albanian Diesel Production by ARMO]. Unpublished data used with permission. Tirana, March 2010.

MT 2008: Municipality of Tirana. Directory of Transport and Mobility. Unpublished data used with permission. Tirana, November 2008.

MTTPW 2010: Ministry of Transport, Telecommunication and Public Works. General Directorate of Services to the Road Transport. Directory of Information. Unpublished data used with permission. Tirana, March 2010.

Mulla, E. and Dhimitri, R (2002); *"The evaluation of sulfur content in fuels and air pollution from sulfurous gases in Korca area"* Polytechnic University of Tirana, Technical Sciences Bulletin No. 2. Tirana, 36-43 (Albanian)

Mulla, E. and Norbeck, J. : (2005) *"Improving urban air quality by lowering the sulfur content in fuels used in vehicles"* Book of Proceedings: Third International Conference. Ecological Chemistry – Latest Advances; Academy of Sciences - Chisinau, Moldova, 352 – 360.

Mulla, E. : (2008) – *The impact of vehicles on the Air Pollution in Tirana City*. 3^{o} Convegno Nazionale sul Particolato Atmosferico. La conoscenza per l'informazione a le strategie di intervento. Bari, Italy, 6-8 Oct. 2008. pg. 82.

Mulla, E. 2009: Studim i ndotesve te ajrit nga djegia e lendeve djegese ne motoret e automjeteve ne qytetin e Tiranes dhe ndikimi i tyre ne cilesine e ajrit. – Disertacion per Graden “Doktor i Shkencave”. Universiteti Politeknik i Tiranes. Tirane, 167 pp.

NICC 2010: National Information Customs’ Center – Statistics Directorate [Imported Diesels D1 and D2 by the Country of their origin]. Unpublished data used with permission. Tirana, March 2010.

Placentino, C.M., Amodio, M., Bruno, P., Cafagna, I., Caselli, M., Daresta, B.E., De Gennaro, G., Di Gilio, A., Francescangeli, A., Ielpo, P., Tutino, M. 2008: Caraterizzazione chimica del PM2.5 e PM10 nella Regione Puglia. Il particolato Atmosferico: La conoscenca per l’informazione e le strategie di intervento. - 3° Convegno Nazionale sul Particolato Atmosferico. Bari. Italy. 6-8 Ottobre 2008. Pp. 79.

SoE, 1999 - State of Environment Report 1997-1998. Republic of Albania. National Environmental Agency. Tirana 1999. Pg. 27.

SoE, 2001 - State of Environment Report 1999-2000. Republic of Albania. National Environmental Agency. Tirana 2001. Pg. 70

SoE, 2003 - State of Environment Report 2001-2002. Republic of Albania. National Environmental Agency. Tirana 2003. Pg. 20.

SoE, 2005: State of Environment Report 2003 - 2004. Republic of Albania. National Environmental Agency. Tirana 2005. Pg. 9.

SoE, 2008: Report on the State of Environment 2005 – 2007. Republic of Albania. Ministry of Environment, Forests and Administration of Waters. Agency of Environment and Forests. Tirana 2008. Pg. 146.

SoE, 2009: Report on the State of Environment 2008. Republic of Albania. Ministry of Environment, Forests and Administration of Waters. Agency of Environment and Forests. Tirana 2009. Pg. 16.

STASH – 1987: Standartet Shteterore, Vellimi I (Nafte, gaz dhe produkte te naftes), Tirane, 1987. pg. 82.

Sterner, Th., 2003: Policy Instruments for Environmental and Natural Resource Management. - Resources for the Future & The World Bank, Washington DC, USA., Swedish International Development Cooperation Agency, Stockholm, Sweden. 504 pp.

Wahlin, P., Palmgren, F., Van Dingenen, R., Raes, F. 2001: Pronounced decrease of ambient particle number emissions from diesel traffic in Denmark after reduction of the sulphur content in diesel fuel. - Atmospheric Environment, 35(21): 3549-3552.

Воздействие сгорания дизельного топлива в автомобилях на загрязнение SO_2 городского воздуха в Тиране, Албания

Едлира F. MULLA[1*]; Ангелин SHTJEFNI[2]; Андонак Lamani (LONDO)[2]
[1] Департамент Химии. Политехнический Университет Тираны.
[2] Департамент Энергетики. Политехнический Университет Тираны.

*Соотвествующий автор: Политехнический Университет Тираны, Площадь “Nënë Tereza”, Тирана, Албания, Тел / Факс: +355 4 222 3707, Email: edimulla@gmail.com

Резюме: Албанское автотранспортное предприятие состоит из 80% дизельных транспортных средств, которые используют дизель с очень высоким содержанием серы и являются относительно "старыми". В данной статье рассматривается важный аспект: сравнение концентраций серы дизельного топлива торгующево в Албании, с дизельным топливом торгующем в стране ЕС, в Греции, и воздействие сгорания дизельного топлива в автомобилях на загрязнение SO_2 городского воздуха в Албании.

Это исследование показало, что: i) дизель D2 имеет среднюю S концентрацию 1020 ppm для импортного топлива, и 1600 ppm S для топлива производимого в стране; ii) Дизель D1, хотя и относительно является более высокого качества топливо, имеет большие различия в отношении содержания S: средняя концентрация S для дизеля D1 импортированным в Албании составляло 210 ppm, в то время как средняя концентрация S дизеля D1 используемых транспортных средств в Греции составляло 27 ppm.

С другой стороны, не смотря на то что концентрации SO_2 в воздухе албанских городов продолжают уважать албанские нормы 60 $\mu g/m^3$, наблюдается значительное увеличение концентрации SO_2 в городском воздухе. Более высокие концентрации SO_2 и тенденции ежегодного увеличения, коррелируются очень хорошо с ежегодным увеличением количества автомобилей и в основном с плотностью движения в определенных перекрестках в городе Тирана.

Ключевые слова: дизель, содержание серы, загрязнение SO_2 воздуха.

PROMITHEAS Network, the origin of which is the Project Development Fund of BSEC, aims to promote scientific cooperation on the energy and climate policy issues between the countries of BSEC and EU and thus to contribute in knowledge transfer to that region, as a basic precondition for the development of human potential that will materialize policies of cooperation.

PROMITHEAS Network has the following members:

KEPA	Energy Policy and Development Centre, Greece
PUT	Polytechnic University of Tirana, Albania
ESC	Energy Strategy Centre, Armenia
GPOGC	Geotechnological Problems of Oil, Gas and Chemistry, Azerbaijan
BSREC	Black Sea Regional Energy Centre, Bulgaria
TUSB	Technical University of Sofia, Bulgaria
EEC	Energy Efficiency Centre, Georgia
NOA	National Observatory of Athens, Greece
AUT	Aristotle University of Thessaloniki –Laboratory of Heat Transfer and Environmental Engineering, Greece
UA	University of Aegean – Department of Environment, Energy Management Laboratory, Greece
INEXCB-Kz	Independent Expert Consulting Board to Promote Scientific Research Activity in Kazakhstan, Kazakhstan
SRC KAZHIMINVEST	Scientific Production Firm KAZIMINVEST, Kazakhstan
PCTC-KG	Public Centre for Tobacco Control, Kyrgyzstan
IPE	Institute of Power Engineering, Moldova
ISPE	Institute for Studies and Power Engineering, Romania
Financial University	Federal State-Funded Educational Institution of Higher Professional Education Financial University under the Government of the Russian Federation
ESSUT	Eastern Siberia State University of Technology, Russian Federation
UOB-CE	University of Belgrade – Centre of Energy, Serbia
SoDeSCo	Society for Development of Scientific Cooperation in Tajikistan, Tajikistan
IWHEA	Institute of Water problems, Hydropower and Ecology Academy, Academy of Sciences, Tajikistan
TUBITAK	Marmara Research Center, Energy Institute, Turkey
MUGLA	Mugla University, Turkey
ESEMI	Energy Saving and Energy Management Institute, Ukraine
IUCPT	Indo-Uzbek Centre for Promotion S&T Cooperation, Uzbekistan

Photos of cover from ManagEnergy and Intelligent Energy - Europe Programme of the European Commission

PROMITHEAS
The Energy and Climate Change Policy Network

Energy Policy and Development Centre (KEPA)
National and Kapodistrian University of Athens (NKUA)

ISSN: 1791 - 6119